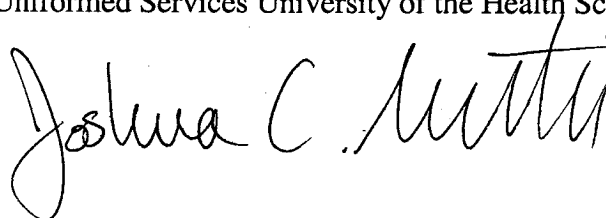The author hereby certifies that the use of any copyrighted material in the thesis manuscript entitled:

"The Influence of Platelet-Derived Growth Factor and Fibroblast Growth Factor 2 on Oligodendrocyte Development and Remyelination"

is appropriately acknowledged and, beyond brief excerpts, is with the permission of the copyright owner.

Joshua Murtie
Molecular and Cell Biology Program
Uniformed Services University of the Health Sciences

Report Documentation Page

Public reporting burden for the collection of information is estimated to average 1 hour per response, including the time for reviewing instructions, searching existing data sources, gathering and maintaining the data needed, and completing and reviewing the collection of information. Send comments regarding this burden estimate or any other aspect of this collection of information, including suggestions for reducing this burden, to Washington Headquarters Services, Directorate for Information Operations and Reports, 1215 Jefferson Davis Highway, Suite 1204, Arlington VA 22202-4302. Respondents should be aware that notwithstanding any other provision of law, no person shall be subject to a penalty for failing to comply with a collection of information if it does not display a currently valid OMB control number.

1. REPORT DATE **2004**	2. REPORT TYPE	3. DATES COVERED **-**

4. TITLE AND SUBTITLE	5a. CONTRACT NUMBER
THE INFLUENCE OF PLATELET-DERIVED GROWTH FACTOR AND FIBROBLAST GROWTH FACTOR 2 ON OLIGODENDROCYTE DEVELOPMENT AND REMYELINATION	5b. GRANT NUMBER
	5c. PROGRAM ELEMENT NUMBER

6. AUTHOR(S)	5d. PROJECT NUMBER
	5e. TASK NUMBER
	5f. WORK UNIT NUMBER

7. PERFORMING ORGANIZATION NAME(S) AND ADDRESS(ES) **Uniformed Servicces universsity of the Health Sciences,F. Edward Herbert School of Medicine,4301 Jones Bridge Road,Bethesda,MD,20814-4799**	8. PERFORMING ORGANIZATION REPORT NUMBER

9. SPONSORING/MONITORING AGENCY NAME(S) AND ADDRESS(ES)	10. SPONSOR/MONITOR'S ACRONYM(S)
	11. SPONSOR/MONITOR'S REPORT NUMBER(S)

12. DISTRIBUTION/AVAILABILITY STATEMENT
Approved for public release; distribution unlimited

13. SUPPLEMENTARY NOTES
The original document contains color images.

14. ABSTRACT

Multiple sclerosis (MS) is a demyelinating disease of the central nervous system (CNS) characterized by repeated episodes of autoimmune-mediated demyelination. Symptoms of the disease range from loss of vision to paralysis with each episode resulting in a decreased remyelination response. If remyelination does not occur, bare axons will not be able to function properly either by inefficient saltatory conduction or by degeneration resulting from a lack of myelin. This study examines the effects of growth factors on recovery from demyelination. Specifically, what roles do plateletderived growth factor (PDGF) and fibroblast growth factor 2 (FGF2) play during remyelination of the central nervous system? This question will be addressed using the cuprizone model of demyelination with significant remyelination. The remyelination response in this model will be examined in FGF2 knockout mice as well as PDGF alpha receptor (PDGFαR) heterozygous mice. This study examines the elimination of FGF2 signaling and the reduction of PDGF signaling in an animal model of demyelination with significant remyelination. The current results demonstrate that the predominant role for FGF2 during development and remyelination is that of an inhibitor.

15. SUBJECT TERMS

16. SECURITY CLASSIFICATION OF:			17. LIMITATION OF ABSTRACT	18. NUMBER OF PAGES **151**	19a. NAME OF RESPONSIBLE PERSON
a. REPORT **unclassified**	b. ABSTRACT **unclassified**	c. THIS PAGE **unclassified**			

ABSTRACT

Title: THE INFLUENCE OF PLATELET-DERIVED GROWTH FACTOR AND
FIBROBLAST GROWTH FACTOR 2 ON OLIGODENDROCYTE DEVELOPMENT
AND REMYELINATION

Author: Joshua C. Murtie Ph.D. (2004)

Thesis Directed By: Regina C. Armstrong Ph.D. Professor, Department of Anatomy
Physiology, and Genetics

ABSTRACT: Multiple sclerosis (MS) is a demyelinating disease of the central nervous
system (CNS) characterized by repeated episodes of autoimmune-mediated
demyelination. Symptoms of the disease range from loss of vision to paralysis with each
episode resulting in a decreased remyelination response. If remyelination does not occur,
bare axons will not be able to function properly either by inefficient saltatory conduction
or by degeneration resulting from a lack of myelin. This study examines the effects of
growth factors on recovery from demyelination. Specifically, what roles do platelet-
derived growth factor (PDGF) and fibroblast growth factor 2 (FGF2) play during
remyelination of the central nervous system? This question will be addressed using the
cuprizone model of demyelination with significant remyelination. The remyelination
response in this model will be examined in *FGF2* knockout mice as well as
PDGF alpha receptor (*PDGFαR*) heterozygous mice. This study examines the
elimination of FGF2 signaling and the reduction of PDGF signaling in an animal model
of demyelination with significant remyelination. The current results demonstrate that the
predominant role for FGF2 during development and remyelination is that of an inhibitor

THE INFLUENCE OF PLATELET-DERIVED GROWTH FACTOR AND

FIBROBLAST GROWTH FACTOR 2 ON OLIGODENDROCYTE

DEVELOPMENT AND REMYELINATION

by

Joshua C. Murtie

Thesis/dissertation submitted to the Faculty of the
Molecular and Cell Biology Program
Uniformed Services University of the Health Sciences
In partial fulfillment of the requirements for the degree of
Doctor of Philosophy 2004

TABLE OF CONTENTS

of oligodendrocyte progenitor differentiation. PDGF was determined to maintain the

normal non-lesioned density of oligodendrocyte progenitors as well as oligodendrocytes.

Furthermore, PDGF was also identified as a mitogen for oligodendrocyte progenitors

during remyelination. Together these data indicate that PDGF and FGF2 are critical

regulators of adult remyelination *in vivo*.

CHAPTER 1

Introduction

Significance

Damage to the adult human central nervous system (CNS) can have severe, long lasting effects on the efficiency with which the CNS functions. One such type of damage is observed in the autoimmune disease multiple sclerosis (MS). MS is characterized by repeated episodes of demyelination in white matter tracts of the brain and spinal cord. The pathology observed in MS lesions is heterogeneous with various effects on oligodendrocyte lineage cell (OLC) populations. Despite this heterogeneity, three characteristics are commonly found in MS patients: myelin damage, oligodendrocyte death, and transection of axons. In fact, four distinct MS pathologies have been observed: (1) cellular autoimmunity; (2) humoral autoimmunity; (3) oligodendrocyte dystrophy; (4) primary oligodendrocyte degeneration (Lucchinetti et al., 2000). Some MS lesions have extremely low densities of oligodendrocytes (Lucchinetti et al., 1999), while other MS lesions contain large populations of OLCs, including oligodendrocyte progenitors (OPs) and premyelinating oligodendrocytes (Maeda et al., 2001; Chang et al., 2002).

Persistence of OLCs in MS lesions indicates that there is potential for remyelination by endogenous cells. In fact, remyelination can occur in MS lesions; however, this ability to remyelinate dissipates with each demyelinating episode (reviewed in Bruck et al., 2003). This remyelination response is characterized by morphological, not chemical, changes in myelin including short internodal length and thin myelin sheaths (Ludwin, 1997). After repeated

episodes of demyelination associated with MS, remyelination does not occur to the extent necessary for full clinical recovery and symptoms become progressively worse.

Demyelination is also associated with traumatic brain and spinal cord injury. Traumatic injury to the central nervous system (CNS) initiates a cascade of events involving numerous tissues and cell types. The initial phase of brain and spinal cord injury (BSCI) is the destruction of bone, vasculature, and nervous tissue itself. Later stages of injury play out over days and involve activation of microglia and infiltration of macrophages, astrocytic reaction, and significant cell death. Axons may be crushed, transected, or demyelinated after traumatic injury; all of which would require remyelination for proper functioning of regenerated or surviving axons that have been demyelinated as a result of injury. These events typically create an environment that does not allow significant recovery and results in the formation of a glial scar. However, demyelination independent of axonal damage is observed in some cases of BSCI (Blight et al., 1993) and simple remyelination without axonal regeneration may be sufficient for recovery. Limited recovery does occur in several animal models of BSCI, and that recovery corresponds with the number of myelinated axons (Blight, 1993).

The initial mechanical injury associated with BSCI initiates a cascade of secondary tissue damage that is long-lasting (Dumont et al., 2001). Initial oligodendrocyte loss is significantly increased at the injury epicenter at four hours while maximal loss of oligodendrocytes occurs days after the injury (Grossman et al., 2001; Crowe et al., 1997; Shuman et al., 1997). This secondary damage is not restricted to oligodendrocytes, but involves destruction of numerous cell types and tissues. Antibodies directed towards myelin components that inhibit neurite outgrowth have proven to be useful with respect to regeneration (Chen et al., 2000). Although

regeneration of axons is sometimes necessary for recovery from BSCI, inducing myelin-directed inflammation may be a dangerous treatment. While clearing myelin is beneficial in the early stages of recovery, factors that promote myelination are necessary for restoration of function in surviving or regenerated axons (Schwab, 2002).

Whether demyelination is the result of autoimmunity or traumatic injury, remyelination is likely to be a critical step in successful recovery. Specifically, complete repair of the damaged CNS is likely to require at least four phases. First, tissue debris must be removed by microglia and macrophages. The destroyed tissue contains neurite growth inhibitors that must be removed in order for regeneration of fiber tracts to occur. Next, recovery of the neuronal population must occur either by regeneration of destroyed fiber tracts or by repair of surviving axons. Oligodendrocyte lineage cells must then respond by myelinating bare axons resulting in successful saltatory conduction. If remyelination does not occur, regenerated axons will not function appropriately. Finally, further damage must be prevented. Immunosuppressive therapy has already been used to prevent secondary tissue damage seen in BSCI as well as to suppress the misdirected immune response in MS. Clearly, understanding the context in which remyelination must occur and the factors influencing remyelination is essential to successful treatment of diseases such as MS and trauma associated with BSCI.

Oligodendrocytes in CNS Development

Oligodendrocyte Development and the Oligodendrocyte Lineage

The CNS is primarily composed of three neural cell types: neurons, astrocytes, and oligodendrocytes with all three cell types originating from neuroepithelial cells of the neural

tube. Formation of CNS structures occurs through the coordinated proliferation, migration, differentiation, and survival of these cell types. Emergence of each cell type is temporally distinct with some overlap. In the rodent CNS, neurogenesis peaks at embryonic day 14 (E14), astrogliogenesis at postnatal day 2 (P2), and oligodendrogliogenesis at P14 (reviewed in Sauvageot and Stiles, 2002). While the peak of oligodendrocyte formation occurs postnatally, the first oligodendrocytes appear in the CNS during late embryonic development. Oligodendrocyte specification begins around E13 and is regulated by a class of basic helix-loop-helix (bHLH) transcription factors known as Olig1 and Olig2 (Lu et al., 2000). Olig function is necessary and sufficient for specification of all oligodendrocytes in the CNS (Lu et al., 2002). Induction of *Olig* gene expression is regulated directly or indirectly by a gradient of Sonic hedgehog emanating from the floor plate (Lu et al., 2000). Oligodendrocytes are the terminally differentiated phenotype in a lineage of cells that can be identified functionally as well as by the use of cell type-specific markers (reviewed in Pfeiffer et al., 1993; Armstrong, 1998; Baumann and Pham-Dinh, 2001). Over time, the markers used to identify various stages in the oligodendrocyte lineage have become associated with cellular responses such as proliferation and migration (Figure 1).

Early stages of the lineage are characterized by the ability to proliferate and migrate. As

cells progress through the lineage, they eventually lose their proliferative and migratory

capabilities and become myelinating oligodendrocytes. Early stage OPs are commonly identified

by expression of the chondroitin sulfate proteoglycan NG2 and by expression of platelet-derived
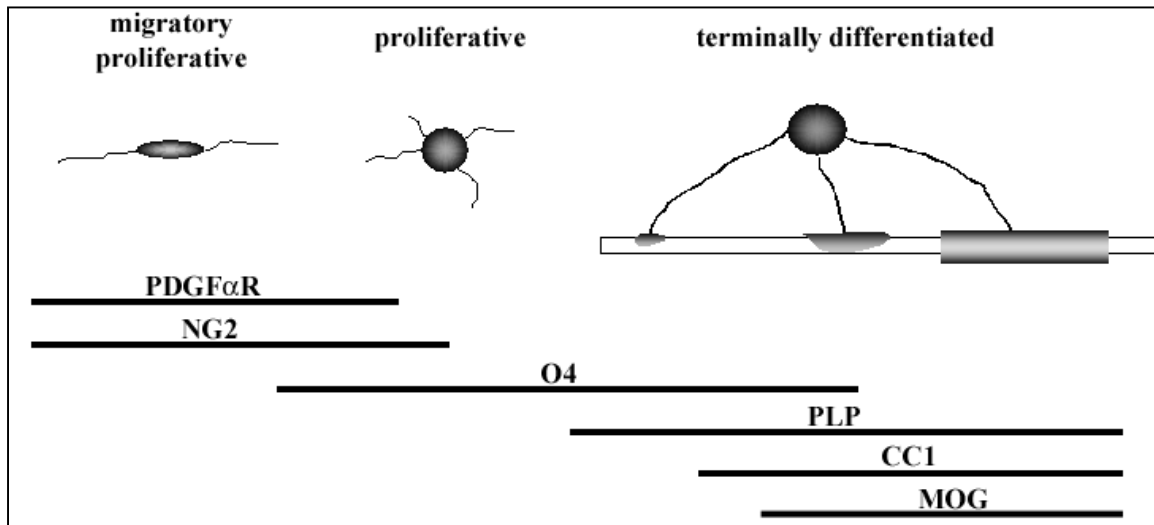

Figure 1: OLC cell type-specific markers including cellular characteristics. As cells mature through the oligodendrocyte lineage they can be identified by various cell type-specific markers. Furthermore, as maturation proceeds, OLCs begin to lose the ability to migrate and proliferate.

growth factor alpha receptor (PDGFαR), while remaining negative for the sulfatide O4. These

early progenitors typically have a bipolar morphology and are highly proliferative and motile.

These characteristics allow OP populations to expand and migrate to the future white matter

tracts of the CNS. Later stage OPs retain PDGFαR and NG2 expression; however they also

begin to express O4. O4-labeled cells are multiprocess-bearing cells that retain a proliferative

capacity, but are generally non-motile. As OPs differentiate into mature oligodendrocytes, they

begin to express myelin protein genes and can be identified by expression of proteins such as

myelin oligodendrocyte glycoprotein (MOG) and proteolipid protein (PLP). During earlier

stages in the lineage, OPs can also be identified by expression of mRNA transcripts of myelin

protein genes such as the PLP splice variant DM/20. In fact, use of these markers has led to the

debate as to whether oligodendrocytes are derived from a single or multiple lineages.

Specifically, cells that express PDGFαR are found in close proximity to similar cell types that

express DM/20 transcripts in the developing CNS; however, cells that express both PDGFαR

and DM/20 mRNA are extremely rare (reviewed in Spassky et al., 2000).

While it may appear that OPs are cells that are fully committed to the oligodendrocyte

lineage, recent studies have demonstrated that OPs are potentially multipotent. Specifically, *in

vitro* and *in vivo* experiments have demonstrated that cells expressing OP markers have the

ability to generate neurons (Mason and Goldman, 2002; Belachew et al., 2003; Nunes et al.,

2003). These results demonstrate that cells once thought of as fully committed to the

oligodendrocyte lineage have the potential to generate other cell types in the proper environment.

Roles of PDGF and FGF2 during CNS Development

During development, OLC proliferation, migration, differentiation, and survival are all

regulated by complex interactions of multiple signals over the appropriate developmental time

course. Growth factors are one type of these critical regulators that have profound influences on

OLC responses. Among these growth factors, PDGF and FGF2 may be critical regulators of

oligodendrocyte generation during myelination and remyelination.

PDGF

There are currently four members of the PDGF ligand family (PDGF-A-D) with two high

affinity receptors (PDGFαR and

PDGFβR). With the recent

identification of ligand family

members PDGF-C and PDGF-D,

and their receptor-binding

properties (Li et al., 2000;

Bergsten et al., 2001; Gilbertson

et al., 2001) it is becoming clear

that PDGF signaling is far more

complex than originally thought.

PDGF ligands homdimerize and

heterodimerize in order to

activate PDGFRs via receptor

dimerization. The binding

properties of PDGFRs with the

four ligand family members are

still not fully characterized;

however, a few general

conclusions can be made.

Figure 2: PDGF ligand/receptor binding properties. Specifically, PDGFαR is known to bind PDGF-A, PDGF-B, or PDGF-C while PDGFβR binds PDGF-B or PDGF-D. It is not currently clear whether PDGF-C and PDGF-D form heterodimers with other PDGF ligands.

PDGFαR can bind PDGF-A, PDGF-B, or PDGF-C, while PDGFβR is known to bind PDGF-B

or PDGF-D (Figure 2; reviewed in Heldin and Westermark, 1999; Li et al., 2000; Bergsten et al., 2001; Gilbertson et al., 2001).

PDGFRs are members of the receptor tyrosine kinase (RTK) family of receptors that have been shown to activate classical RTK signal transduction pathways including PI3 kinase, MAP kinase, PKC, and PLC-γ (reviewed in Claesson-Welsh, 1996). However, while *in vivo* studies demonstrate the considerable overlap in signal transduction between PDGFαR and PDGFβR they also demonstrate the distinct functions of each receptor (Klinghoffer et al., 2001). Within the oligodendrocyte lineage, PDGFαR and not PDGFβR is expressed; therefore, homodimerization of PDGFαR is the only mechanism by which PDGF signal transduction occurs in OLCs.

PDGF-A is expressed in the CNS by neurons and astrocytes in the CNS (Pringle et al., 1992; Yeh et al., 1993; Maxwell et al., 1998). Elimination of PDGF-A as with that seen in *PDGF-A* knockout mice, has severe developmental implications. *PDGF-A* knockout mice have dramatically decreased numbers of OPs and oligodendrocytes in the developing spinal cord (Fruttiger et al., 1999). *PDGF-A* knockout mice also exhibit severe hypomyelination and die within the first few postnatal weeks. *PDGFαR* knockout mice also have severe developmental abnormalities. The homozygous null *PDGFαR* mutation is also lethal and mice generally die between E14 and E16 (Soriano, 1997). Since development is arrested prior to the wave of oligodendrocyte development, it is difficult to interpret the impact of complete PDGFαR loss on OLCs using *PDGFαR* knockout mice. However, as the current study demonstrates, *PDGFαR*

heterozygotes have a normal lifespan and may be used to study the effects of decreased

PDGFαR expression.

A combination of *in vitro* and *in vivo* studies has demonstrated multiple potential roles

for PDGF in OLC responses. PDGF is well characterized as an OP mitogen *in vitro* as well as *in*

vivo during early development (Richardson et al., 1988, Barres et al., 1993; Calver et al., 1998;

Fruttiger et al., 1999). During CNS development *in vivo*, overexpression of PDGF from neurons

results in a dramatic increase in OP cell number (Calver et al, 1998). This increase in OP cell

number was directly proportional to the amount of PDGF expression indicating that PDGF is the

limiting factor determining OP cell number during development (van Heyningen et al., 2001).

Mice overexpressing PDGF also have a transient overpopulation of oligodendrocytes during

development (Calver et al., 1998). The transient nature of this overpopulation indicates that

PDGF concentration is not the determinant of final oligodendrocyte density.

Additional roles for PDGF have been demonstrated *in vitro*. PDGF acts as a survival

factor for OPs and newly formed oligodendrocytes (Barres et al., 1992) and also acts as a

chemoattractant for OPs *in vitro* (Armstrong et al., 1990). These characteristics are extremely

important if proven to be active *in vivo*. PDGF may potentially act as a survival factor for OPs *in*

vivo as is seen with increased numbers of OPs in the developing spinal cord of mice

overexpressing PDGF from neurons (Calver et al., 1998). If in fact PDGF also acts as a survival

factor and chemoattractant *in vivo*, then PDGF plays a significant role in regulating all of the

major cellular processes of OLCs during development.

FGF2

The FGF family of ligands is a complex group of ligands that currently has 23 members with four high affinity receptors. Expression patterns of the 23 family members and four high affinity receptors differ greatly in timing and in location. FGFRs are members of the RTK receptor family and have been shown to activate signal transduction pathways similar to those activated by other RTKs, including the MAP kinase, PKA, and PKC pathways (Baron et al., 2000). Adding a further layer of complexity to FGF signaling, cell surface heparin and heparan sulfate have been shown to bind FGFs with a lower affinity than FGFRs, but a significantly greater affinity than other sulfated glycosaminoglycans (Shing et al., 1984, Moscatelli et al., 1987; Saksela et al., 1988). The interaction of low affinity and high affinity receptors became evident when removal of cell surface heparan sulfate eliminated the activation of high affinity FGFRs by FGF ligand (Rapraeger et al., 1991; Yayon et al., 1991). In light of this evidence, it appears that binding of FGF ligand to cell surface heparan sulfate induces a conformational change in FGF ligand structure, allowing ligand to interact with high affinity FGFRs.

During early postnatal development, FGFR1-3 are expressed by diverse cell types in the CNS including astrocytes, neurons, and OLCs (Bansal et al., 2003). FGFR expression is crucial for proper development as *FGFR1* knockout mice die between E7 and E10 due to deficits during gastrulation (Deng et al., 1994; Yamaguchi et al., 1994) and *FGFR2* knockout mice mice do not develop due to failure in placenta formation (Xu et al. 1998). *FGFR3* knockout mice survive postnatally and display decreased oligodendrocyte density without altered OP density, proliferation, or OLC survival (Oh et al., 2003). Furthermore, FGFR expression is differentially regulated as cells progress through the oligodendrocyte lineage (Bansal et al., 1996).

Specifically, FGFR1 expression increases with OLC maturation. FGFR2 expression is low in early stages of the lineage and highest in oligodendrocytes. FGFR3 expression peaks at the late oligodendrocyte progenitor stage and declines with further maturation.

Of the FGF ligands expressed in the CNS (FGF1, FGF2, FGF3, FGF5, and FGF9), FGF2 is of direct significance to oligodendrocyte development. FGF2 expression is dramatically increased during the peak of myelination around the second postnatal week in rodents (Kuzis et al., 1995), and thus may play a significant role in regulating developmental myelination. Furthermore, FGFR expression developmentally precedes FGF2 expression. Therefore, FGF2 expression may be the limiting factor with regard to the role of FGF2 during CNS development. *In vitro* studies have demonstrated diverse roles for FGF2 in the oligodendrocyte lineage. FGF2 promotes migration and proliferation of early stage oligodendrocyte lineage cells (McKinnon et al., 1990; Decker et al., 2000; Magy et al., 2003) while inhibiting differentiation at later stages in the lineage (Bansal and Pfeiffer, 1997). Furthermore, treatment of oligodendrocytes with FGF2 *in vitro* induces apoptosis (Muir and Compston, 1996). Determining specific roles for FGF2 *in vivo* has proven difficult since there is potentially considerable redundancy in FGFR activation by various FGF ligands. However, *FGF2* knockout mice display subtle phenotypes such as decreased cortical neuron and glia density (Vaccarino et al., 1999). This decreased glial density can be further characterized by analysis of *FGF2* knockout mice indicating that there was no change in oligodendrocyte density in the normal white matter (Armstrong et al., 2002). *In vivo* FGF2 signaling in the oligodendrocyte lineage during development is complex and may be regulated by differential expression of FGFRs at different stages in the lineage. Furthermore, the

distinct FGFR expression profiles at different stages in the oligodendrocyte lineage may result in distinct effects of FGF2 at those respective lineage stages.

Persistence of OPs in the Adult CNS

As development proceeds into adulthood, the density of OPs gradually decreases but does not disappear. Multipotent stem cells have been identified in the adult parenchyma. These cells are thought to preferentially generate astrocytes or oligodendrocytes, but have been shown to generate neurons as well (reviewed in Goldman, 2003). Immature OLCs also persist in the adult human and rodent CNS and with them the potential for remyelination by endogenous cells (Armstrong et al., 1992, Gensert and Goldman, 1997, Chang et al., 2002; Goldman, 2003). These immature OLCs express the OP marker PDGFαR and respond to administration of PDGF (Wolswijk and Noble, 1992; Shi et al., 1998; Frost et al., 2003). Despite the resemblance to neonatal OPs, adult OPs respond differently to environmental cues. These characteristics in addition to the presence of immature OLCs and premyelinating oligodendrocytes in demyelinated MS lesions (Wolswijk, 2002; Chang et al., 2002) further support the potential for growth factor-based treatment of demyelinating diseases.

Remyelination in the Adult CNS

Animal Models of Demyelination

To study demyelinating diseases, several animal models of demyelination and remyelination have been utilized. Each of these models has its own characteristics that provide

unique opportunities to address specific cellular responses. Some models such as murine

hepatitis virus strain-A59 (MHV-A59), Theiler's murine encephalitis virus (TMEV), and

experimental autoimmune encephalomyelitis (EAE) all incorporate an immune complement to

the disease model similar to that seen in human MS. However, other models such as the

cuprizone neurotoxicant model and lysolecithin injection model are independent of B and T cell

involvement and rely on the cellular toxicity of a copper chelator and detergent respectively.

The MHV-A59 model of CNS demyelination relies on an intracranial injection of the

coronavirus. After virus injection, numerous cell types become infected including

oligodendrocytes, astrocytes, neurons, macrophages, endothelial cells, hepatocytes, and others

(Weiner, 1973; Lavi et al., 1987, Stohlman et al., 1995; Lavi et al., 1999; Navas et al., 2001;

reviewed in Matthews and Paterson, 2002). The first detectable immune response to MHV-A59

infection is the presence of anti-viral IgM antibodies at 6 days post infection (dpi; Stohlman et

al., 1995) with CD8+ and CD4+ T cells peaking at 7 dpi and 9 dpi respectively (Williamson et

al., 1991). The direct mechanism of demyelination is currently unknown. It is not clear whether

MHV-A59 infection results in the activation of autoreactive T cells via epitope spreading or if

the immune response is directed at clearing MHV-A59-infected oligodendrocytes. As a result of

the infection, mice undergo severe weight loss and varying degrees of transient focal

demyelination throughout the spinal cord with corresponding paresis or paralysis (reviewed in

Houtman and Fleming, 1996; Matthews et al., 2002). Interestingly, the severity of the motor

deficit can be judged using a simple "hang-time" behavioral test. This test involves determining

how long a mouse can hang upside down on a standard cage top. Severely affected mice have

significant difficulties supporting their own body weight. As remyelination occurs, severely

affected mice regain this ability and their "hang-time" increases. Affected mice typically undergo spontaneous remyelination and full motor function recovery.

The TMEV model of demyelination is based on infection by the TMEV picornavirus and has several distinguishing features. TMEV infection results in long-term pathology lasting the life of the animal. It is not dependent on viral cytotoxicity, but rather on an autoimmune response resulting from molecular mimicry (reviewed in Dal Canto et al., 1996; Olson et al., 2001). Demyelination in the TMEV model is characterized by clearly demarcated lesions found throughout the spinal cord with corresponding paresis. In contrast to the MHV-A59 model, TMEV-infected mice generally do not recover. Thus, the TMEV model provides an excellent opportunity to study the potential for remyelination in a setting in which autoimmunity is continuously active.

In contrast to viral models, demyelination may also be induced by immunizing rats with myelin components such as MBP, MOG, or galactocerebroside (reviewed in Swanborg, 2001). Alternatively, demyelination may be induced through adoptive transfer of autoreactive T cells specific for myelin component epitopes (Lannes-Vieira et a., 1994). EAE results in paresis or paralysis of one or more limbs. The severity of this motor deficit is typically judged using a clinical scoring system in which a score of 1 represents mild paresis and a score of 4 is the most severe. In terms of mechanism, it is clear that demyelination is induced by a host autoimmune response either by immunization or adoptive transfer. In effect, the mechanism of demyelination is not unlike that seen in the TMEV model. However, the induction of the host autoimmune response through immunization with "self" antigen is clearly unique.

Models such as lysolecithin injection rely on a mechanism of demyelination independent of autoimmunity. In this model, the lysolecithin is stereotactically injected into a white matter tract in the brain or spinal cord. Common areas of injection include the caudal cerebellar peduncle (Woodruff and Franklin, 1999), the corpus callosum (Gensert and Goldman, 1997), and the dorsal column (Larsen et al., 2003). Lysolecithin injection induces significant loss of myelin and oligodendrocytes, astrocytosis, and dystrophy of neurons in the injection site (Woodruff and Franklin, 1999). Demyelination associated with the lysolecithin model is extremely rapid compared to alternative models. Specifically, demyelination occurs within a matter of days and remyelination has begun approximately two weeks after injection (Woodruff and Franklin, 1999). In comparison to other models, the rapidity of demyelination and remyelination using lysolecithin is a unique benefit to the model.

The cuprizone neurotoxicant model of demyelination is independent of B and T cell infiltration, and does not require detergent-mediated cellular toxicity. The direct mechanism of cuprizone action is still unknown; however, it is thought that ingestion of this copper chelator interferes with the extremely high metabolic demands of myelinating oligodendrocytes (reviewed in Matsushima and Morell, 2001). The cuprizone model is highly reproducible with mice undergoing a predictable time course of demyelination with significant remyelination. Furthermore, demyelination is observed in the corpus callosum and superior cerebellar peduncle with high reproducibility of timing and extent of demyelination (Ludwin, 1978). 8-week-old mice undergo near complete demyelination of the corpus callosum over a period of 6 weeks with significant lesion repopulation and remyelination by oligodendrocytes (Hiremath et al., 1998; Armstrong et al., 2002). Cuprizone is administered as a percentage of milled chow weight that is

mixed and fed to the mice ad libitum. The percentage of cuprizone mixed with milled chow

ranges between 0.2% and 0.3% based on mouse strain. Specifically, 0.2% cuprizone

administered to a hybrid Black Swiss/129 Sv:Ev strain will not induce significantly reproducible

demyelination whereas it is sufficient to induce reproducible demyelination in C57Bl/6 mice

(Hiremath et al., 1998; Morell et al., 1998; Armstrong et al., 2002). Interestingly, a

remyelination response can be observed prior to the end of cuprizone treatment (Mason et al.,

2000). It is thought that this response is the result of endogenous OPs proliferating and

differentiating within the demyelinated lesion due to the fact that endogenous OPs are not

eliminated by cuprizone treatment. Supporting this rationale are observations using long-term

administration of cuprizone. Sixteen-week administration of cuprizone results in chronic

demyelination with second attempt at recovery by endogenous cells observed 12 weeks into the

treatment. This second attempt is not as robust as the first, observed after 6 weeks. Depletion of

the endogenous OP pool is predicted to be the cause of this weaker attempt at recovery (Mason

et al., 2001). The typical time course of cuprizone administration and associated pathology is as

follows: 1) decrease in myelin gene expression is observed 2 weeks into cuprizone treatment; 2)

mature oligodendrocyte apoptosis and a coincident decrease in oligodendrocyte density peaks

after 3 weeks; 3) infiltration of microglia/macrophages gradually increases until it peaks after

approximately 5 weeks; 4) OP density also increases in the lesion site after 5 weeks; 5) cuprizone

treatment is halted after 6 weeks at which time myelin gene expression, oligodendrocyte density,

and myelinated fibers all increase (Mason et al., 2000).

Roles of PDGF and FGF2 during Remyelination

The use of animal models of demyelination has demonstrated the potential impact of growth factors on remyelination after experimental demyelination. It is no surprise, as several studies have shown, that manipulation of growth factor concentration in the remyelinating environment has profound effects on the success or failure of remyelination. Several studies have demonstrated that administration of exogenous PDGF or FGF2 can have distinct effects on remyelination *in vivo* (Allamargot et al., 2001; Ruffini et al., 2001). In lysolecithin-induced lesions, remyelination was enhanced when exogenous PDGF was administered (Allamargot et al., 2001). Stereotactic injection of lysolecithin and PDGF into the corpus callosum results in increased OLC proliferation, increased oligodendrocyte density within the lesion, and decreased lesion size. Previous studies have demonstrated the potential for endogenous PDGF to play a significant role in spontaneous remyelination (Redwine and Armtrong, 1998). MHV-A59-mediated lesions have an approximately 15-fold increase in the number of dividing OPs, characterized by expression of PDGFαR and incorporation of BrdU. Furthermore, PDGF-A ligand expression was also significantly elevated in astrocytes in response to demyelination (Redwine and Armstrong, 1998).

Unlike administration of exogenous PDGF, studies in which PDGF-A or PDGFαR expression are eliminated during remyelination have proven difficult until the current study, because both *PDGF-A* and *PDGFαR* homozygous null mutations are lethal during development and do not allow for remyelination experiments. Despite these difficulties, remyelination studies have been completed in an environment in which PDGF is inhibited. The putative PDGF inhibitor trapidil has been used to inhibit PDGF signaling in a lysolecithin injection model of demyelination (McKay et al., 1997; McKay et al., 1998). Despite this inhibition of PDGF

signaling, trapidil is not the ideal method with which to study the effects of PDGF inhibition since it may inhibit signaling through other RTKs. Daily intraperitoneal injections of trapidil over the course of lysolecithin mediated demyelination results in decreased oligodendrocyte density and decreased remyelination of lesions. Furthermore, remyelinated axons typically have thinner myelin sheaths.

Studies in which FGF2 levels were increased above normal levels also show significant effects on remyelination (Ruffini et al., 2001). Intrathecal injection of a replication deficient herpes simplex virus type-1 vector encoding human FGF2 improves the pathology observed in an EAE model of demyelination. These experiments indicate that virally infected cells do in fact express high levels of FGF2 and these cells were commonly in direct contact with cerebrospinal fluid. Furthermore, autoreactive T cell levels were decreased while increases in OP density and myelinating oligodendrocytes were observed (Ruffini et al., 2001).

As with *PDGF-A* and *PDGFαR* knockout mice, *FGFR1*, *FGFR2*, and *FGFR3* knockout mice have complicating factors that make it difficult or impossible to conduct remyelination studies. However, *FGF2* knockout mice are viable and have presented an excellent opportunity to determine the role of FGF2 during remyelination. Furthermore, *FGF2* knockout mice might be preferable to *FGFR* knockout mice since it is not clear what the specific receptor-ligand interactions may be *in vivo*. The MHV-A59 and cuprizone models of demyelination and remyelination have been analyzed in *FGF2* knockout mice with significant effects on OLC populations (Armstrong et al., 2002). Both models of demyelination and remyelination demonstrate similar effects. The absence of FGF2 during remyelination promotes repopulation of demyelinated lesions by oligodendrocytes. This enhanced lesion repopulation does not

coincide with changes in OP proliferation or OLC survival. Furthermore, *in vitro* analysis of

mixed glial cultures from remyelinating spinal cords demonstrates that differentiation of OPs to

mature oligodendrocytes is inhibited by the presence of FGF2.

  While the effects of growth factors such as PDGF and FGF2 on oligodendrocyte

development and remyelination are beginning to be determined through a combination of *in vitro*

and *in vivo* studies, the effect of these growth factors on cellular processes such as proliferation,

migration, differentiation, and survival are not well characterized at the cellular level *in vivo*.

Furthermore, the differences between *in vitro* results and *in vivo* roles must be determined along

with differences between the myelinating and remyelinating environments. The current study

demonstrates the importance of FGF2 during postnatal development and its effects on OLC

responses *in vivo*. Furthermore, *FGF2* knockout mice are used to extend previous analysis of

remyelination and determine the *in vivo* mechanism by which enhanced lesion repopulation

occurs. Additionally, while the role of PDGF during development is well characterized, the role

of PDGF during remyelination is not. Therefore, *PDGFαR* heterozygotes are used to determine

the cellular impact of decreased PDGFαR expression during remyelination.

CHAPTER 2

Fibroblast Growth Factor 2 (FGF2) and FGF Receptor Expression in an Experimental Demyelinating Disease with Extensive Remyelination

Donna J. Messersmith[1,2#], Joshua C. Murtie[3#], Tuan Q. Le[1], Emma E. Frost[1] and Regina C. Armstrong[1,2,3*]

[1] Department of Anatomy and Cell Biology,[2] Program in Neuroscience,[3] Program in Molecular and Cell Biology
Uniformed Services University of the Health Sciences

[#]The first two authors contributed equally to this manuscript.

ABSTRACT

Fibroblast growth factor 2 (FGF2) is an excellent candidate to regulate remyelination based upon its proposed actions in oligodendrocyte lineage cell development in conjunction with its involvement in CNS regeneration. To assess the potential for FGF2 to play a role in remyelination, we examined the expression pattern of FGF2 and FGF receptors (FGFRs) in an experimental demyelinating disease with extensive remyelination. Adult mice were intracranially injected with murine hepatitis virus strain A-59 (MHV-A59) to induce focally demyelinated spinal cord lesions that spontaneously remyelinate, with corresponding recovery of motor function. Using kinetic RT-PCR analysis of spinal cord RNA, we found significantly increased levels of FGF2 mRNA transcripts which peaked during the initial stage of remyelination. Analysis of tissue sections demonstrated that increased levels of FGF2 mRNA and protein were localized within demyelinated regions of white matter, including high FGF2 expression associated with astrocytes.

The expression of corresponding FGF receptors was significantly increased in lesion areas during the initial stage of remyelination. In normal and lesioned white matter, oligodendrocyte lineage cells, including progenitors and mature cells, were found to express multiple FGFR types (FGFR1, FGFR2, and/or FGFR3). In addition, in lesion areas astrocytes expressed FGFR1, FGFR2, and FGFR3. These findings indicate that during remyelination, FGF2 may play a role in directly regulating oligodendrocyte lineage cell responses and may also act through paracrine or autocrine effects on astrocytes, which are known to synthesize other growth factors and immunoregulatory molecules that influence oligodendrocyte lineage cells.

INTRODUCTION

Remyelination involves a recapitulation of developmental events occurring in a pathological environment. FGF2 is likely to be an important regulator of remyelination based upon its proposed actions in oligodendrocyte lineage cell development in conjunction with its association with CNS injury.

FGF2 is expressed in the developing and adult CNS, and its role may be accentuated in pathological states by enhanced expression and activation. In normal CNS tissues FGF2 is synthesized by neurons and astrocytes, and in some areas microglia (Hatten et al., 1988; Woodward et al., 1992; Gonzalez et al., 1995; Redwine et al., 1997). Pathological conditions induce FGF2 synthesis by astrocytes and macrophage/microglia cells (Logan et al., 1992; Mocchetti et al., 1996; Liu et al., 1998). In wound fluids, FGF2 activity may be enhanced by heparanases that degrade the ectodomain of soluble syndecan-1, which then converts from an inhibitor of FGF2 to become a potent activator (Kato et al., 1998). The range of effects of FGF2 in CNS pathology have not been fully elucidated. Improvement in the survival of injured neurons has been demonstrated with FGF2 administration (Grothe and Unsicker, 1992; Teng et al., 1999). *In vitro* data and developmental studies suggest that FGF2 may also influence oligodendrocyte lineage cell responses following CNS demyelination (Wolswijk and Noble, 1995; Armstrong, 2000).

In the CNS, FGF2 can act through 3 high affinity receptors (FGFR1, R2, R3 IIIc isoforms) along with multiple low affinity receptors expressed on a wide variety of neural cell types (Chellaiah et al., 1994; Ornitz et al., 1996). *In vitro*, FGF2 appears to influence every stage of oligodendrocyte development. FGF2 is an important factor for *in vitro* treatment of embryonic

stem cells to generate oligodendrocytes (Ben-Hur et al., 1998; Brustle et al., 1999). FGF2 may

act independently, or in combination with other factors, to induce oligodendrocyte progenitor

(OP) proliferation and migration (McKinnon et al., 1990; Milner et al., 1997; Simpson and

Armstrong, 1999). Differentiation of oligodendrocyte lineage cells is arrested and/or reversed in

the presence of FGF2 (Grinspan et al.,1996; Bansal and Pfeiffer, 1997). Consistent with these *in

vitro* findings, exogenous FGF2 increases the number of promyelinating oligodendrocytes and

retards myelination *in vivo* (Goddard et al., 1999). These diverse effects of FGF2 on

oligodendrocyte lineage cells may reflect the differential expression of FGFRs with cell

maturation (Bansal et al., 1996) and the interplay of FGF2 with other regulatory molecules.

The present study examines the expression of FGF2 ligand and receptor types in a murine

model of transient focal demyelination that is followed by extensive remyelination and recovery

of motor function. We determine the temporal pattern of FGF2 expression relative to the major

stages in this disease progression, and the spatial distribution of FGF2 relative to focal lesions. In

normal and lesioned areas, we characterize expression of FGFR1, FGFR2, and FGFR3 by

specific glial cell types, including oligodendrocyte lineage cells as required for predicting a role

in the extensive remyelination accomplished in this model.

RESULTS

Increased expression of FGF2 peaks during the early remyelination stage of MHV-A59 disease progression.

Kinetic RT-PCR analysis (Figure 1) was used to measure changes in the abundance of

FGF2 mRNA transcripts during the progression of demyelination and subsequent remyelination

in mice intracranially infected with MHV-A59 virus or PBS. Motor function was monitored to demonstrate loss of function and subsequent recovery (Figure 1A), which corresponds histopathologically with the progression of demyelination and remyelination (Redwine and Armstrong, 1998). During the stage of maximal demyelination, affected mice exhibited impaired limb movement [clinical score average of 2.0 at 10 days post injection, dpi; n = 7]. The ability of MHV-A59 infected mice to support their weight while hanging upside down from a wire cagetop was significantly impaired at 10 dpi, in comparison to prior to the MHV injection when they easily performed the task. By 4 wpi, in correlation with histological signs of early remyelination (Redwine and Armstrong, 1998), mice almost completely recovered motor function. FGF2 mRNA transcript levels (Figure 1B) began to increase after the period of maximal motor impairment (10 dpi) and increased to 533% of control values during the early remyelination phase (28 dpi). Subsequent to the initial remyelination phase and associated functional recovery (42 dpi), FGF2 mRNA transcript abundance decreased to 213% of control levels.

Increased expression of FGF2 is localized to focal white matter lesions.

This 4 wpi time point, with associated motor function improvement, defined a reproducible stage of early remyelination for examining the peak expression of FGF2 mRNA transcripts to determine the localization of FGF2 mRNA transcripts in lesioned versus non-lesioned spinal cord tissue (Figure 2A, B). In both PBS (control) and MHV-A59 injected mice at 4 wpi, FGF2 mRNA transcripts were readily detected in the perinuclear cytoplasm of neurons in spinal cord gray matter. Focal areas of demyelinated white matter lesions in MHV-infected spinal cords were identified by loss of myelin, using dark field microscopy (not shown; Redwine and Armstrong, 1998; Armstrong, 2000), as well as by signs of vacuolation, gliosis, and cellular

infiltrates. Lesioned white matter consistently exhibited a high density of cells with intense signal from hybridization with the FGF2 antisense ribonucleotide probe. In comparison, non-lesioned white matter exhibited a relatively low FGF2 signal associated with glial-like cells distributed throughout spinal cord sections. Similar results were obtained with two different antisense FGF2 ribonucleotide probes (not shown). Ribonucleotide probes transcribed as the sense strand were not used as controls for non-specific hybridization since expression of antisense FGF2 mRNA transcripts has been reported (Grothe and Meisinger, 1995). The specificity of the FGF2 antisense hybridization was confirmed by the marked decrease of signal in tissue sections from knockout mice lacking FGF2 mRNA transcripts (Figure 2C).

Immunostaining of similar sections (4 wpi with MHV-A59 or PBS) with an antibody against FGF2 ligand (Figure 2D) demonstrated increased FGF2 immunoreactivity in lesion areas that corresponded with the increased expression of FGF2 mRNA transcripts. Intense FGF2 immunoreactivity was associated with cells that appeared to be large reactive astrocytes in the lesions, and also in astrocyte-like cells in adjacent gray matter. The specificity of the FGF2 immunoreactivity was confirmed by lack of signal after peptide antigen absorption as well as by marked loss of immunostaining using tissue sections from FGF2 null mice (not shown).

Reactive astrocytes exhibit intense FGF2 mRNA signal in lesions.

Although a previous study in a rat model of experimental demyelination reported a lack of FGF2 mRNA expression by astrocytes (Liu et al., 1998), our results indicated FGF2 mRNA transcripts were associated with multiple cell types, including extremely high signal in cells with an astrocytic morphology (Figure 2). Therefore, FGF2 mRNA expression by astrocytes was examined by *in situ* hybridization for FGF2 mRNA followed by immunostaining for GFAP, an

intermediate filament protein used to identify astrocytes (Figure 3). In normal spinal cord

tissue, FGF2 mRNA signal was detected in GFAP immmunolabeled cells mainly in the gray

matter, less frequently in white matter, and also in cells along the central canal (Figure 3A, B).

Sections from MHV-A59 affected mice exhibited increased GFAP immunoreactivity, which was

mildly increased throughout the gray matter and severely increased in focal white matter lesions

(Figure 3C). Intense FGF2 hybridization signal was clearly associated with GFAP

immunolabeled astrocytes within and near the lesions (Figure 3C, black arrows). Small

microglia-like cells also exhibited FGF2 hybridization signal within and near the lesions at 4 wpi

(Figure 3C, white arrows), consistent with the report by Liu et al. (1998) which used several

markers to identify microglia expressing FGF2.

Expression of FGFR types in normal and lesioned spinal cord tissues.

To determine the range of potential cell types within the spinal cord environment that

could potentially be regulated by local FGF2 levels during remyelination, we characterized the

expression pattern of FGFR1, FGFR2, and FGFR3 in normal and lesioned spinal cord tissue

sections using *in situ* hybridization and/or immunodetection.

FGFR1 was expressed in multiple cell types with particularly high levels in neurons,

which were evident by the distinctive morphology and organization within the gray matter

laminae (Figure 4A). Within normal white matter (Figure 4 A, B), FGFR1 was present in

distributed cells of various morphologies, which is consistent with our previous report using cell

type-specific markers to demonstrate that oligodendrocytes, OPs, and astrocytes exhibited

immunolabeling with a monoclonal antibody recognizing mainly FGFR1 (Redwine et al., 1997).

In areas of demyelinated lesions at 4 wpi, there was a significant increase of cells detected with

in situ hybridization for FGFR1 (Figure 4C, E, F) and a corresponding increase in FGFR1

immunostaining intensity (Figure 4D). Similar results were obtained with two different FGFR1

ribonucleotide probes but signal was not present when the sense strand was used as the probe in

parallel *in situ* hybridization reactions (not shown). In lesions, as in normal tissue, FGFR1

appeared to be expressed by cells of multiple glial morphologies, with the most intense

immunoreactivity being apparent in cells with the distinctive morphology of reactive astrocytes

(Figure 4D). We previously reported that OPs exhibit increased density in lesion areas and are

immunolabeled by a monoclonal antibody recognizing mainly FGFR1 (Redwine and Armstrong,

1998). We wanted to more specifically characterize FGFR1 expression by adult OPs due to the

proposed requirement of FGFR1 for neonatal OP migration (Osterhout et al., 1997). We detected

FGFR1 mRNA in many, but not all, bipolar NG2 immunolabeled OPs cultured from spinal cords

at 4 wpi with MHV-A59 (Figure 5 A, B). FGFR1 mRNA was actually more consistently

detected in cells with several processes than in bipolar cells (Figure 5 C, D).

In normal white matter, FGFR2 appeared to be expressed by cells with an

oligodendrocytic morphology and distribution, as previously reported (Asai et al., 1993; Yazaki

et al., 1994; Miyake et al., 1996; Belluardo et al., 1997). We confirmed the oligodendroglial

phenotype of FGFR2 immunolabeled cells by simultaneous *in situ* hybridization detection of

PLP mRNA (Figure 6 A, B). In early remyelinating lesions at 4 wpi, we expected decreased

expression of FGFR2 since the density of mature oligodendrocytes, identified by detectable by

PLP mRNA, is still decreased within lesions (Redwine and Armstrong, 1998). Surprisingly, in

contrast to the lack of FGFR2 immunolabeling by astrocytes in normal white matter, reactive

astrocytes in these lesions exhibited strong FGFR2 immunolabeling (Figure 6 C, D).

The most striking overall difference in expression level of FGFR types between normal and demyelinated white matter was consistently observed for FGFR3 mRNA and protein detection (Figure 7). In normal spinal cord, FGFR3 was detected in neurons of the gray matter and in distributed glial-like cells of the white matter (Figure 7A). Within demyelinated white matter lesions (4 wpi) the density of cells labeled by FGFR3 mRNA was significantly increased (Figure 7 B, F), and the FGFR3 immunoreactivity was correspondingly increased (Figure 7 C, D). Immunolabeling with cell type-specific markers was demonstrated that multiple cell types express FGFR3 mRNA and protein in normal and lesioned white matter (Figure 8). In normal white matter, OPs identified by expression of PDGFαR were double-immunolabeled for FGFR3 (Figure 8A). Mature oligodendrocytes, identified by the CC1 monoclonal antibody, also were double-immunolabeled for FGFR3 (Figure 8 B, C). A subset of white matter astrocytes and microglia, identified by GFAP and by Mac-1 immunoreactivity, respectively, also showed FGFR3 double-immunolabeling in normal tissue (not shown). In each cell type, the subcellular distribution of FGFR3 immunoreactivity was stronger in the nucleus than the cytoplasm in the normal tissue. This subcellular distribution is consistent with previous reports of FGFR3 immunoreactivity (Johnston et al., 1995; Sogos et al., 1998). In the demyelinated lesions (4 wpi), reactive astrocytes exhibited strong nuclear and cytoplasmic FGFR3 immunoreactivity (Figure 8 D), as did many microglia (not shown), consistent with findings in kainic acid lesioned rat brain (Ballabriga et al., 1997). We more specifically examined FGFR3 expression by OPs because, as noted above, the density of OPs in early remyelinating lesions is increased while that of identifiable mature oligodendrocytes is still decreased. In addition, FGFR3 is expressed by neural progenitors during development (Peters et al., 1993), and so might continue to be

expressed by adult progenitors. To clearly identify individual OPs, we cultured cells from

MHV-lesioned spinal cord at 4 wpi. OPs immunolabeled for NG2 consistently exhibited FGFR3

mRNA signal at the bipolar stage as well as after multiple processes were elaborated (Figure 8 E-

H).

DISCUSSION

Mice infected with the MHV-A59 coronavirus exhibit focal areas of transient

demyelination throughout the spinal cord that are subsequently completely remyelinated, with

corresponding recovery of motor function. Using this experimental model, we found that FGF2

ligand mRNA expression is significantly increased during an early stage of remyelination. This

increased FGF2 expression is spatially localized to areas of demyelination, with especially

intense FGF2 mRNA and protein signal associated with reactive astrocytes. We also found that

FGFR expression is significantly increased within lesions during this early stage of

remyelination. With respect to remyelination, FGFR expression by OPs in the adult CNS is of

particular interest since these cells appear to be a source of remyelinating cells in experimental

models (Franklin et al., 1997; Gensert and Goldman, 1997; Carroll et al., 1998; Keirstead, 1998;

Redwine and Armstrong, 1998). We demonstrate FGFR1 and FGFR3 expression by OPs, which

we have previously shown express PDGFαR and exhibit vigorous proliferation during

remyelination in this model (Redwine and Armstrong, 1998). We also show that in normal adult

CNS, mature oligodendrocytes express FGFR3 in addition to previously reported expression of

FGFR1 and/or FGFR2 (Asai et al., 1993; Yazaki et al., 1994; Gonzalez et al., 1995; Miyake et

al., 1996; Belluardo et al., 1997; Redwine et al., 1997; Jiang et al., 1999). The differential

expression of FGFR types by oligodendrocyte lineage cells may provide a mechanism for FGF2 to differentially influence proliferation, migration, differentiation and/or survival as required for oligodendrocyte lineage cells to repopulate lesions and accomplish stable remyelination.

FGF2 expression is subject to both transcriptional and translational control mechanisms (Touriol et al., 1999; Willis, 1999; Ueba et al., 1999), which may be influenced by environmental factors (Gomez-Pinilla and Dao, 1999; Jiang et al., 1999). Although we have not yet identified the molecular signals that trigger the observed upregulation of FGF2, the increased expression of FGF2 in this MHV-A59 model does not appear to reflect a response that is specific to this method of inducing demyelination, or to components specific to this lesion environment. Inflammatory demyelination of experimental autoimmune encephalomyelitis (Liu et al., 1998) as well as toxin-induced demyelination using lysolecithin injection (Hinks and Franklin, 1999) each exhibit increased FGF2 expression. Whether increased expression of FGFRs also occurs in these other demyelinating models has not been addressed.

FGF2 synthesized by cells within and near lesions may be released to act in a paracrine and/or autocrine manner in the remyelination process. Although lacking a signal sequence for secretion, FGF2 can be released from cells via mechanisms that are not yet clear but may involve an ATP-dependent non-ER/golgi pathway and interactions with the 27 KDa heat shock protein (HSP27)(Florkiewcz et al., 1995; Mignatti et al., 1992; Piotrowicz et al., 1997). Our preliminary studies of MHV-A59 lesions demonstrate that reactive astrocytes have increased immunoreactivity for HSP27 (unpublished observation), which may thus facilitate FGF2 secretion through a molecular chaperone mechanism.

A potentially important interaction relative to growth factor regulation of remyelination is that FGF2 increases expression of PDGFαR (McKinnon et al., 1990) and NG2 on neonatal OPs (Nishiyama et al., 1996b). In response to demyelination, increased local expression of FGF2 (present results) might augment OP expression of PDGFαR and NG2. Indeed, our previous studies of MHV-A59 lesions, similarly analyzed during early remyelination at 4 wpi, demonstrated increased local expression of PDGFαR and NG2 as well as a dramatic increase of proliferating OPs detected by *in vivo* incorporation of bromodeoxyuridine (Redwine and Armstrong, 1998). In these lesioned tissues, PDGF ligand was upregulated (Redwine and Armstrong, 1998) but was not as markedly increased or as distinctly localized to the lesions as has been found in the present analysis of FGF2. PDGF and FGF2 acting in combination induce OPs from neonatal CNS to grow as a self-renewing line and induce OPs from adult CNS to display proliferative, migratory, and morphological characteristics similar to neonatal cells (Bogler et al., 1990; Wolswijk and Noble, 1992; Engel and Wolswijk, 1996). Thus, in response to demyelination, local increases of FGF2 might also play a role in remyelination by enhancing OP responses to PDGF.

Our results indicate that oligodendrocyte lineage cells in normal and lesioned white matter express a repertoire of FGFRs. FGFR expression can be modulated by CNTF and FGF2 (Bansal et al., 1996; Bansal and Pfeiffer, 1997; Jiang et al., 1999), and therefore may be regulated by these and other cytokines and growth factors in the lesion environment. The functional results of FGF2 exposure can be diverse, and may depend upon the FGFR types expressed in conjunction with differential activation of intracellular signalling pathways within a given cell (Vaccarino et al., 1999). In studies of normal CNS tissues, FGFR1 is expressed at

relatively high levels by neurons (Asai et al., 1993; Yazaki et al., 1994; Gonzalez et al., 1995; Belluardo et al., 1997). In contrast, FGFR2 expression is not detected in neurons but has been well characterized as being expressed in mature oligodendrocytes (Asai et al., 1993; Belluardo et al., 1997; Bansal et al., 1996). However, oligodendrocytes and/or OPs have also been reported to express FGFR1 (Gonzalez et al., 1995; Bansal et al., 1996; Redwine et al., 1997; Jiang et al., 1999). FGFR1 has been proposed to play a role in migration of neonatal OPs (Osterhout et al., 1997) and may modulate myelination by mature oligodendrocytes (Harari et al., 1997). Our findings from remyelinating tissue support the possibility of a role for FGFR1 in some OPs, at a bipolar and thus potentially migratory stage, as well as in more differentiated cells.

FGFR3 is most abundantly expressed in germinal epithelium during CNS development, and then detected in distributed glial-like cells in the adult (Peters et al., 1993; Yazaki et al., 1994). Differences in the sensitivity of detection methods may explain why oligodendrocyte lineage cells and astrocytes were identified as expressing FGFR3 in our work while a previous study reported that only astrocytes express FGFR3 in adult rat brain (Miyake et al., 1993). *In vitro* analysis has demonstrated that the IIIc variant of FGFR3 is associated with a late oligodendrocyte precursor stage as neonatal OPs differentiate (Bansal et al., 1996). The FGFR3 splice variant IIIc can be activated by several FGF family members, including FGF2, while the IIIb isoform is preferentially activated by FGF1 (Ornitz et al., 1996). In addition, the IIIc form is present in brain, while FGFR3 IIIb is not detected (Chellaiah et al., 1994), supporting the potential for FGF2 to serve as a relevant ligand for the FGFR3 we observed *in situ*.

The effects of FGF2 in lesions may be extended by the potential to modulate astrocytic responses since astrocytes express multiple FGFR types (Gonzalez et al., 1995; Bansal et al.,

1996; Ballabriga et al., 1997; Redwine et al., 1997; present results). In response to demyelination astrocytes produce growth factors that may regulate oligodendrocyte lineage cells, such as FGF2, insulin-like growth factor-I, and PDGF-A (Komoly et al., 1992; Redwine and Armstrong, 1998; present results). Thus, FGF2 might directly and/or indirectly contribute to oligodendrocyte lineage cell responses during remyelination.

The present findings demonstrate that the appropriate combinations of ligand and receptor expression patterns are present in remyelinating lesions for hypothesizing that FGF2 could serve a potential regulatory role in the oligodendrocyte lineage response during remyelination. Attempts to use FGF2 null mice to determine the *in vivo* role of FGF2 in this remyelination model have not been possible due to morbidity of the MHV-A59 virus in this strain of mice (unpublished observation). Further analyses will be required to reveal positive, or possibly even negative, regulatory effects that may be mediated by FGF2, presumably interacting with specific FGFR splice variants and acting in combination with other factors. Detailed understanding of the cellular and molecular events that bring about successful remyelination in such model systems should facilitate the development of therapies for manipulating the cell populations and/or the lesion environment to promote repair in human demyelinating conditions, such as multiple sclerosis.

MATERIALS AND METHODS

MHV-A59 Injection and Preparation of Mouse Spinal Cord Tissue

As previously described (Redwine and Armstrong, 1998), MHV-A59 stock was injected intracranially into 28 day old C57Bl/6 female mice (Charles River, Wilmington, MA) to produce

focal areas of demyelination throughout the rostrocaudal extent of the spinal cord. Throughout

the disease progression, motor impairment and recovery was quantified by recording the period

of time mice were able to hang upside down supporting their weight by gripping the metal

cagetop bars (Redwine and Armstrong, 1998). Additionally, a clinical score was assigned as

follows: 0 for no paralysis; 1-5 indicates paresis/paralysis in one to five appendages; 6 indicates

morbidity (Redwine and Armstrong, 1998).

Kinetic Reverse Transcriptase-Polymerase Chain Reaction (RT-PCR) for RNA Quantitation

RNA was isolated from individual spinal cords using TRIZOL Reagent (Life

Technologies, Gaithersburg, MD). The RT reaction was carried out separately from 2 μg total

RNA from each mouse using random hexamer primers. According to the methods detailed for

the ABI PRISM 7700 "TaqMan" System (PE Applied Biosystems; Foster City, CA), mouse

FGF2 primers (forward primer CCCACCAGGCCACTTCAA from nucleotide 60; reverse

primer TCTCTCTTCTGCTTGGAGTTGTAGTT from nucleotide 204) were designed to flank

an intervening FGF2 probe (CCCAAGCGGCTCTACTGCAAGAACG from nucleotide 82) that

was labeled with a fluorochrome (6-FAM) on the 5' end as well as a fluorescence quencher

(TAMRA) on the 3' end. The total RNA values and RT reaction efficiency was normalized by

measuring 18s rRNA for each sample in parallel.

Immunofluorescence Detection of FGF2 and FGFRs

The anti-FGF2 rabbit polyclonal antiserum (Santa Cruz Biotechnology; Santa Cruz, CA)

was shown by western blotting and immunohistochemistry to recognize mouse FGF2. The rabbit

polyclonal anti-FGFR antisera used were raised against peptide sequences designed to differentially detect FGFR1 (Sigma), FGFR2 (Santa Cruz Biotechnology), and FGFR3 (Santa Cruz Biotechnology), and previously characterized (Johnston et al., 1995; Pirvola et al., 1995; Ballabriga et al., 1997; Del Rio-Tsonis et al., 1997; Rao et al., 1998; Sogos et al., 1998; Cohen and Chandross, 2000).

Mice were perfused with 4% paraformaldehyde and the spinal cords were processed as in Redwine and Armstrong, 1998. Fifteen μm thick transverse cryostat sections were permeabilized with 10% Triton X-100 in PBS for 10 min and non-specific binding sites were blocked by a 30 min incubation in a solution of 25% normal goat serum, 0.4% Triton X-100, 1% bovine serum albumin, and 100 mM L-lysine. Sections were incubated overnight at 4°C with anti-FGFR or anti-FGF2 rabbit polyclonal antibodies (100 μg/ml stock diluted 1:500) which was subsequently detected with a donkey anti-rabbit IgG antibody conjugated with Cy3. The specificity of the primary antisera (anti-FGF2, -FGFR2, -FGFR3) immunodetection was demonstrated by pre-incubation with a 100x excess of the corresponding peptide antigen overnight at 4°C, which abolished subsequent immunoreactivity.

Immunofluorescence with Glial Cell Type-Specific Markers

Two color indirect immunofluorescence was used to detect FGFR immunoreactivity associated with distinct glial cell types, identified by immunoreactivity for cell type-specific marker antigens. Platelet-derived growth factor α receptor (PDGFαR) or NG2 chondroitin sulfate proteoglycan (see below) were used to identify OPs in adult rodent CNS (Nishiyama et al., 1996a, 1997; Reynolds and Hardy, 1997; Trapp et al., 1997; Redwine and Armstrong, 1998; Nishiyama et al., 1999). To double immunolabel with the rabbit polyclonal anti-FGFR, PDGFαR

was recognized with a rat monoclonal (APA5; Pharmingen; San Diego, CA) and detected with biotinylated anti-rat IgG followed by tyramide amplification (Renaissance indirect blue kit; New England Nuclear; Boston, MA) to deposit AMCA (blue fluorescence). Mature oligodendrocytes expressing FGFRs were identified by immunolabeling for CC1, or by *in situ* hybridization for proteolipid protein (PLP)(see below). CC1 monoclonal antibody immunostains the cell body of mature oligodendrocytes without labeling the myelin, which facilitates cell identification (Fuss et al., 2000). The CC1 antibody (100 µg/ml; Oncogene Research Products; Cambridge, MA) was used at 1:20 dilution, which using our conditions did not double immunolabel with an astrocyte marker, glial fibrillary acidic protein (GFAP) or with NG2 (unpublished observations). Double immunolabeling to detect FGFRs in astrocytes utilized a mouse monoclonal IgG1 anti-GFAP antibody (Boehringer Mannheim). Microglia were identified with anti-Mac-1 rat monoclonal IgG2b (Boehringer Mannheim) detected using tyramide deposition of AMCA (see above).

All secondary antibodies were affinity-purified F(ab')$_2$ fragments with minimal cross-reactivity to serum proteins from the other species used in each protocol (Jackson Immunoresearch; West Grove, PA). For single and multi-label immunostaining protocols, the sets of primary and secondary antibodies were tested for potential cross-reactivity by omitting each primary antibody from the protocol.

In Situ Hybridization

In situ hybridization and preparation of digoxigenin-labeled riboprobes was performed as previously detailed (Redwine and Armstrong, 1998), with minor modifications to adjust the hybridization temperature and washes for each probe sequence. Digoxigenin was detected with an alkaline phosphatase-conjugated sheep anti-digoxigenin (Fab fragment; Boehringer

Mannheim) antibody followed by reaction with NBT/BCIP substrate (DAKO, Carpinteria,

CA), dehydration in progressive ethanol solutions, and mounting with Permount (Fisher; Fair

Lawn, NJ).

The digoxigenin-labeled ribonucleotide probes used to detect FGF2 transcripts were

prepared from cDNA templates complementary to a 477 bp fragment of the rat FGF2 mRNA

(Shimasaki et al., 1988; Dr. Andrew Baird, Ciblex Corporation, San Diego, CA) or a 475 bp

ribonucleotide probe to the mouse FGF2 mRNA (nucleotides 1-475; Dr. Gail Martin, University

of California at San Francisco; Hebert et al., 1990). The FGFR1 ribonucleotide probe (Dr. Alka

Mansukhani, New York University School of Medicine) contained 1.2 kb of the 5' end of the

murine *flg* receptor (nucleotides 1-1177). Similar results were also observed using a smaller

probe which hybridized to nucleotides 843-1170 of the mouse FGFR1 sequence (Dr. David

Ornitz; Washington University Medical School, St. Louis). The FGFR3 ribonucleotide probe

(Dr. David Ornitz) hybridizes to nucleotides 1233-1663 of the mouse sequence, which should

detect each of the differentially spliced FGFR3 isoforms (Chellaiah et al., 1994; Johnston et al.,

1995; Ornitz et al., 1996). These cDNA probes have been shown to be specific for each of the

FGFR types based upon detection of appropriate size bands and differential expression on

Northern blots of neonatal rat oligodendrocyte lineage cells (Bansal et al., 1996). The cDNA

template for the proteolipid protein (PLP) ribonucleotide probe (Dr. Lynn Hudson, National

Institutes of Health) is complementary to a 980 bp fragment of mouse PLP mRNA (Hudson et

al., 1987).

In Situ Hybridization Combined with Immunostaining

The *in situ* hybridization reaction was carried out, as described above, followed by immunostaining. However, since the NBT/BCIP precipitate can impair distinction of the immunostaining reaction, adjustments to the protocols were chosen based upon the optimal combination of detection methods required by the subcellular localization and relative intensity of each signal. The immunoreactivity for GFAP was detected as a brown DAB precipitate, using the ABC Elite kit (Vector Labs), which could be distinguished from the blue/purple NBT/BCIP hybridization reaction. PLP mRNA was detected with a Cy3-conjugated anti-digoxin mouse monoclonal (Jackson Immunoresearch) that recognizes digoxigenin and the anti-FGFR2 was detected with a FITC-conjugated anti-rabbit secondary antibody.

Preparation and Immunostaining of Glial Cell Cultures from Remyelinating Spinal Cord

Since the OPs have small cell bodies with very little cytoplasm, cell cultures were prepared to more readily detect NG2 immunofluorescence along the cell membrane of the soma and processes relative to the NBT/BCIP reaction in the cytoplasm. Mice infected with MHV-A59 were sacrificed at 4 weeks post injection (wpi) and glial cell cultures were prepared from the spinal cords, as previously detailed (Armstrong et al., 1990). For each glial cell isolation spinal cords were combined from 6 severely affected mice, as determined from the hang time assay of motor function. Cells were grown in DMEM supplemented with 10% FBS (Life Technologies). After 2 days *in vitro*, cells were fixed with 4% paraformaldehyde and processed for *in situ* hybridization, as detailed above with the omission of the proteinase K digestion. After incubation in NBT/BCIP, OPs were

identified by immunostaining with anti-NG2 rabbit polyclonal antisera (kindly provided by Dr. Joel Levine, Stony Brook, NY and by Dr. William Stallcup, La Jolla, CA) detected with Cy3-conjugated anti-rabbit secondary antibody.

FGF2 Null Mice

FGF2 knockout mice (generously provided by Dr. Doetschman, University of Cincinnati; Zhou et al., 1998) were used as controls for testing the specificity of the *in situ* hybridization detection of FGF2 mRNA transcripts and of the immunofluorescence detection of FGF2 protein. These mice do not have detectable FGF2 wild-type messages or transcripts containing exon 2 and 3 sequences (Zhou et al., 1998).

Imaging and Documentation

Immunostaining and *in situ* hybridization results were captured with either 400 ASA Ektachrome color film or a Spot 2 digital camera (Diagnostic Instuments, Sterling Heights, MI) using single channels filter sets for Cy3, FITC, and AMCA or a triple-band pass filter (Chroma Technologies, Brattleboro, VT) to simultaneously view multiple channels. At least 3 different MHV affected mice and 3 different PBS injected mice were examined for each result presented, and exhibited similar results to the representative areas shown.

Unbiased Stereology Analysis

Expression of FGFR1 or FGFR3 mRNA was quantitated using the optical "disector" method of morphometric analysis (Long et al., 1998; Bjugn, 1993; Bjugn and Gundersen, 1993). The cell density was estimated using the Stereologer System (Systems Planning & Analysis Inc, Alexandria, VA). Analysis was performed on lumbar spinal cord sections within ventrolateral white matter lesions from MHV-injected mice and

within corresponding ventrolateral white matter areas of matched PBS-injected control spinal cords, prepared on the same slide. Sections from 3 MHV-injected and 3 PBS-injected mice were analyzed for each nucleotide riboprobe. Optical "disectors" composed of mainly vacuolar spaces within lesions were not included in the analysis.

ACKNOWLEDGEMENTS
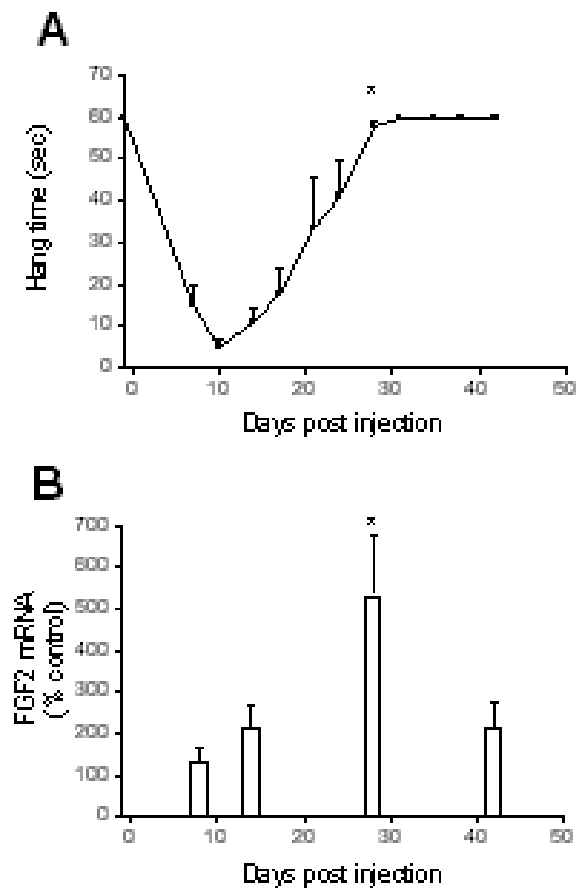
Figure 1

FIGURE 1. *FGF2 mRNA peak expression corresponds with recovery of motor function.* **A**:Mice intracranially injected with MHV-A59 or PBS were tested for limb motor impairment (hang time) and sacrificed for RNA isolation from spinal cords. Analysis was carried out in parallel for MHV-injected and age-matched PBS-injected (control) mice at various days post injection (dpi) throughout the progression of demyelination and remyelination. Limb motor impairment was scored by the time that mice could support their weight by grasping the bars of a cage top. Hang time scores indicate significant motor function impairment at 7 through 21 dpi, with maximal impairment at 10 dpi (p <0.001 for 7, 10, 14, 21 dpi each; compared to pre-injection baseline values in which each mouse recorded a maximal time of 60 sec for this assay; ANOVA with Tukey's post-hoc analysis) with almost complete recovery at 28 dpi (* = p <0.001 for 28 dpi vs 10 dpi; ANOVA with Tukey's post-hoc analysis). **B:** FGF2 mRNA transcript abundance was determined in these behaviorally tested mice by kinetic RT-PCR analysis using the ABI PRISM 7700 "Taqman" System. FGF2 mRNA values were normalized to 18s rRNA values for the cDNA sample generated from the same RT reaction. FGF2 mRNA transcript levels for MHV affected mice were 533% higher than PBS control values at the 28 dpi stage when motor function recovery was almost complete. FGF2 mRNA values from MHV affected mice were significantly elevated at this 28 dpi stage of the disease progression (p <0.05 for 28 dpi vs 8 dpi; ANOVA with Tukey's post-hoc comparison). The same mice were used in the behavioural tests and the RNA isolation (8 dpi, N = 4 MHV and 3 PBS; 14, 28 and 42 dpi, N = 3 MHV and 3 PBS for each dpi). Hang time scores shown are combined for all mice so that values for a given dpi include the mice sacrificed on that dpi as well as mice that were sacrificed for RNA isolation at any later dpi. Error bars indicate standard error of the mean.
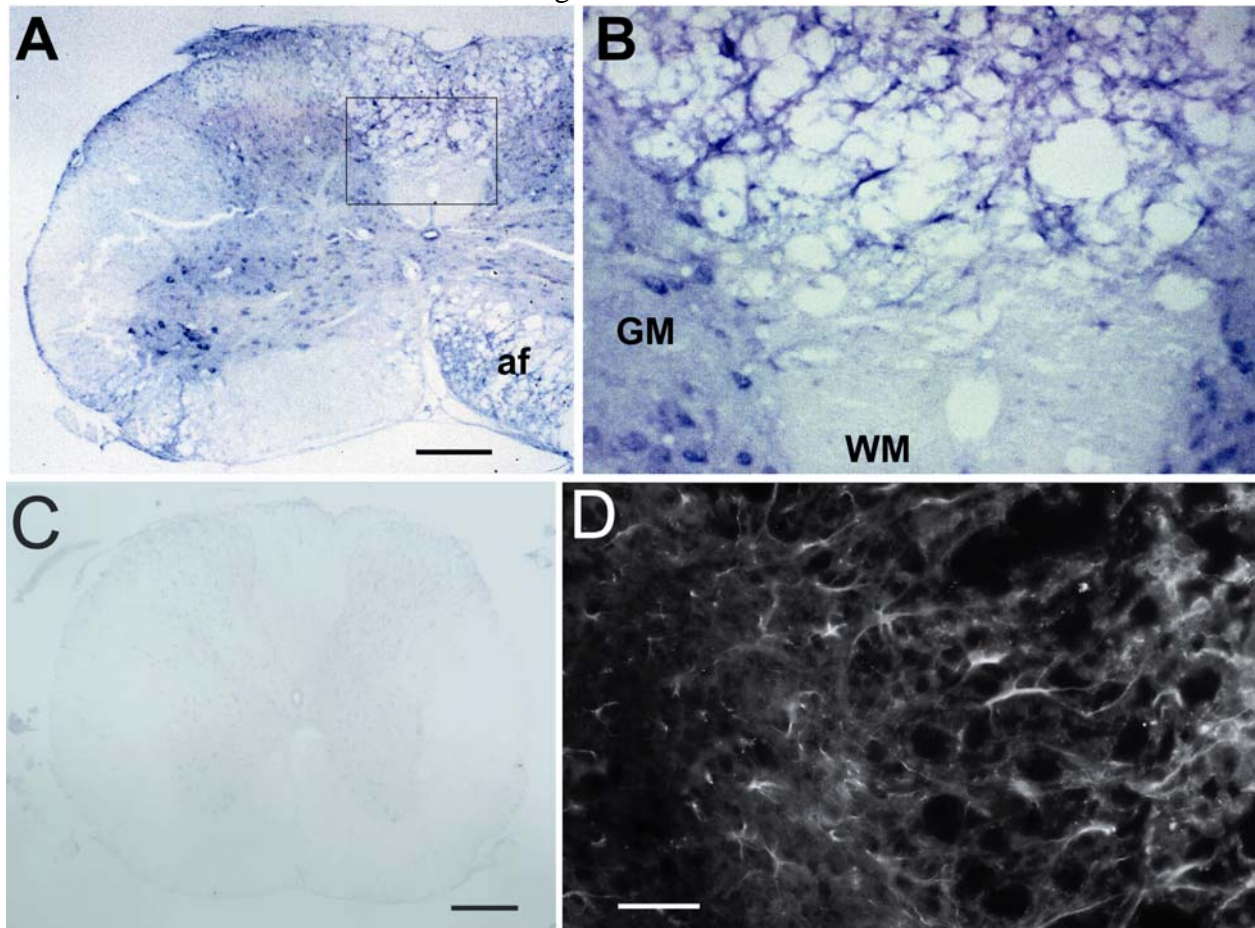
Figure 2

FIGURE 2. *Increased expression of FGF2 mRNA and protein is localized to white matter lesion areas*.
In situ hybridization for FGF2 mRNA transcripts (A, B, C) and immunofluorescence for FGF2 protein (D).
A: In spinal cord sections from lesioned mice (MHV, 4 wpi), FGF2 mRNA signal is evident in neurons (as
in controls, not shown) and is strong in lesioned white matter areas. **B**: Higher magnification (dorsal
column region from box in A) shows signal in the cell body and processes of astrocyte-like cells that is
clearly increased in the vacuolated lesion area (upper dorsal column area) relative to the normal-appearing
white matter (lower dorsal column area). **C**: Similar FGF2 mRNA signal was not found in sections of
FGF2 null mice (no injections), demonstating the specificity of the FGF2 mRNA detection. **D**: In sections
of lesioned white matter, FGF2 immunoreactivity was most evident in cells with an astrocytic morphology,
similar to the findings with FGF2 mRNA detection. A, C scale bars = 200 μm. D scale bar = 50 μm.
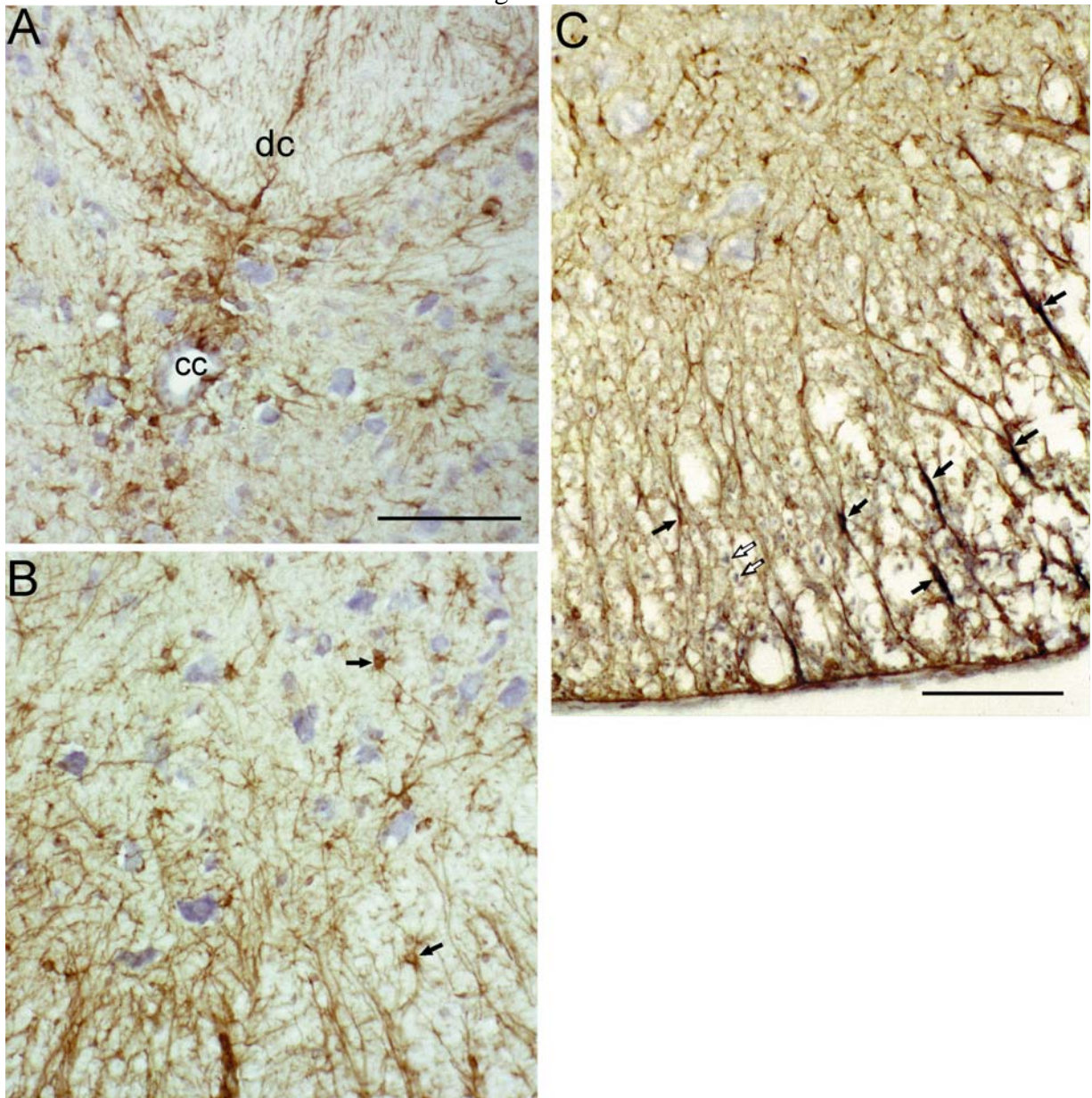
Figure 3

FIGURE 3. *Reactive astrocytes exhibit high levels of FGF2 mRNA transcripts.* *In situ* hybridization for FGF2 (blue, NBT/BCIP reaction) combined with immunostaining for GFAP (brown, DAB reaction) to identify astrocytes. **A, B**: In control sections of spinal cord (PBS, 4 wpi), the FGF2 mRNA transcripts are most abundant in neurons throughout the gray matter (A shows adjacent to central canal (cc) and dorsal column (dc), B shows ventral horn). FGF2 mRNA is also detected in cells around the central canal and in astrocytes of the gray matter and white matter (examples at arrows in B). **C**: In sections of lesioned spinal cord (MHV, 4 wpi), the overall immunoreactivity for GFAP (brown) is increased and very intense within the vacuolated lesion area, consistent with gliosis. The FGF2 mRNA signal is extremely intense within astrocytes in the lesions (black arrows) and appears as almost black, due to the NBT/BCIP dark blue combining with the brown anti-GFAP reaction. In the lesioned tissue the NBT/BCIP reaction had to be weaker in the neurons (large cells in C compared to B) to allow detection of GFAP in astrocytes with intense NBT/BCIP. Scale bars (A, C) = 100 μm. B same magnification as A.

Figure 4
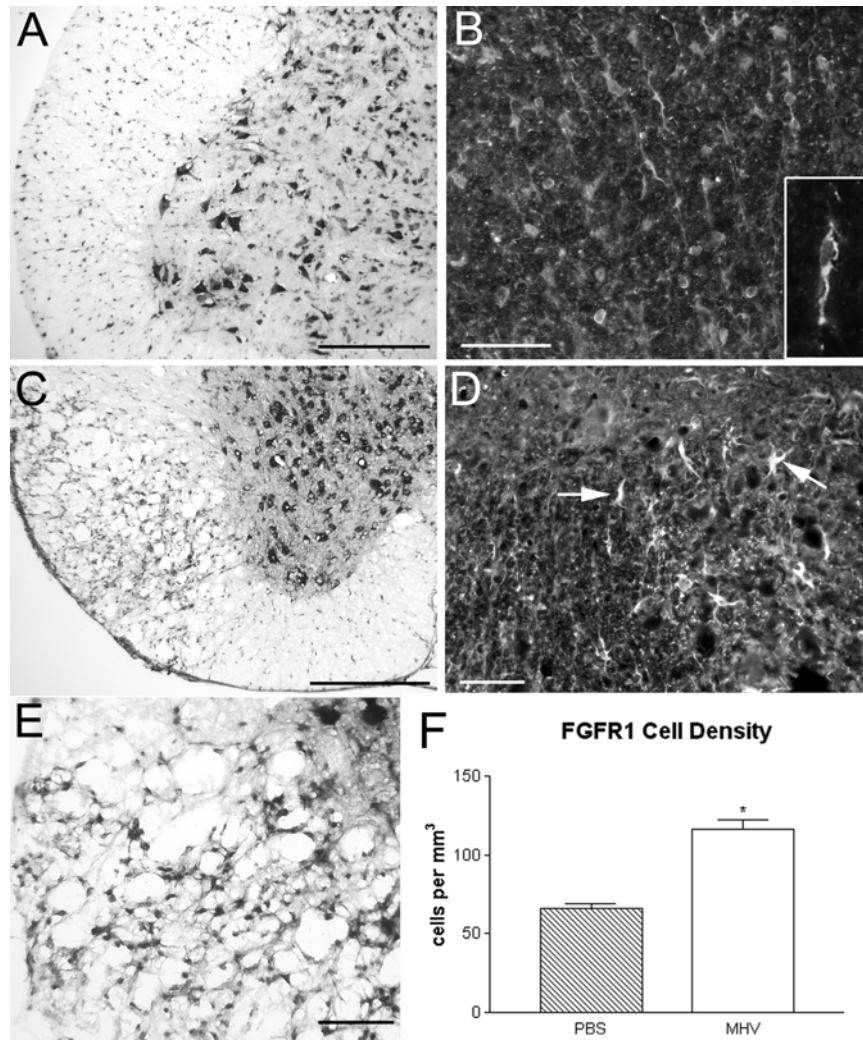
FIGURE 4. *Increased expression of FGFR1 is localized to white matter lesions*. *In situ* hybridization for FGFR1 mRNA (A, C, E) and immunostaining for FGFR1 protein (B, D). **A**: In sections from normal spinal cord (PBS, 4 wpi) FGFR1 mRNA is most abundant in gray matter cells with a neuronal morphology, and is also detected in distributed white matter cells. **B**: Immunofluorescence of FGFR1 protein in normal spinal cord (PBS, 4 wpi) showing expression in cells of multiple glial morphologies, including an apparently bipolar cell (enlarged as inset). **C**: In sections from lesioned spinal cord (MHV, 4 wpi) FGFR1 mRNA is more abundant in the vacuolated lesioned white matter (lateral funiculus) than in normal appearing white matter (ventral funiculus). **D**: A similar increase of FGFR1 immunofluorescence is evident in lesioned (right side of field) relative to non-lesioned white matter (left side of field) in sections from mice 4 wpi with MHV. Signal is most intense in cells with a reactive astrocyte morphology (arrows). **E**: Higher magnification of FGFR1 mRNA in lesioned white matter shows a high density of labeled cells. **F**: Numerical density of cells expressing FGFR1 mRNA in ventrolateral spinal cord white matter in sections from mice injected with MHV-A59 (white bar) or PBS-injected control (hatched bar). Numerical density of cells in lesioned white matter that are expressing FGFR1 mRNA is significantly increased over a similar region of control white matter from matched PBS-injected mice (N = 3 MHV mice and 3 PBS mice; *p = 0.002, ANOVA). All stereological analyses represented here had a coefficient of error (CE) of 0.12 or less. Error bars show standard error of the mean. A, C scale bars = 100 μm. B, D, E scale bars = 50 μm.
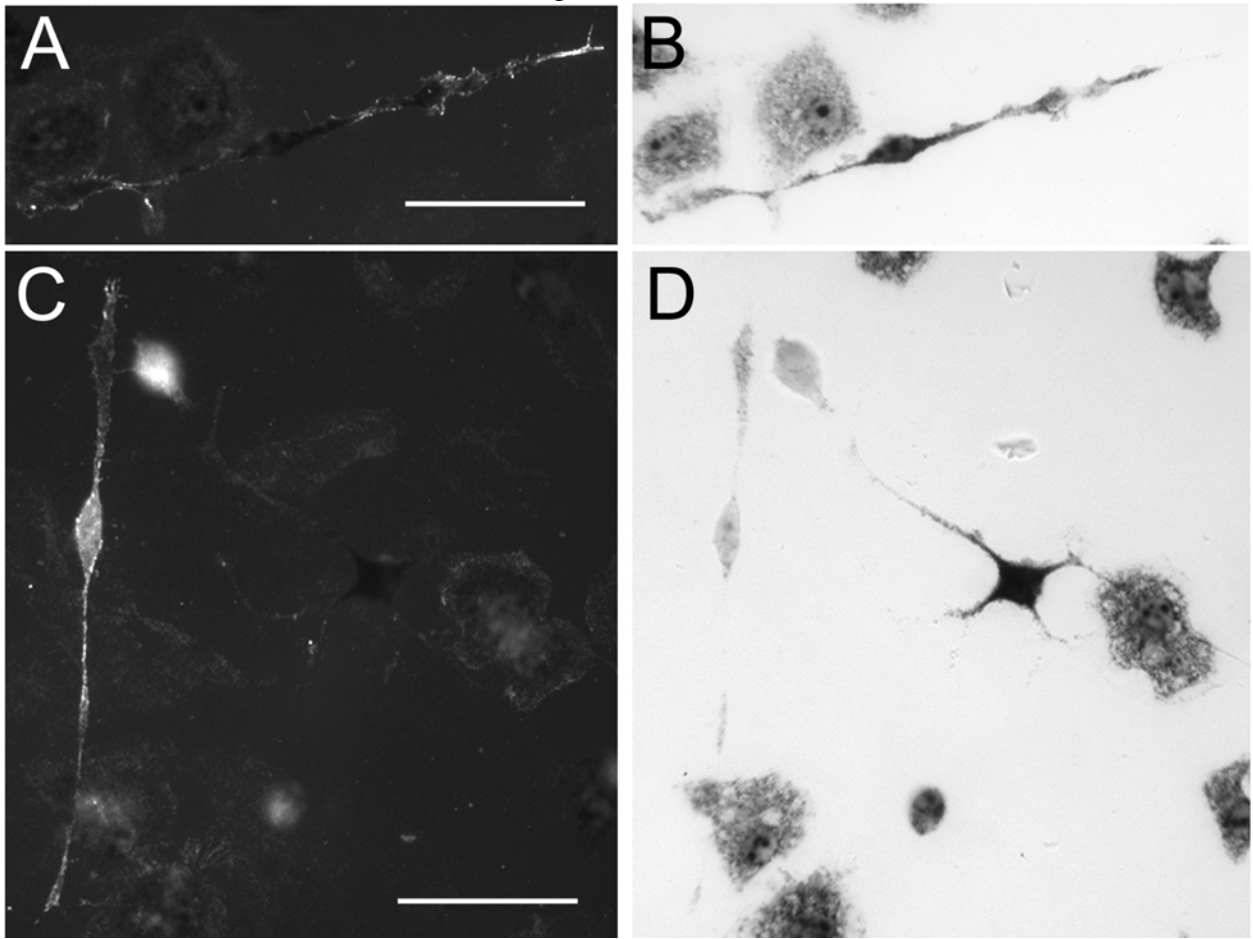
Figure 5

FIGURE 5. *FGFR1 mRNA expression in oligodendrocyte lineage cells cultured from lesioned spinal cords.* Cells isolated from MHV lesioned mice at 4 wpi, grown in culture for 2 days to allow process extension, and then labeled with anti-NG2, detected with immunofluorescence (A, C), and *in situ* hybridization for FGFR1 mRNA detection with NBT/BCIP substrate (B, D). **A, B**: A bipolar oligodendrocyte progenitor cell with cell surface immunofluorescence for NG2 (A) evident in the processes and strong FGFR1 mRNA signal (B) in the cytoplasm, which blocks imaging of the majority of NG2 epifluorescence. **C, D**: A bipolar oligodendrocyte cell with cell surface immunofluorescence for NG2 (C, left side) does not have FGFR1 mRNA signal (D). An adjacent multipolar cell has strong FGFR1 mRNA signal (D). The ameboid cells are microglia, which are abundant in cultures of lesioned spinal cord (Armstrong et al., 1990a). Microglia exhibited variable levels of FGFR1 mRNA transcripts but were never as intensely labeled as were the oligodendrocyte lineage cells. Scale bars = 50 μm.
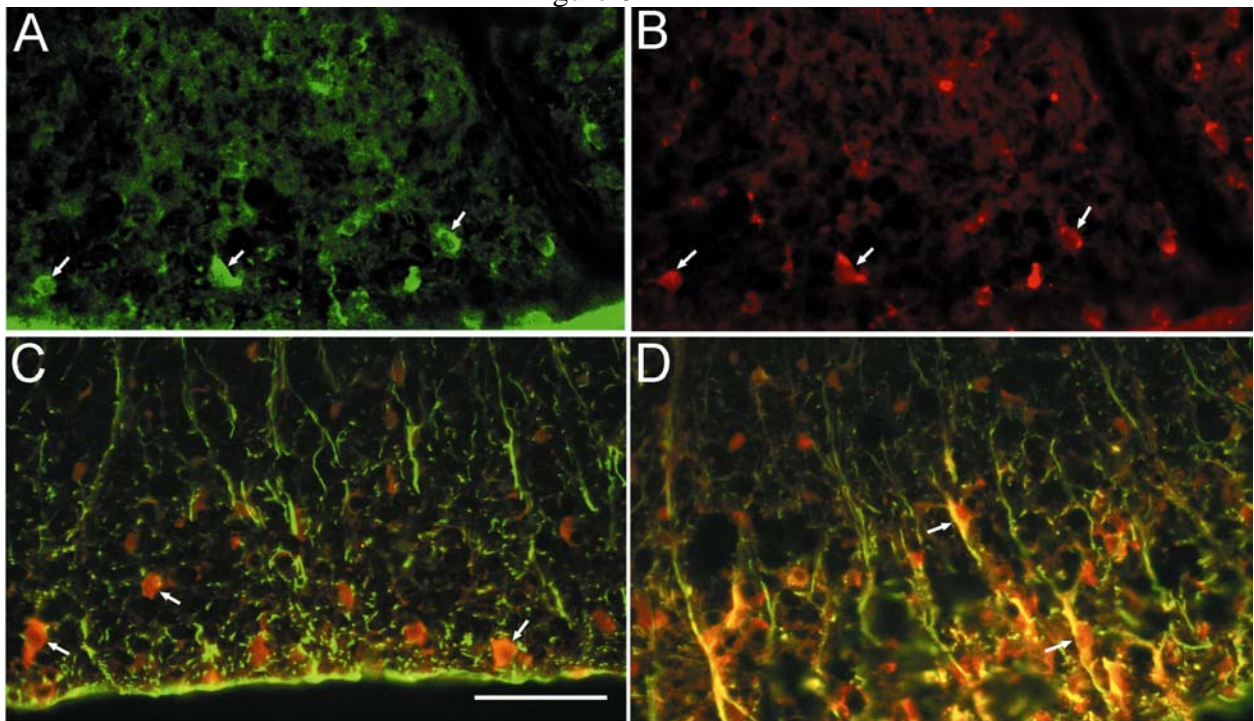
Figure 6

FIGURE 6. *Cell type-specific expression of FGFR2 is altered in lesioned white matter*.
Immunofluorescence detection of FGFR2 (A, C, D) with cell type-specific markers using PLP mRNA
detection for oligodendrocytes (B) or double immunofluorescence with anti-GFAP for astrocytes (C, D). **A,
B**: In normal spinal cord white matter (PBS, 4 wpi), FGFR2 immunofluorescence was present (green in A)
in the same cells that exhibited PLP mRNA (red in B)(arrows indicate examples of double labeled
oligodendrocytes). **C**: In normal spinal cord white matter (PBS, 4 wpi), astrocytes labeled with anti-GFAP
(green) are not double immunolabeled for FGFR2 (red). **D**: In lesioned white matter (MHV, 4 wpi), anti-
GFAP immunoreactivity (green) increases consistent with gliosis and FGFR2 immunoreactivity (red) is
now found in cells that include astrocytes (double immunolabeled cells appear yellow). Scale bar in C = 50
μm.
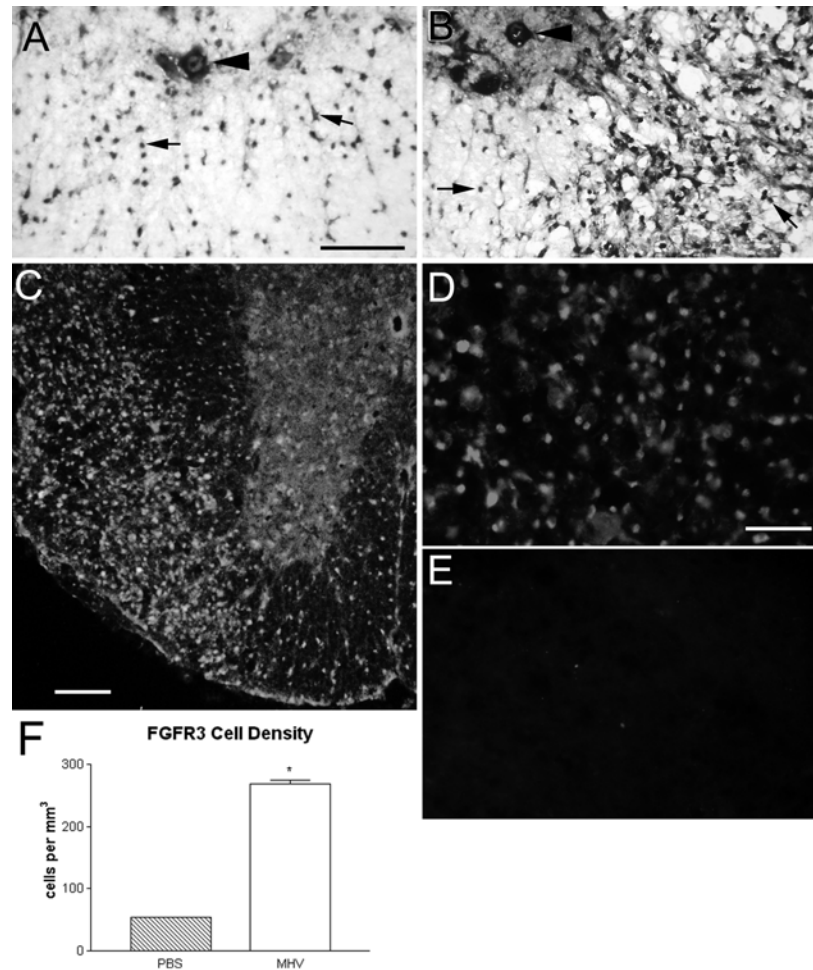
Figure 7

FIGURE 7. *Increased density of FGFR3 expressing cells in areas of white matter lesions*. *In situ* hybridization for FGFR3 mRNA (A, B) and immunostaining for FGFR3 protein (C, D). **A**: In sections from normal spinal cord (PBS, 4 wpi) FGFR3 mRNA is detected in gray matter neurons (large cells, arrowhead) and in distributed small glial-like cells of the gray matter and white matter (arrows). **B**: In sections of lesioned spinal cord (MHV, 4 wpi) FGFR3 mRNA is expressed in both large neuronal cells (arrowhead) and small glial-like cells (arrows), with a marked increase in the density of labeled cells in the lesioned area of white matter (lesion associated with vacuolation, right side of field) relative to the non-lesioned white matter (left side, ventral to gray matter). **C**: A similar increase in the density of cells expressing FGFR3 within lesions is detected by immunofluorescence analysis of sections from lesioned spinal cord (MHV, 4 wpi). **D**: Higher magnification of FGFR3 immunofluorescence within a lesioned area of white matter shows variable intensities of nuclear and cytoplasmic signal. **E**: In sections prepared as in (D) the immunoreactivity is abolished by incubation of the anti-FGFR3 antisera with the peptide antigen prior to immunostaining. F: Numerical density of cells expressing FGFR3 mRNA in spinal cord sections of mice injected with MHV-A59 (white bar) or PBS-injected control (hatched bar). Numerical density of cells in lesioned white matter that are expressing FGFR3 mRNA is significantly increased over a similar region of control white matter from matched PBS-injected mice (N = 3 MHV mice and 3 PBS mice; *p = < 0.001, ANOVA). All stereological analyses represented here had a coefficient of error (CE) of 0.12 or lower. Error bars show standard error of the mean. A, B scale bar in A = 100 μm. C scale bar = 100 μm. D, E scale bar in D = 50 μm.
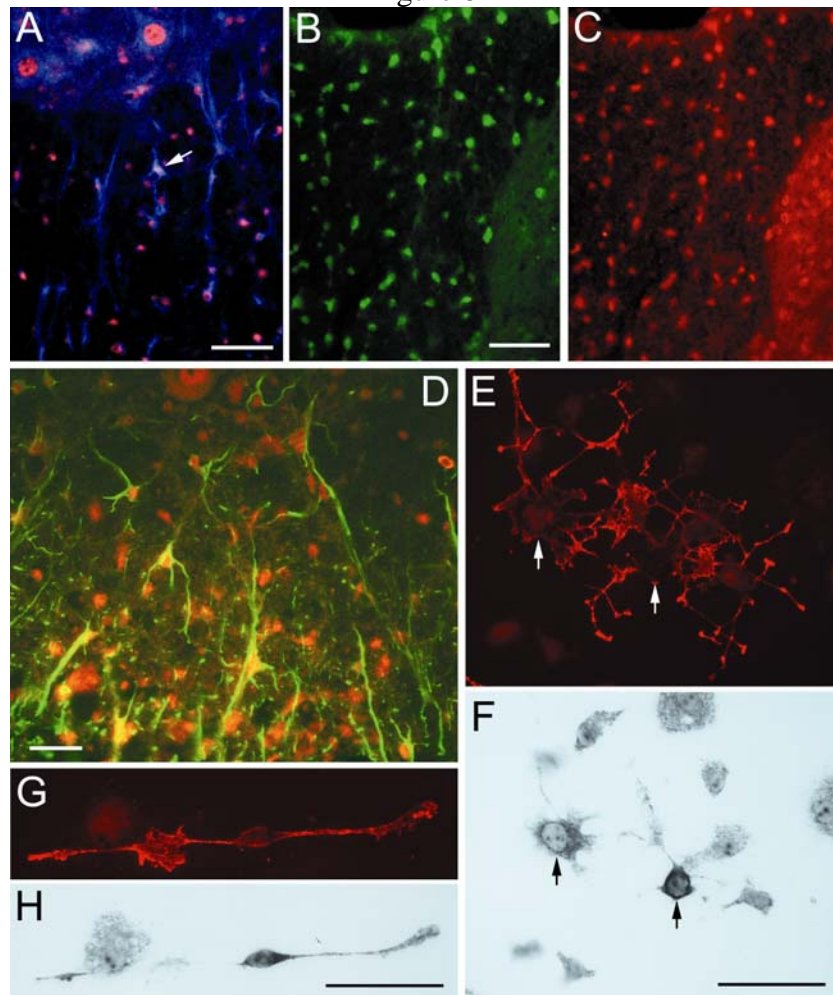
Figure 8

FIGURE 8. *Expression of FGFR3 by multiple glial cell types*. FGFR3 expression detected by immunofluorescence (A, C, D) or *in situ* hybridization (F, H). Immunofluorescence identification of oligodendrocyte progenitors with PDGFαR (A) and anti-NG2 (E, G), mature oligodendrocytes with CC1 monoclonal antibody (B), and astrocytes with anti-GFAP (D). **A**: In sections of normal spinal cord, FGFR3 immunofluorescence (red) is present in the nucleus and cytoplasm of cells (example at arrow) with a characteristic small, elongated oligodendrocyte progenitor morphology that express PDGFαR (blue). **B, C**: In sections of normal spinal cord, mature oligodendrocytes in the white matter that are immunolabeled with CC1 (B, green) are also immunolabeled with anti-FGFR3 (C, red channel of same field as B). **D**: In lesioned white matter (MHV, 4 wpi), anti-GFAP immunoreactivity increases consistent with gliosis and FGFR3 immunoreactivity (red) is intense in the astrocyte cell body and processes (double immunolabeled cells appear yellow). E-H show cells isolated from MHV lesioned mice at 4 wpi, grown in culture for 2 days to allow process extension, and then labeled with anti-NG2, detected with immunofluorescence (E, G), and *in situ* hybridization for FGFR3 mRNA detection with NBT/BCIP substrate (F, H). **E, F**: Cells with multiple processes that have not yet lost NG2 expression (red, E) exhibit perinuclear NBT/BCIP reaction product for FGFR3 mRNA (F) that blocks the NG2 epifluorescence from the cell bodies (arrows indicate cell bodies). **G, H**: Bipolar cells immunolabeled for NG2 (red, G) consistently exhibited perinuclear FGFR3 mRNA signal (H). The ameboid cells (F,H) are microglia, which are abundant in cultures of lesioned spinal cord (Armstrong et al., 1990a). Microglia exhibit variable FGFR3 mRNA signal intensity. The ameboid cell in H shows only gray associated with phase contrast imaging and serves as an indicator of a cell that is not labeled for FGFR3 mRNA. All scale bars = 50 μm.

CHAPTER 3

Fibroblast Growth Factor 2 (FGF2) Inhibits Oligodendrocyte Progenitor Differentiation *In Vivo* During Development and Remyelination

Joshua C. Murtie[1], Yong-Xing Zhou[2], Tuan Q. Le[2], and
Regina C. Armstrong[1,2]

[1]Program in Molecular and Cell Biology and [2]Department of Anatomy, Physiology, and Genetics at the Uniformed Services University of the Health Sciences, Bethesda, MD

ABSTRACT

The role of fibroblast growth factor 2 (FGF2) on oligodendrocyte lineage cell (OLC) responses during myelination and remyelination was determined using wild-type and *FGF2* knockout mice. In wild-type mice, FGF2 expression increases approximately three-fold between the first and second postnatal weeks, a time corresponding with the peak of myelination in the central nervous system (CNS). At postnatal day (P7), replication-incompetent retrovirus encoding enhanced green fluorescent protein (GFP) was injected into the mouse spinal cord white matter to label endogenous cycling cells. On P28, mice were perfused and differentiation of retrovirally labeled cells was quantified by morphological characteristics and immunolabeling, using CC1 for oligodendrocytes and NG2/platelet-derived growth factor α receptor (PDGFαR) for oligodendrocyte progenitors (OPs). Within the population of GFP-labeled cells, the proportion of oligodendrocytes was higher in *FGF2-/-* mice, indicating that endogenous FGF2 inhibits the differentiation of OPs during development in wild-type mice. FGF2 expression also increases dramatically in response to CNS demyelination (Messersmith et al., 2000; Armstrong et al., 2002). Retrovirus injection into the corpus callosum of adult mice prior to induction of transient demyelination allowed lineage tracing of newly generated oligodendrocytes that contribute to remyelination. Comparison of wild-type and *FGF2-/-* mice indicates that FGF2 inhibits differentiation of OPs into mature oligodendrocytes during remyelination. Previous *in vitro* studies have revealed potential roles for FGF2 in OLC migration, proliferation, differentiation, and survival. Our *in vivo* analysis demonstrates that the predominant *in vivo* role of FGF2 on OLCs is inhibition of OP differentiation during both myelination and remyelination.

During development, growth factors regulate proliferation, migration, and differentiation of neural stem cells and progenitors to coordinate the formation of CNS structures. Myelination is an excellent example of cellular interactions regulated by growth factor signaling (Calver et al., 1998; Fruttiger et al., 1999; Ye et al., 2002). Pathological scenarios ranging from traumatic injury to autoimmune diseases, such as multiple sclerosis (MS), result in demyelination and impaired nerve conduction. Functional recovery from diseases such as MS is likely to require amelioration of disease progression as well as remyelination of viable axons. While remyelination can occur in the CNS, repair is typically incomplete and diminishes with each subsequent demyelinating episode (Prineas et al., 1993; Raine et al., 1993). Populations of immature OLCs are present in MS lesions (Wolswijk, 2002; Chang et al., 2002), and may have the potential to remyelinate if induced to differentiate into myelinating oligodendrocytes. In this context, growth factors may play a significant role in regulating the cellular responses required for remyelination in a potentially non-permissive lesion environment.

Among the growth factors that may regulate OLC responses during both myelination in development and remyelination in pathological contexts, FGF2 has been implicated in multiple effects that differ with lineage progression. Specifically, FGF2 has been shown to enhance proliferation and migration of early stage OPs while inhibiting differentiation of cells at later stages in the lineage (McKinnon et al., 1990; Bansal and Pfeiffer, 1997; Decker et al., 2000; Jiang et al., 2001). These differential effects have been identified *in vitro* and may be the result of varying FGF receptor (FGFR) expression profiles (Bansal et al., 1996; Messersmith et al., 2000). In the CNS, FGF2 and FGFR

expression levels increase during postnatal development and in response to demyelination (Riva and Mocchetti, 1991; Kuzis et al., 1995; Messersmith et al., 2000; Bansal et al., 2003).

While FGF2 can elicit multiple OLC responses *in vitro*, the role of endogenous FGF2 *in vivo* has not been demonstrated *in vivo* relative to the regulation of OLCs. Our previous studies show that the absence of FGF2 leads to enhanced lesion repopulation by oligodendrocytes during early remyelination (Armstrong et al., 2002). FGF2 acts in the context of many signals, which may differ between myelinating and remyelinating environments. Therefore, we characterized the effects of FGF2 at the cellular level, *in vivo*, during both myelination and remyelination. We find that FGF2 does not play a significant role in OLC proliferation or survival *in vivo* during either myelination or remyelination. Importantly, our retroviral lineage tracing studies reveal a predominant role of FGF2 as an inhibitor of OP differentiation during both myelination and remyelination.

RESULTS

Developmental expression of FGF2 in the normal spinal cord

During development, FGF2 expression increases postnatally in the rat CNS during the period corresponding with the peak of myelination (Matthews and Duncan, 1971; Riva and Mochetti, 1991; Kuzis et al., 1995). Confirming this developmental time-course in mice, real time kinetic RT-PCR for FGF2 revealed a dramatic increase in FGF2 mRNA expression in the wild-type mouse spinal cord from P1 to 4 weeks of age (Figure 1A). At 3 months of age, FGF2 mRNA expression had decreased to normal adult levels

from the developmental peak at 4 weeks. Since FGF2 expression can be regulated at the post-transcriptional level as well as the transcriptional level (Touriol et al., 1999; Li and Murphy, 2000), Western blots were used to assess protein expression. Protein expression of the 3 mouse FGF2 isoforms (18 kd, 21 kd, and 22kd) was most notably increased between P7 and P15, with only a slight subsequent decrease observed at 3 months of age (Figure 1B, C).

FGF2 null mice do not overproduce oligodendrocytes during the peak of myelination (P15)

OLCs have been shown to express FGFR isoforms 1, 2, and 3 at different developmental stages and thus have the potential to respond to increased expression of endogenous FGF2 in the postnatal CNS (Bansal et al., 1996). With this in mind, we used complementary techniques to analyze diverse OLC responses in the developing spinal cord of wild-type (*FGF2+/+*) and knockout mice (*FGF2-/-*). *FGF2-/-* mice did not express detectable levels of FGF2 mRNA (data not shown) or protein (Figure 1B), confirming the original characterization of the null phenotype (Zhou et al., 1998).

We first compared the density of oligodendrocytes identified by PLP mRNA or CC1, to assess OLC responses that may accumulate to alter the oligodendrocyte population. Analysis at P15, the approximate peak of oligodendrocyte development, revealed a significant difference between *FGF2* genotypes. Quantification of PLP *in situ* hybridization using P15 lumbar spinal cord sections indicated that the total oligodendrocyte density was higher in *FGF2+/+* mice relative to *FGF2-/-* mice, with the biggest difference found in the white matter (Figure 2A). A similar result was found with counts from CC1 immunofluorescence of P15 lumbar spinal cord sections (Figure 2 C

and D; P15 lumbar CC1 counts in white matter: 1567 ± 70 cells/mm^2 for *FGF2+/+* mice, n = 3 vs. 1141 ± 44 cells/mm^2 for *FGF2-/-* mice, n = 3, p = 0.007). Therefore, the difference in cell density does not appear to be attributable to an effect of FGF2 on *PLP* gene transcription. Furthermore, oligodendrocyte quantification is presented as density to minimize variability between sections. The area of transverse lumbar sections was similar between FGF2 genotypes (1.539 ± 0.116 mm^2 for *FGF2+/+* mice, n = 4 vs. 1.151 ± 0.156 mm^2 for *FGF2-/-* mice, n = 6, p = 0.109) so that differences in cell density correspond with differences in cell number rather than changes in tissue section area.

Previous studies have shown that during postnatal development, the peak of oligodendrogenesis actually reflects an overproduction of oligodendrocytes, by approximately 50%, followed by matching of oligodendrocyte and axon number that results in the density found in adults (Barres and Raff, 1999). The superfluous oligodendrocytes may be premyelinating oligodendrocytes that eventually die after failing to make contact with bare axons (Trapp et al., 1997). PLP mRNA *in situ* hybridization (Figure 2B) should detect premyelinating and myelinating oligodendrocytes since PLP transcription precedes myelin formation (Mallon et al., 2002). Therefore, the effect of FGF2 genotype on the density of oligodendrocytes, identified by PLP mRNA, was examined across postnatal development to compare P15 with an earlier stage of myelination (P7) and with adult mice (3 mth).

Since analysis of P15 spinal cord revealed that the most dramatic difference in oligodendrocyte cell density occurred in the white matter (Figure 2A), we used white matter cell counts to illustrate the developmental time course (Figure 2B). Similar results were observed for total sections and for gray matter (not shown). As expected, across

lumbar spinal cord sections, the density of oligodendrocytes peaks in *FGF2+/+* mice at P15 and then declines to adult levels. Interestingly, this overproduction of oligodendrocytes was not observed in *FGF2-/-* mice when the density was examined across different ages.

The effect of *FGF2* genotype appeared to be specific to developmental age and did not appear to reflect a difference in the rostrocaudal progression of oligodendrogenesis. In P15 spinal cord, *FGF2* genotype correlated with a significant difference in white matter oligodendrocyte density at both lumbar (Figure 2) and cervical (1883 ± 48 cells/mm^2 for *FGF2+/+* mice, n = 5 vs. 1697 ± 58 cells/mm^2 for *FGF2-/-* mice, n = 8, p = 0.047) levels. In addition, *FGF2* genotype did not cause a change in the densities of PLP mRNA+ cells in P7 spinal cord sections when analyzed in the lumbar enlargement (Figure 2) or in the cervical enlargement (1062 ± 63 cells/mm^2 for *FGF2+/+* mice, n = 5 vs. 998 ± 40 cells/mm^2 for *FGF2-/-* mice, n = 5, p = 0.417).

Time course of myelination is not dependent on FGF2

Myelination was assessed in *FGF2-/-* and *FGF2+/+* mice, using MOG immunofluorescence (Figure 3) and toluidine blue staining (not shown) of the postnatal spinal cord at lumbar levels. Within the lumbar dorsal column white matter, myelination of the fasciculus cuneatus was nearing completion at P7 while myelination of the fasciculus gracilis was ongoing. At P15, myelination of both the fasciculus gracilis and fasciculus cuneatus was complete and myelination of the corticospinal tract was ongoing. This time course and pattern of myelination was similar for both genotypes, and corresponds with previous studies of normal rodent spinal cord development (Schwab and Schnell, 1989). Therefore, the absence of FGF2 did not affect the pattern of

myelination observed at either P7 or P15. Similarly, the pattern of myelination was not notably different in cerebellum or corpus callosum of P15 mice (not shown).

Quantification of pixel intensity revealed no difference in MOG immunofluorescence in either the dorsal column of P7 or P15 lumbar spinal cord sections or the corpus callosum of the P7 or P15 brain (Figure 3, quantification not shown). This lack of an effect of FGF2 expression on myelination is not necessarily in contradiction with our quantification of oligodendrocyte densities. Premyelinating oligodendrocytes may contribute to the overproduction of oligodendrocytes observed at P15 in *FGF2+/+* mice but not in *FGF2-/-* mice (Figure 2). Therefore, the density of myelinating oligodendrocytes could be similar in each genotype or at least sufficient for similar myelin formation. However, quantitative distinction of premyelinating versus myelinating populations was not feasible in the current study.

Differentiation of OPs is inhibited by FGF2 during myelination

Previous *in vitro* studies have reported that FGF2 inhibits differentiation of OPs (reviewed in Bansal and Pfeiffer, 1997). Using replication-incompetent retrovirus encoding GFP, we monitored OLC differentiation over the period of myelination *in vivo*. Injection of NIT-GFP retrovirus into P7 lumbar dorsal column selectively labeled endogenous dividing cells in spinal cord white matter. On P28, mice were perfused and the retrovirally labeled population was analyzed.

Greater than 90% of GFP-labeled cells were identified as OLCs, *i.e.* OPs or oligodendrocytes, in both FGF2 genotypes. OPs were identified by immunofluorescence for PDGFαR and NG2 combined with detection of GFP expression (Figure 4). The proportion of GFP-positive cells identified as OPs was significantly lower in *FGF2-/-*

mice (Figure 5B). Oligodendrocytes were identified by the presence of multiple processes that bifurcate and extend parallel to axons (Figure 4B). Counts of oligodendrocytes identified by morphology were confirmed by CC1 immunofluorescence in combination with GFP detection (Figure 5B). The proportion of GFP-positive cells that were identified as oligodendrocytes was significantly higher in *FGF2-/-* mice, as compared to *FGF2+/+* mice (Figure 5A, B). Together, this proportional shift in the generation of oligodendrocytes and OPs indicates that in wild-type mice, endogenous FGF2 inhibits *in vivo* differentiation of OPs to generate oligodendrocytes.

There was no difference between genotypes in the proportion of total GFP-labeled cells that were not identified as oligodendrocytes or OPs (Figure 5). A very small proportion ($< 5\%$) of the total GFP-labeled population was identified as astrocytes (Figure 4C, D) based upon association with blood vessels. The remaining cells had morphologies that appeared to be stages of OLCs but were not specifically recognized by NG2, PDGFαR, or CC1.

These findings indicate that in the absence of FGF2, endogenous cycling cells are more likely to differentiate into oligodendrocytes. Since mature oligodendrocytes are post-mitotic cells, this precocious differentiation in *FGF2-/-* mice would be expected to generate fewer oligodendrocytes as a given cycling OP may not complete the normal number of rounds of asymmetric divisions.

OLC proliferation, migration, and survival in the absence of FGF2

In vitro studies have indicated potential effects of FGF2 on OLC proliferation, survival, and migration. We considered the effect of FGF2 genotype on each of these cellular processes in the developing spinal cord. The mitogenic effects of FGF2 on OPs

have been well established *in vitro* (McKinnon et al., 1990). Therefore, the absence of FGF2 may reduce OP proliferation *in vivo,* effectively reducing the pool from which mature oligodendrocytes may be formed. OP cell density and proliferation was estimated to address this possible mechanism of influencing oligodendrocyte density. *In situ* hybridization for PDGFαR to identify OPs was combined with immunodetection of BrdU (4 hr terminal pulse) in the P7 and P15 lumbar spinal cord (Figure 6A). As expected, dividing (PDGFαR+/BrdU+) and non-dividing (PDGFαR+/BrdU-) OP density decreased significantly between P7 and P15 in both genotypes. This result is consistent with OP proliferation decreasing as oligodendrocyte maturation progresses. In addition, NG2 immunoreactivity with DAPI chromosomal stain was used to identify OPs actively undergoing mitosis (Figure 6C and D). Neither method revealed a significant difference in OP proliferation based on genotype.

We next examined whether the difference in oligodendrocyte density between *FGF2-/-* and *FGF2+/+* mice at P15 was due to a different extent apoptosis in the absence of FGF2. TUNEL analysis of P7 and P15 lumbar spinal cord sections revealed an extremely low number of labeled cells in both *FGF2-/-* (5.0 ± 1.0 cells/mm^2 at P7, n = 4; 4.6 ± 0.7 cells/mm^2 at P15, n = 6) and *FGF2+/+* (4.7 ± 0.5 cells/mm^2 at P7, n = 4; 4.6 ± 1.1 cells/mm^2 at P15, n = 6) mice. Therefore, apoptosis, as detected by TUNEL, was not significantly affected by *FGF2* genotype.

In vitro studies have shown that FGF2 effects OLC migration (McKinnon et al., 1993; Simpson and Armstrong, 1999; Decker et al., 2000). The majority of OLC developmental migration occurs prior to maximal FGF2 expression. In addition, there was no effect of *FGF2* genotype on oligodendrocyte density at P7 in the cervical or

lumbar spinal cord white matter or gray matter (Figure 2B and data not shown).

Therefore, it is unlikely that the absence of FGF2 had a profound effect on the normal

migration patterns of OLCs *in vivo* that could account for the genotypic differences

observed at P15.

Differentiation of OPs is inhibited by FGF2 during remyelination

Our previous study showed that the absence of FGF2 resulted in a significant

increase in oligodendrocyte density during remyelination (87%; Armstrong et al., 2002).

After 3 weeks of recovery from cuprizone demyelination, *FGF2-/-* mice exhibited

enhanced oligodendroglial repopulation of lesions (325 ± 5 cells/mm^3 x 10^3) compared to

FGF2+/+ mice (247 ± 16 cells/mm^3 x 10^3). Since FGF2 inhibited differentiation of OPs

during development (Figure 5), we used retroviral lineage tracing to determine if FGF2

had the same effect during remyelination. Replication-incompetent retrovirus was

stereotactically injected directly into the corpus callosum three days prior to the start of

treatment with cuprizone ingestion. Mice were then fed cuprizone for a 6-week treatment

period followed by 3 weeks on normal chow to allow recovery and OLC regeneration.

This design effectively labels the endogenous cycling cells of the corpus callosum and

allows the tracking of the progeny of these cells over the full course of demyelination and

remyelination. Experiments using DAP retrovirus encoding membrane-associated

alkaline phosphatase in this experimental design (Figure 7A) confirmed previous reports

that endogenous cycling cells of the adult white matter contribute to remyelination after

transient demyelination (Gensert and Goldman, 1997). Similar cell types (Figure 4A, B)

were found with NIT-GFP retroviral labeling during remyelination as in development

with one exception; no GFP-labeled astrocytes (Figure 4C, D) were observed in our

remelination analysis. This finding is consistent with previous reports that endogenous cycling cells of the adult white matter do not generate astrocytes in this context (Gensert and Goldman, 1996; 1997).

After recovery from cuprizone demyelination, the proportion of GFP-positive cells that were morphologically identified as oligodendrocytes was significantly higher in the absence of FGF2 (Figure 7B). This quantification by morphology was confirmed with CC1 immunohistochemistry in combination with GFP detection. Consistent with this result, the proportion of GFP-positive cells identified as OPs (*i.e.* immunolabeled with NG2 and PDGFαR) was significantly decreased in *FGF2-/-* mice (Figure 7C). Together with our similar results from the developing spinal cord, these data indicate that a significant role for FGF2 is as an inhibitor of OP differentiation *in vivo* during remyelination.

DISCUSSION

The effects of FGF2 expression in the CNS during embryonic development are beginning to be deciphered by analysis of *FGF2* knockout mice (Ortega et al., 1998; Dono et al., 1998; Vaccarino et al., 1999). The present study analyzed *FGF2-/-* mice in comparison with wild-type mice to demonstrate the effect of FGF2 upregulation on OLC responses during postnatal development and in CNS pathologies. An increase in FGF2 mRNA and protein expression occurs between P7 and P15 in mouse spinal cord. This period corresponds with a postnatal wave of OP differentiation into mature oligodendrocytes. In the adult CNS, FGF2 levels are typically low in white matter, but increased FGF2 expression appears to be a universal response to demyelination (Liu et al,

1998; Hinks and Franklin, 1999; Messersmith et al., 2000; Armstrong et al., 2002). This FGF2 expression pattern combined with *in vivo* expression of FGFRs by OLCs (Messersmith et al., 2000; Bansal et al., 2003) sets up the expectation that FGF2 plays a role during myelination as well as remyelination. Indeed, administration of excess FGF2 in the developing CNS impairs the generation of myelinating oligodendrocytes and formation of myelin (Goddard et al., 1999; 2001). In addition, during remyelination, impairing FGF2 expression during remyelination has profound effects on regeneration of OLCs (Armstrong et al., 2002). However, the mechanism by which FGF2 acts on OLCs at the cellular level *in vivo* remains poorly understood in development as well as remyelination.

In the developing CNS, there is a complex interaction between FGF family members and their high affinity receptors (FGFRs). Three FGFR types (FGFR1, 2, and 3) can be activated by FGF2 and are expressed by diverse cell types in the postnatal CNS (Bansal et al., 2003). *In vitro*, FGFRs 1-3 are differentially regulated during progression through the oligodendrocyte lineage (Bansal et al., 1996). These studies indicate that FGFR1 is expressed at all OLC stages and increases with maturation or with FGF2 treatment. FGFR2 expression is low in early stages of the lineage and highest in oligodendrocytes. FGFR3 expression peaks at the late progenitor stage and declines with further maturation. *In vivo*, FGFRs are expressed coincident with oligodendrocyte lineage development (Bansal et al., 2003). However, astrocytes also express FGFRs *in vivo* and could respond to FGF2 by producing growth factors and immunoregulatory molecules that regulate OLC responses (Komoly et al., 1992; Ballabriga et al., 1997; Messersmith et al., 2000). FGFR upregulation precedes the postnatal increase in FGF2

ligand expression (Kuzis et al., 1995). As a result, it appears that FGF2 ligand expression regulates the timing of FGF2 effects during postnatal CNS development.

The only study to date of oligodendrocyte development using an *FGFR* knockout mouse model has showed more oligodendrocytes in wild-type mice then in *FGFR3-/-* mice, without altered OP number, OP proliferation, or OLC survival (Oh et al., 2003). This result was attributed to delayed oligodendrocyte differentiation in *FGFR3-/-* mice, which led to the interpretation that endogenous FGFR3 activation promotes OP differentiation (Oh et al., 2003). While our results in *FGF2-/-* mice may appear contradictory, OP differentiation was not directly examined in this FGFR3 analysis. Also, it is possible that activation of FGFR3 promotes differentiation while FGF2 signaling inhibits differentiation, since FGFR3 can bind multiple members of the FGF ligand family. Effects on OLCs in *FGFR3-/-* mice were noted as early as P2 in spinal cord (Oh et al., 2003), a time point that corresponds with very low relative levels of FGF2 expression (present study). Therefore, the effects on early oligodendrocyte development in *FGFR3* null mice might reflect a loss of signaling from an FGF family ligand other than FGF2.

FGF2 inhibition of OP differentiation is well characterized *in vitro* (McKinnon et al., 1990; Bansal and Pfeiffer, 1997; Decker et al., 2000; Jiang et al., 2001). In the current study, the lack of overproduction of oligodendrocytes observed at P15 in *FGF2-/-* mice could result from a positive or negative effect on differentiation, depending on the stage affected within the lineage, and/or from an effect on OLC proliferation or survival. Lineage tracing with replication-incompetent retroviral infection has allowed us to analyze differentiation *in vivo* by observing cumulative effects on the fate of newly

generated cells. We show that absence of FGF2 promotes differentiation of OPs during development and during remyelination. Specifically, progression from the NG2/PDGFαR-positive progenitor stage to the oligodendrocyte stage is enhanced *in vivo* in the absence of FGF2.

In the current study, FGF2 inhibition of OP differentiation was observed without significant effects in proliferation or survival assays during development (current study) or remyelination (Armstrong et al., 2002). Differences in oligodendrocyte density without a corresponding change in the OP population may appear somewhat surprising, but was similarly found in *FGFR3-/-* mice as previously discussed. Our proliferation assay used a 4 hr terminal pulse of BrdU so that the proliferating cell types could be identified, without a subsequent period allowing differentiation. In addition, this short BrdU pulse provided an estimate of the proportion of cycling cells within the OP population, which was also similar between the *FGF2* genotypes. Since OPs can divide asymmetrically to generate an oligodendrocyte and a replacement OP, a change in the number of OP generations can change oligodendrocyte density more than OP density. Further detailed analysis would be needed to identify a genotypic difference in symmetric versus asymmetric divisions and in the number of OP cell generations prior to exit from the cell cycle. The OP population size does not appear to be influenced by FGF2 expression but rather seems dependent upon PDGF signaling during both development (Calver et al., 1998) and remyelination (Murtie et al., submitted). The population of BrdU labeled cells that were not identified as OPs by PDGFαR expression also was not affected by *FGF2* genotype. However, our analysis does not fully address the potential

for FGF2 effects on neural stem cells that could proliferate in sites that were not examined, such as the subventricular zone.

A subtle differential effect of *FGF2* genotype on cell survival could also contribute to the oligodendrocyte densities observed; but relatively few apoptotic cells were identified in our analyses (current study and Armstrong et al., 2002). After the examined P15 time point of spinal cord development, a greater extent of cell death is likely to occur in wild-type mice to compensate for initial overproduction of oligodendrocytes. Previous analysis of normal development has shown that approximately 50% of newly generated or premyelinating oligodendrocytes are produced in excess and then die due to failure to contact axons and myelinate (Barres et al., 1992). However, the *FGF2-/-* mice do not appear to overproduce oligodendrocytes during development.

While the predominant effect of FGF2 on OLC responses appears to be the same in development as it is in remyelination, the cumulative result on the oligodendrocyte population density is opposite. During development, *FGF2-/-* mice do not undergo the normal overproduction of oligodendrocytes at the peak of myelination. During early remyelination, the absence of FGF2 increased oligodendrocyte density (Armstrong et al., 2002). These results may reflect the interaction of FGF2 with the combination of signals that regulate oligodendrocyte population density *in vivo* during development and remyelination. For example, during late postnatal development, oligodendrocyte number becomes less dependent on soluble mitogens, such as PDGF, so that axonal signals regulate the final oligodendrocyte density *in vivo* (Trapp et al., 1997; Calver et al., 1998; Barres and Raff, 1999). The current study examines the postnatal period of FGF2

upregulation that corresponds with ongoing myelination (P7), progressing through the peak of myelination (P15), and completion of myelination (P28 and 3 months of age). During demyelination, FGF2 is upregulated as axons are stripped of myelin and then progressively remyelinate. With this in mind, an OLC is more likely to contact a bare axon and potentially different axonal signals during demyelination and early remyelination than during the late developmental window examined. This comparison of contexts may indicate that removal of FGF2 inhibition of differentiation allows OPs to respond more optimally to match oligodendrocyte density to relevant axonal signals.

The current study identifies significant effects of FGF2 on OLCs in the context of complex environmental signals *in vivo*. We identify a common role for FGF2 in inhibiting OP differentiation during development and remyelination. However, the cumulative result of this effect on the OLC population differs between development and remyelination, indicating that the environmental context during remyelination may not simply recapitulate developmental signals. With regard to demyelinating diseases such as MS, our results indicate that increased FGF2 expression in lesions may be detrimental during remyelination. In fact, chronic MS lesions contain considerable populations of immature and premyelinating oligodendrocytes (Maeda et al., 2001; Wolswijk, 2002; Chang et al., 2002). Also, FGF2 expression has been demonstrated in subpopulations of astrocytes in MS lesions (Holley et al., 2003). Understanding signals, such as FGF2, that may inhibit immature OLCs in lesions from differentiating into myelinating oligodendrocytes may reveal strategies to promote more efficient differentiation and remyelination. Together these data illustrate the importance of FGF2 signaling *in vivo*

and indicate potential benefits of modulating FGF2 signaling in the treatment of CNS pathology.

MATERIALS AND METHODS

Animals

Mice were bred and maintained in the USUHS animal housing facility and all procedures were performed in accordance with guidelines of the National Institutes of Health, the USUHS Institutional Animal Care and Use Committee, and the Society for Neuroscience.

FGF2 knockout (*FGF2-/-*) mice and wild-type (*FGF2+/+*) mice, of the same 129 Sv-Ev:Black Swiss genetic background, were obtained from breeding heterozygous pairs (generously provided by Dr. Doetschman, University of Cincinnati). The *FGF2* knockout was generated by a targeted deletion replacing a 0.5 kb portion of the *FGF2* gene including 121 bp of the promoter and the entire first exon with an *Hprt* mini-gene (Zhou et al., 1998). Mice were genotyped using PCR analysis of tail DNA to identify wild-type *FGF2* and the targeted allele, as described in Zhou et al. (1998). *FGF2-/-* mice do not have detectable wild-type or truncated FGF2 mRNA or protein transcripts (Zhou et al., 1998).

Cuprizone Experimental Demyelination

Male 8 wk old mice were placed on a diet of 0.3% (w/w) cuprizone (finely powdered oxalic bis(cyclohexylidenehydrazide); Aldrich, Milwaukee, WI) thoroughly mixed into milled chow (Harlan Teklad; Madison, WI), which was available *ad libitum*. Mice were maintained on the cuprizone diet until being returned to normal chow pellets

after 6 wks. Cuprizone ingestion results in a reproducible pattern of corpus callosum demyelination followed by spontaneous remyelination during subsequent wks on normal chow (Matsushima and Morell, 2001; Armstrong et al., 2002).

Tissue Preparation and Histopathological Analysis

Mice were perfused with 4% paraformaldehyde, then brains and spinal cords were dissected prior to overnight post-fixation in 4% paraformaldehyde (Redwine and Armstrong, 1998). Segments of spinal cord and brain were cryoprotected and embedded in OCT compound for immunostaining, *in situ* hybridization, and TUNEL staining. Myelination and demyelination were evaluated in 7-μm paraffin sections using either toluidine blue staining or Luxol fast blue with periodic acid-Schiff reaction (Mason et al., 2001; Armstrong et al., 2002).

Kinetic RT-PCR

After euthanasia, spinal cords were rapidly removed and homogenized. RNA was isolated using Stat-60 (TEL-TEST, Inc, Friendswood, TX). For each mouse, 2 μg total RNA was reverse transcribed using random hexamer primers. According to the methods detailed for the ABI PRISM 7700 "TaqMan" System (PE Applied Biosystems, Foster City, CA), mouse FGF2 primers (forward primer CCCACCAGGCCACTTCAA from nucleotide 60; reverse primer TCTCTCTTCTGCTTGGAGGTTGTAGTT from nucleotide 204) were designed to flank an intervening FGF2 probe (CCCAAGCGGCTCTACTGCAAGAACG from nucleotide 82) that was labeled with a fluorochrome (6-FAM) on the 5' end as well as a fluorescence quencher (TAMRA) on the 3' end. The total RNA values and RT reaction efficiency was normalized by

measuring 18S rRNA for each sample in parallel. Full-length FGF2 plasmid cDNA was used to generate the standard curve.

Western Blots

Spinal cords were rapidly removed and homogenized in protein lysis buffer (1x PBS, 2% SDS, 1% NP-40, 0.5% Na deoxycholate). Spinal cord homogenates were incubated with protease inhibitors for 30 min at 4°C under constant rotation and then centrifuged at 15,000 rpm for 20 min at 4°C, prior to affinity purification by overnight incubation at 4°C with prewashed heparin-sepharose CL-6B (Pharmacia Biotech, Sweden). Proteins were solubilized from the heparin-sepharose beads by the addition of 2x Laemmli sample buffer and incubation at 65°C for 20 min. Human recombinant FGF2 (18 kd; R&D Systems, Minneapolis, MN) was used as a positive control. Homogenates from *FGF2-/-* mice were used as a negative control.

Eluates were electrophoresed in a 14% Tris-Glycine Gel. Kaleidoscope Standards (BIO-RAD, Hercules, CA) and proteins were transferred to an Immobilon-P PVDF membrane (Millipore, Bedford, MA). Before transfer, the membrane was wetted in 100% methanol for 15 seconds, washed in water for 2 min, and equilibrated in transfer buffer for more than 1 min. The gel was also equilibrated in transfer buffer for more than 1 min. Proteins were transferred at 16 volts for 90 min in transfer buffer. After washing the membrane in two brief rinses of distilled water, nonspecific binding was blocked by incubating at room temperature with 3% non-fat milk (BIO-RAD, Hercules, CA) in 1x PBS without Mg^{2+} and Ca^{2+} for 30 min. The blocking solution was replaced with the same buffer containing anti-FGF2 antibody (monoclonal anti-human fibroblast growth factor-basic, clone FB-8; Sigma, St. Louis, MO; 1:200 dilution), and the membrane

incubated overnight at 4°C with gentle agitation. The membrane was washed in distilled

water twice and incubated with anti-mouse Ig conjugated to horseradish peroxidase

(Amersham Pharmacia Biotech, UK; 1:3000 dilution) at room temperature for 1 hr. Blots

were rinsed in PBS with 0.05% Tween 20 twice, and washed an additional 3 times in

PBS with 0.05% Tween 20 for 10 min each. Immunolabeled protein bands were detected

with ECL chemiluminescent reagent (Pierce, Rockford, IL) and by exposure to BioMax

film (Kodak, Rochester, NY). FGF2 protein quantification was completed using

Metamorph image analysis software (Universal Imaging, West Chester, PA) and

normalized to actin loading controls.

In Situ Hybridization

In situ hybridization and preparation of digoxigenin-labeled riboprobes were

performed as previously detailed (Redwine and Armstrong, 1998; Messersmith et al.,

2000). Antisense riboprobes were used to detect mRNA transcripts for proteolipid

protein (PLP; gift from Dr. Lynn Hudson; National Institutes of Health; Hudson et al.,

1987) and PDGF alpha receptor (PDGFαR; gift from Dr. Bill Richardson; University

College London; Fruttiger et al., 1999). The digoxigenin-labeled riboprobes were

hybridized to 15-μm cryosections of brain or spinal cord tissues. Digoxigenin was

detected with an alkaline phosphatase-conjugated sheep anti-digoxigenin antibody

(Boehringer Mannheim, Indianapolis, IN), followed by reaction with NBT/BCIP

substrate (DAKO, Carpinteria, CA).

BrdU Incorporation and Detection

In situ hybridization combined with bromodeoxyuridine (BrdU) incorporation

was carried out as detailed previously (Redwine and Armstrong, 1998). Mice were

injected intraperitoneally with 200 mg/kg BrdU (Sigma, St. Louis, MO) at 4 hrs and 2 hrs

prior to sacrifice. After *in situ* hybridization detection, sections were treated with HCl

and then incubated overnight with a monoclonal anti-BrdU antibody directly conjugated

with horseradish peroxidase (diluted 1:15; Boehringer Mannheim). Peroxidase activity

was detected by incubation with 3,3'-diaminobenzidine (DAB; Vector Labs, Burlingame,

CA).

Apoptosis

P7 and P15 mouse spinal cord tissues were analyzed for cells undergoing

apoptosis. Cryosections (15 μm) were processed using a modified TUNEL assay

(ApopTag Plus peroxidase *in situ* apoptosis detection kit; Intergen, Purchase, NY). The

3'-OH DNA ends, generated by DNA fragmentation typically observed with apoptotic

cells, were labeled with digoxigenin-dUTP using terminal deoxynucleotidyl transferase

(TdT). The digoxigenin tag was then detected with an anti-digoxigenin antibody

conjugated with peroxidase to yield a dark brown reaction product with DAB substrate.

The sections were lightly counterstained with methyl green to detect nuclei.

Immunohistochemistry

To identify oligodendrocyte progenitors *in situ*, 15-μm cryosections were

immunostained for NG2 and PDGFαR (Messersmith et al., 2000; Armstrong et al.,

2002). Primary antibodies used were rabbit polyclonal anti-NG2 antibody (1:500; gift

from Dr. William Stallcup, La Jolla, CA) and rat monoclonal anti-PDGFαR antibody

(APA5 used at 1:200; Pharmingen, San Diego, CA). Donkey anti-rabbit IgG F(ab')$_2$

fragment conjugated with Cy3 (Jackson Immunoresearch, West Grove, PA) was used to

detect NG2 while the PDGFαR was detected with biotinylated donkey anti-rat IgG

F(ab')$_2$ fragment (Jackson Immunoresearch) followed by coumarin tyramide amplification (New England Nuclear, Boston, MA). Additional sections were immunostained for NG2 and also stained with DAPI (Sigma) to detect nuclei and identify OPs undergoing mitosis.

Mature oligodendrocytes were identified with CC1, which immunostains oligodendrocyte cell bodies without labeling myelin (Fuss et al., 2000). The CC1 antibody (Oncogene Research Products, Cambridge, MA) was detected with donkey anti-mouse IgG F(ab')$_2$ fragment conjugated with Cy3 (Jackson Immunoresearch). The CC1 immunostaining conditions were previously tested to ensure that CC1 did not label astrocytes or NG2-labeled cells (Messersmith et al., 2000).

Myelin was immunostained with monoclonal antibody 8-18C5, which recognizes myelin oligodendrocyte glycoprotein (MOG; hybridoma cells provided by Dr. Minetta Gardinier; University of Iowa, Iowa City, IA; Linnington et al., 1984).

Retrovirus Production

A 293 cell line stably transfected with pNIT-GFP, a replication-incompetent retroviral expression vector encoding GFP, (provided by Dr. Fred Gage; Salk Institute, La Jolla, CA; Palmer et al., 1999) was transiently transfected with pMD.G (plasmid containing the vesicular stomatitis virus glycoprotein) and cultured for two days. Virion-containing supernatants were concentrated 100-fold by centrifugation at 50,000 x g at 4^0 C for 150 min. Viral pellets were reconstituted in Hanks balanced salt solution to a final concentration of 100x the original volume. Titers, typically 10^5 cfu/mL, were determined by GFP expression after infection of NIH 3T3 cells with serial dilutions of concentrated virus.

Replication-incompetent DAP retrovirus, encoding membrane-associated human placental alkaline phosphatase, was generated from a stable NIH 3T3 producer cell line (Fields-Berry et al., 1992). Producer cells were grown to confluence and the supernatant was collected after 3 days and concentrated 100-fold by centrifugation at 50,000 x g at 4^0 C for 150 minutes. Alkaline phosphatase was detected with NBT/BCIP substrate (DAKO, Carpinteria, CA).

Stereotactic Surgery and Retrovirus Injection

Development: P7 male mouse pups were placed on cooling blocks and anesthetized with isoflurane using the A.D.S. 1000 anesthesia delivery system (Engler Engineering Corporation; Hialeah, FL) with a mouse anesthesia mask (Stoelting Physiology Research Instruments; Wood Dale, IL). Partial laminectomy was performed to expose the L5 spinal cord through the intervertebral space. A range of viral titers (10, 30, or 60 cfu in 1.0 μL) was injected into the dorsal column through a pulled glass pipette (outer diameter $\leq$ 50 μm) mounted on a Hamilton syringe at a rate of 0.2 μL per min (Levison et al., 1999). After surgery, the wounds were closed with a single wound clip and the pups were returned to their mother.

Remyelination: Three days prior to cuprizone treatment, 8-week-old male mice were anesthetized with isoflurane and body temperature was maintained with 37^0 C isothermal heating pads. Heads were stabilized in the stereotaxic apparatus using cushioned ear bars and a burr hole was drilled into the skull at the following coordinates: bregma –1.0 mm and 0.25 mm lateral to the sagittal suture (Franklin and Paxinos, 1997). In these adult mice, virus (10^2 cfu in 1.0 μL) was injected directly into the corpus

callosum at a depth of 1.875 mm and a rate of 0.2 µL per minute. After injection, the

burr hole was sealed using Gelfoam and the wound closed with a single wound clip.

After appropriate intervals for retroviral lineage tracing (see Results), mice were

transcardially perfused with 3% paraformaldehyde in 0.1M phosphate buffer followed by

fixation overnight at 4^0 C in 3% paraformaldehyde solution. Tissues used for

immunohistochemistry were cryoprotected in 30% sucrose overnight at 4^0 C after

overnight fixation. Cryoprotected tissue was then embedded in OCT compound and

stored at -80^0 C.

Imaging, Quantification, and Statistical Analysis

Images of immunostaining and *in situ* hybridization results were captured with a

Spot 2 digital camera on an Olympus IX-70 microscope. Fluorescence channels were

imaged singly or in combination using narrow band pass filter sets for Cy3, FITC/GFP,

and AMCA or a triple band pass filter (Chroma Technologies, Brattleboro, VT). Images

were prepared as panels using Adobe Photoshop. Immunofluorescence signal intensity

within a given area was quantified from digital images using Metamorph Software

(Universal Imaging Corp., West Chester, PA) to select the region of interest and calculate

the average pixel intensity of the region.

For cell density quantification, entire 15 µm-thick transverse sections of spinal

cord were sampled. All labeled cells within each section were counted and the area was

measured to determine cells/mm^2. Each category analyzed included 3 or more tissue

sections per mouse and 3 or more mice per condition. Specific numbers of animals per

sample are noted in text and/or figure legends. Unpaired Student's *t*-tests were used to

identify significant differences between genotypes and/or treatments. The significance of proportions generated in lineage tracing was tested using the χ^2 statistical test.

Acknowledgements
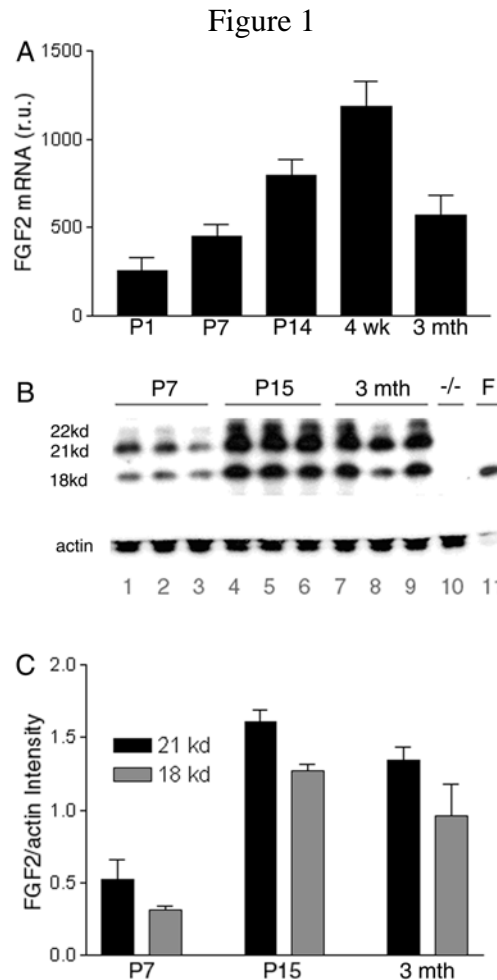
Figure 1

Figure 1: *FGF2 expression during postnatal development.* *FGF2+/+* mice were used to determine the relative levels of FGF2 mRNA and protein expression during postnatal development in the spinal cord. (**A**) Semi-quantitative kinetic RT-PCR. FGF2 mRNA levels were normalized to 18S rRNA values for the cDNA sample generated from the same RT reaction. Full-length FGF2 plasmid cDNA was used to generate the standard curve. N = 3 mice per time point; r.u., relative units. (**B**) Western blotting for the 3 mouse isoforms of FGF2 (18, 21, and 22 kd) shows FGF2 protein expression from mice in triplicate at postnatal day (P) 7 (lanes 1-3), P15 (lanes 4-6), and 3 months (lanes 7-9). *FGF2-/-* spinal cord (P15) homogenate was used as a negative control (lane 10). Human recombinant 18 kd FGF2 was used as a positive control (lane 11). (**C**) Quantification of the 18 and 21 kd isoforms from the Western blot shown in panel B using actin to normalize for total protein loaded per lane. Protein quantification confirms increased FGF2 expression levels during the progression of myelination (P7 to P15). Values shown represent the mean ± SEM (**A**, **C**).
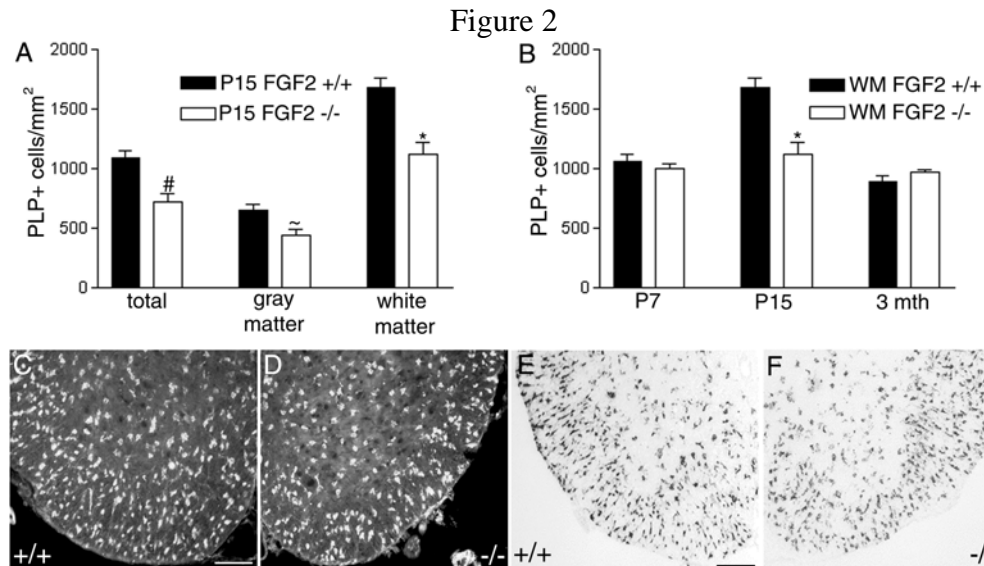
Figure 2

Figure 2: *Oligodendrocytes in the developing spinal cord.* The density of oligodendrocytes was calculated in both *FGF2+/+* and *FGF2-/-* mice in the lumbar spinal cord using *in situ* hybridization for PLP mRNA. (**A**) Density of PLP mRNA labeled cells was quantified in the total P15 spinal cord sections as well as separately in the spinal cord white matter and gray matter (*FGF2+/+*, n = 5; *FGF2-/-*, n = 7). Oligodendrocyte density was significantly different in *FGF2-/-* mice as quantified in the total area of transverse spinal cord sections (#, p = 0.005). This difference in total oligodendrocyte density was accounted for by significant differences in the gray matter (~, p = 0.001) and white matter (*, p = 0.002), with the most pronounced decrease observed in the white matter. (**B**) Density of PLP mRNA-labeled cells in white matter (WM) was determined at postnatal days 7 (P7; *FGF2+/+*, n = 5; *FGF2-/-*, n = 5) and 15 (P15), and in adults (3 mth; *FGF2+/+*, n = 3; *FGF2-/-*, n = 4). In *FGF2+/+* mice, a normal overproduction of oligodendrocytes is observed at P15. In *FGF2-/-* mice, this overshoot does not occur. Values shown represent the mean ± SEM (**A, B**). Representative images of *FGF2+/+* (**C, E**) and *FGF2-/-* (**D, F**) P15 spinal cord sections immunolabeled with CC1 (**C, D**) and PLP mRNA (**E, F**). Scale bars = 100 μm.

Figure 3
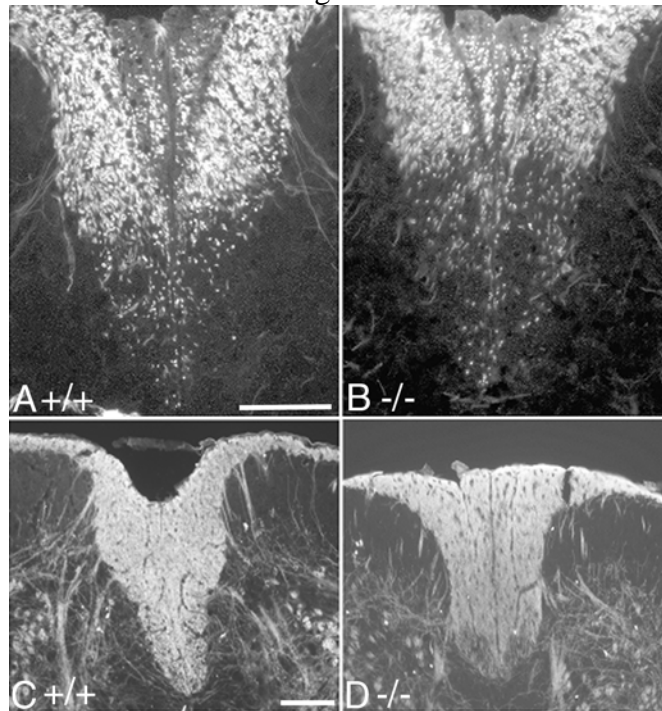
Figure 3: *Myelination of the developing spinal cord.* MOG immunolabeling of the dorsal columns at lumbar levels shows no changes in the pattern of myelination. (**A**, **B**) Myelination is the same in *FGF2+/+* (**A, C**) and *FGF2-/-* (**B, D**) mice at P7 (**A**, **B**) and P15 (**C**, **D**). Myelination of the fasciculus cuneatus was near completion at P7 with myelination of the fasciculus gracilis ongoing. The corticospinal tract was not yet myelinated at P7. Myelination of the fasciculus gracilis is complete by P15. Myelination of the entire dorsal column is complete at P15 with the exception of the most ventral aspect of the corticospinal tract in both genotypes. Scale bars = 100 μm.
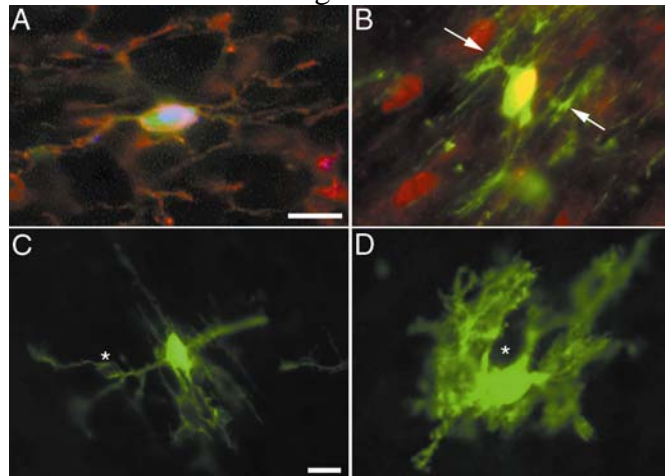
Figure 4

Figure 4: *Cell types generated from lineage tracing studies.* Multiple cell types were generated from endogenous cycling cells in CNS white matter tracts that were heritably labeled with NIT-GFP retrovirus. (**A**) GFP-positive (green) cells were characterized as oligodendrocyte progenitors by PDGFαR (blue) and NG2 (red) immunostaining. (**B**) Oligodendrocytes expressing CC1 (red) and GFP (green) have T-shaped bifurcated processes (arrows), a distinct characteristic of oligodendrocyte morphology. (**C**, **D**) GFP-positive cells with morphologies consistent with astrocytes were identified by their association with blood vessels (* denotes contact with blood vessels). Scale bars = 10 μm (**A**, **B**, **C**, **D**).
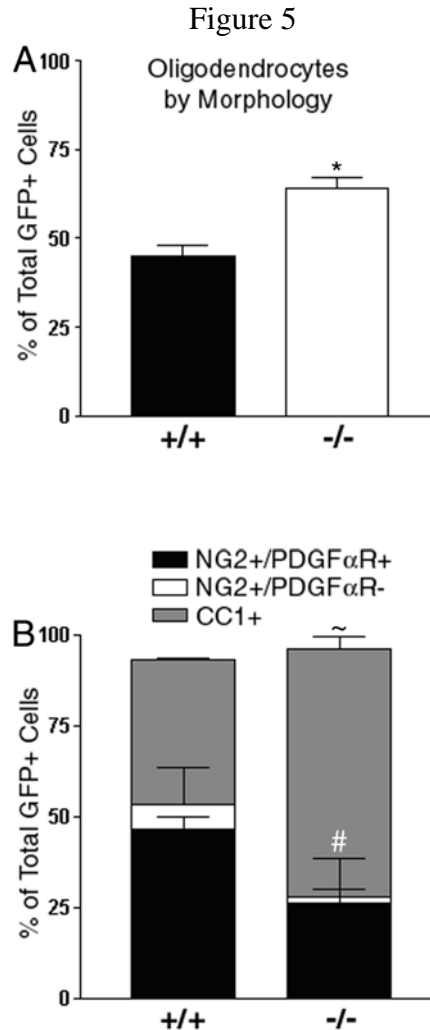
Figure 5: *Oligodendrocyte lineage cell differentiation during myelination.* Oligodendrocyte lineage cell differentiation was examined using NIT-GFP retroviral infection to monitor cumulative differentiation spanning the peak period of myelination (P7-P28). (**A**) The proportion of GFP-labeled cells that were morphologically identified as oligodendrocytes was significantly higher in *FGF2-/-* mice (n = 6 mice; 442 cells) compared to *FGF2+/+* mice (n = 10 mice; 230 cells) during myelination (*, p = 0.001). (**B**) Retroviral infection was combined with immunolabeling for cell type-specific antigenic markers to reveal the proportion of GFP-labeled cells that were oligodendrocyte progenitors (NG2+/PDGFαR+ or NG2+/PDGFαR-) or oligodendrocytes (CC1+). *FGF2-/-* mice (n = 3; 144 cells) have a significantly lower proportion of GFP-labeled oligodendrocyte progenitors (#, p = 0.007) and a significantly higher proportion of GFP-labeled oligodendrocytes (~, p = 0.001) compared to *FGF2+/+* mice (n = 3 mice; 464 cells). Values shown represent the proportional mean ± standard error of the proportion.

Figure 6
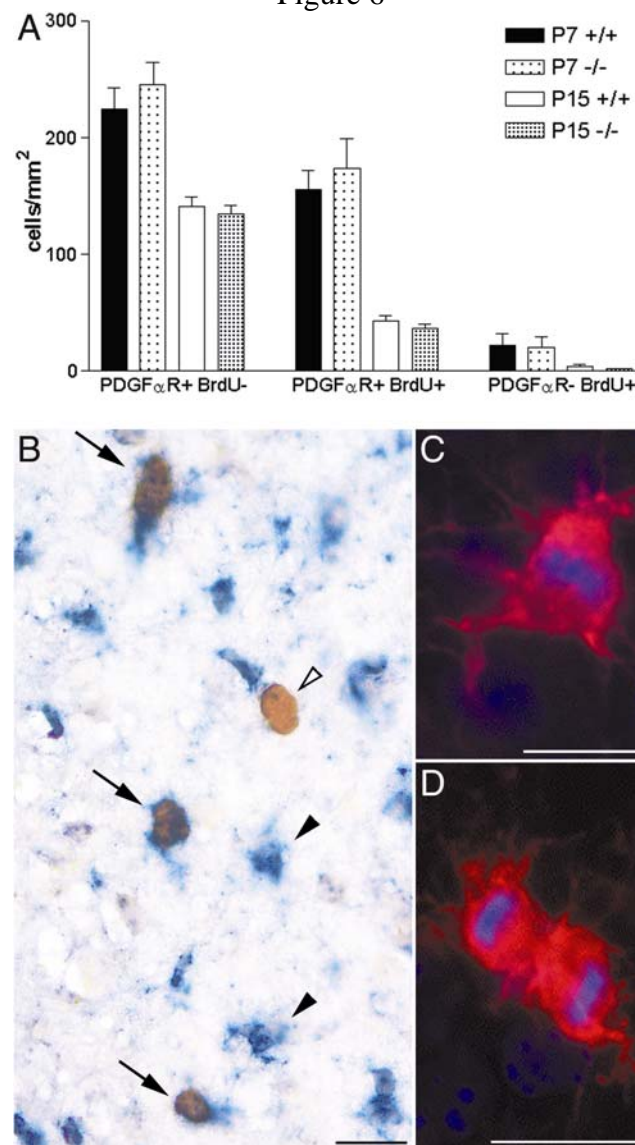
Figure 6: *Oligodendrocyte progenitor proliferation during early postnatal development.* (**A**) Proliferation of oligodendrocyte progenitors was assessed using *in situ* hybridization for PDGFαR mRNA in combination with BrdU immunodetection (4 hr terminal pulse) in P7 and P15 lumbar spinal cord sections. Marked decreases were observed in dividing (PDGFαR+/BrdU+) and non-dividing (PDGFαR+/BrdU-) oligodendrocyte progenitor densities between P7 (*FGF2+/+*, n = 5; *FGF2-/-*, n = 5) and P15 (*FGF2+/+*, n = 4; *FGF2-/-*, n = 6). The density of dividing and non-dividing oligodendrocyte progenitors was not changed in *FGF2-/-* mice compared to *FGF2+/+* mice at P7 or P15. There were no genotypic differences in the population of dividing cells that was not identified by cell type-specific markers (PDGFαR-/BrdU+) at P7 or P15. Values shown represent the mean ± SEM. (**B**) Representative images of PDGFαR mRNA *in situ* hybridization (cells labeled blue) in combination with BrdU (nuclei labeled brown) immunodetection show non-dividing (PDGFαR+/BrdU-; black arrowheads) as well as dividing (PDGFαR+/BrdU+; black arrows) oligodendrocyte progenitors. Dividing cells that were not identified by cell type-specific markers (PDGFαR-/BrdU+; arrowhead outline) are also present. Scale bar = 25 μm (**B**). (**C, D**) Mitotic oligodendrocyte progenitors were identified with DAPI DNA stain (blue) and immunolabeling with NG2 (red). Representative images show mitotic oligodendrocyte progenitors in metaphase (**C**) and telophase (**D**). Scale bars = 25 μm (**C, D**).
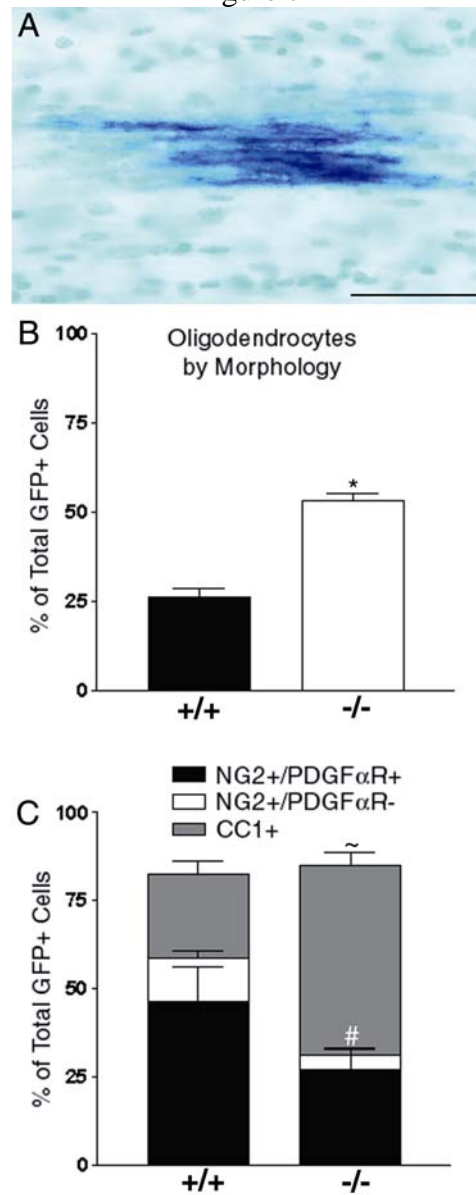
Figure 7

Figure 7: *Oligodendrocyte lineage cell differentiation during remyelination.* (**A**) DAP replication-incompetent retrovirus encoding alkaline phosphatase was used to label the endogenous cycling cells of the corpus callosum prior to cuprizone demyelination. After remyelination, membrane-associated alkaline phosphatase substrate deposition is found on parallel tracks oriented with axons in the corpus callosum, indicative of remyelination by cells generated from the endogenous cycling cells of the normal adult white matter. Scale bar = 50 μm. (**B**) Based on morphological characteristics, the proportion of GFP-labeled cells that were identified as oligodendrocytes was significantly higher (*, p = 0.001) in *FGF2-/-* mice (n = 5 mice; 2084 cells) compared to *FGF2+/+* mice (n = 3 mice; 927 cells) during early remyelination. (**C**) Retroviral lineage tracing was combined with immunolabeling for cell type-specific markers to identify GFP-labeled cells as oligodendrocyte progenitors (NG2+/PDGFαR+ or NG2+/PDGFαR-) or oligodendrocytes (CC1+). *FGF2-/-* mice (n = 3) have a significantly lower proportion of GFP-labeled oligodendrocyte progenitors (#, p = 0.001; *FGF2+/+*, n = 261 cells; *FGF2-/-*, n = 182 cells) and a significantly higher proportion of GFP-labeled oligodendrocytes (~, p = 0.003; *FGF2+/+*, n = 118 cells; *FGF2-/-*, n = 95 cells) compared to *FGF2+/+* mice (n = 3). Values shown represent the proportional mean ± standard error of the proportion.

CHAPTER 4

Impaired Oligodendrocyte Regeneration From PDGFαR Deletion is Improved by Absence of FGF2

Joshua C. Murtie[1], Yong-Xing Zhou[2], Tuan Q. Le[2], Adam C. Vana[3] and Regina C. Armstrong[1,2,3]

[1] Program in Molecular and Cell Biology, [2]Department of Anatomy, Physiology, Genetics, and [3] Program in Neuroscience at the Uniformed Services University of the Health Sciences, Bethesda, MD

ABSTRACT

The role of platelet-derived growth factor (PDGF) in oligodendrocyte lineage cell (OLC) responses in the adult central nervous system (CNS) was determined using *PDGF alpha receptor* (*PDGFαR*) heterozygous (+/-) mice. Resting densities of oligodendrocyte progenitors (OPs) and oligodendrocytes in the corpus callosum were reduced in adult *PDGFαR+/-* mice compared to *PDGFαR+/+* mice. When fed the demyelinating agent cuprizone, *PDGFαR+/-* and *PDGFαR+/+* mice underwent a similar disease progression. However, in response to demyelination, *PDGFαR* heterozygotes had impaired OP proliferation and amplification as well as oligodendroglial repopulation of demyelinated lesions. To test the putative cooperation between PDGFαR signaling and fibroblast growth factor 2 (FGF2) as OP mitogens, *FGF2* knockout mice were crossed with *PDGFαR* heterozygotes. In demyelinated lesions, OP amplification was not further impaired in *PDGFαR+/- FGF2-/-* mice, as compared to *PDGFαR+/-* mice. In fact, oligodendrocyte regeneration was improved. We propose a model in which PDGFαR signaling promotes OP proliferation in response to demyelination while FGF2 predominantly inhibits OP differentiation during remyelination.

INTRODUCTION

Demyelination in the CNS, such as in multiple sclerosis lesions, can result in neurological deficits due to impaired nerve conduction and associated axonal damage. Remyelination can occur in the adult CNS; however, the ability to remyelinate becomes limited with additional demyelinating episodes (reviewed in Bruck et al., 2003). Immature OLCs persist in the adult rodent and human CNS, and may have the potential to enhance remyelination in response to the appropriate signals (Armstrong et al., 1992; Gensert and Goldman, 1997; Chang et al., 2002; Goldman, 2003). Studies in diverse models of demyelination show that proliferation of OPs is a prerequisite for extensive remyelination. These OPs in the adult rodent and human CNS have been identified by expression of NG2 and PDGFαR (Nishiyama et al., 1997; Keirstead et al., 1998; Redwine and Armstrong, 1998).

In vitro and *in vivo* developmental studies have demonstrated OLC responses to PDGF ligands. PDGF is a potent mitogen for OPs both *in vitro* and *in vivo* during early CNS development (Richardson et al., 1988; Calver et al., 1998; Fruttiger et al., 1999). *In vitro* studies indicate a similar mitogenic effect of PDGF on OPs that persist in the adult CNS (Wolswijk and Noble, 1992; Shi et al., 1998; Frost et al., 2003). Overexpression of PDGF from neurons results in a dramatic increase in the number of OPs in the developing CNS (Calver et al., 1998). This increase in cell number is directly proportional to the level of PDGF expression, suggesting that PDGF is a limiting factor in the generation of OPs during development (van Heyningen et al., 2001). Oligodendrocyte density is also elevated in mice overexpressing PDGF; however, this overpopulation is transient so that oligodendrocyte density in the normal mature CNS is

expected to be dependent on axonal signals rather than the supply of soluble trophic factors (Barres and Raff, 1993; Calver et al., 1998).

The absence of PDGF results in dramatic failure to appropriately generate OPs, oligodendrocytes, and myelin in the developing spinal cord in *PDGF-A* knockout mice (Fruttiger et al, 1999). This finding demonstrates the importance of OLC responses to endogenous PDGF. Unfortunately, *PDGF-A* knockout mice die within the first few postnatal weeks and so are not useful for remyelination studies. PDGF ligands directly regulate OLC responses through activation of PDGFαR, the only PDGFR expressed by OLCs (Hart et al., 1989; McKinnon et al., 1990). Homozygous deletion of *PDGFαR* is lethal during late embryonic development due to a host of abnormalities, including incomplete cephalic closure and apoptosis of migrating neural crest cells (Soriano, 1997). Despite the significant developmental deficits in homozygous null mice, *PDGFαR* heterozygotes express half the normal amount of PDGFαR but do not show gross abnormalities (Soriano, 1997). Thus, *PDGFαR* heterozygotes are a useful model for studying the contribution of PDGF signaling in OLCs of the adult CNS, which may be especially important for OP proliferation that is required for remyelination.

In an experimental model of CNS demyelination followed by spontaneous remyelination, PDGF ligand expression is upregulated and the density of proliferating cells expressing PDGFαR is dramatically increased in lesions (Redwine and Armstrong, 1998). The current study demonstrates the importance of PDGFαR signaling in OLCs in the normal adult CNS and in a demyelinating disease model. *PDGFαR* heterozygotes have decreased OP and oligodendrocyte densities in the normal adult white matter. In response to demyelination, OP proliferation and amplification of the OP population was

significantly reduced in *PDGFαR* heterozygotes. Furthermore, oligodendroglial repopulation of lesions was impaired in *PDGFαR+/-* mice as compared to *PDGFαR+/+* mice.

In vitro studies have demonstrated a cooperative interaction between PDGF and FGF2 signaling (Bogler et al., 1990; McKinnon et al., 1990). As with PDGF, FGF2 can act *in vitro* as a mitogen for OPs from neonatal and adult CNS (McKinnon et al., 1990; Wolswijk and Noble, 1992; Frost et al., 2003). Administration of PDGF and FGF2 in combination induces OPs cultured from neonatal and adult rodents to proliferate as self-renewing stem cells (Bogler et al., 1990; Wolswijk and Noble, 1992). Our lab has shown that FGF2 inhibits OP differentiation during development and remyelination, so that FGF2 removal in *FGF2* knockout mice enhances oligodendroglial repopulation of demyelinated lesions (Armstrong et al., 2002; Murtie et al., submitted). The present study now uses *PDGFαR* heterozygotes crossed with *FGF2* knockout mice to evaluate the potential for PDGF and FGF2 to cooperatively influence OLC responses during remyelination.

Based on the current results and our analysis of *FGF2* knockout mice, we propose a model in which PDGF and FGF2 signaling mediate distinct effects on OLCs. Endogenous PDGFαR signaling promotes OP proliferation in response to demyelination while FGF2 predominantly inhibits OP differentiation during remyelination.

RESULTS

Oligodendrocyte and OP density is lower in non-lesioned white matter of adult PDGFαR heterozygotes

In 8-week old *PDGFαR* heterozygotes, proteolipid protein (PLP) mRNA *in situ* hybridization was used to quantify oligodendrocyte density in the corpus callosum. Oligodendrocyte density was significantly reduced in the non-lesioned corpus callosum of *PDGFαR+/-* mice compared to *PDGFαR+/+* mice (Figure 1A). OP density was concurrently decreased in the non-lesioned corpus callosum of *PDGFαR* heterozygotes based on quantification of PDGFαR mRNA *in situ* hybridization (Figure 1B). OP density counts were confirmed using NG2 immunostaining (Figure 1C). OP proliferation was estimated using a 4-hour terminal pulse of BrdU. Very few cells with incorporated BrdU were detected in the corpus callosum (28.31 ± 4.50 cells/mm^2 *PDGFαR+/+*, n = 3; 20.70 ± 1.68 cells/mm^2 *PDGFαR+/-*, n = 3), as expected for the relatively low rate of cell division typically observed in non-lesioned adult white matter.

Oligodendrocyte repopulation of demyelinated lesions is impaired in PDGFαR heterozygotes

The contribution of PDGF signaling to OP proliferation in response to demyelination was tested using dietary cuprizone to induce demyelination. Myelin oligodendrocyte glycoprotein (MOG) immunostaining (Figure 2) and histological staining (not shown) demonstrated that *PDGFαR* heterozygotes undergo the same predictable time course of demyelination and spontaneous remyelination that has been previously reported for adult mice fed cuprizone (Matsushima and Morell, 2001; Armstrong et al., 2002). By 3 weeks into the cuprizone treatment, demyelination is not

yet consistently evident in the corpus callosum (Figure 2A), but there is already

substantial loss of oligodendrocytes (Figure 3C). Demyelination of the corpus callosum

is complete by 6 weeks (Figure 2B). After a further 3 weeks on normal chow to allow

remyelination to proceed, extensive MOG immunoreactivity is again present throughout

the corpus callosum (Figure 2C).

Analysis of oligodendrocyte density over the course of demyelination using PLP

mRNA *in situ* hybridization revealed a dramatic decrease in lesion repopulation by

oligodendrocytes in *PDGFαR* heterozygotes (Figure 3). In *PDGFαR+/+* mice,

oligodendrocyte regeneration is sufficient to regain normal density throughout the

remyelinating corpus callosum after 3 weeks of recovery from cuprizone treatment. In

contrast, the oligodendroglial repopulation response in *PDGFαR+/-* mice was impaired

so that the oligodendrocyte density did not return to the level found in non-lesioned

PDGFαR heterozygotes.

Proliferation is reduced in PDGFαR heterozygotes

Although PDGFαR expression correlates with the vigorous OP proliferation

response to demyelination (Redwine and Armstrong, 1998), a mitogenic function of

PDGFαR signaling has not been demonstrated *in vivo* during remyelination. Previous

studies have documented that maximal OP proliferation is observed in the corpus

callosum after 5 weeks of cuprizone treatment (Armstrong et al., 2002). Therefore, we

used the 5-week time point to analyze OP proliferation in the corpus callosum using

PDGFαR mRNA *in situ* hybridization in combination with detection of BrdU

incorporated during a 4-hour terminal pulse (Figure 4). NG2 immunostaining was not

used to quantify OP density during remyelination because the intense NG2

immunoreactivity on OP cell bodies and processes throughout demyelinated lesions makes accurate cell counts extremely difficult (Keirstead et al., 1998; our unpublished observations).

Total OP density was dramatically reduced in *PDGFαR+/-* mice as compared to *PDGFαR+/+* mice (Figure 4). The density of OPs without detectable BrdU (PDGFαR+, BrdU- cell phenotype) was significantly reduced in *PDGFαR+/-* mice relative to *PDGFαR+/+* mice. Proliferating OP density (PDGFαR+, BrdU+ cell phenotype) was significantly reduced in *PDGFαR+/-* mice as well. Finally, the density of BrdU labeled cells that were not identified as OPs (PDGFαR-, BrdU+ cell phenotype) was also significantly reduced in *PDGFαR* heterozygotes compared to *PDGFαR* wild-type mice. This value could include several cell types with responsive yet undetectable levels of PDGFαR, such as newly formed oligodendrocytes. In addition, several reports have shown that reactive astrocytes express low levels of PDGFαR and may also have the potential to respond to PDGF (Redwine and Armstrong, 1998; Maeda et al., 2001).

To test the potential cooperative interaction of FGF2 and PDGFαR signaling in OP proliferation, OP density and BrdU incorporation was assessed in *PDGFαR+/-* mice crossed with *FGF2-/-* mice. Our previous analysis demonstrated that *FGF2* knockout alone did not significantly alter OP density or proliferation (data reproduced for comparison in Figure 4; Armstrong et al., 2002). As in *PDGFαR+/-* mice, OP proliferation was significantly impaired in *PDGFαR+/-* mice crossed with *FGF2-/-* mice (p = 0.006 for comparison of 75.34 ± 9.81 cells/mm^2 *PDGFαR+/- FGF2-/-* mice, n = 5, with 119.38 ± 42.16 cells/mm^2 *PDGFαR+/+ FGF2+/+* mice, n = 4). Importantly, loss

of FGF2 in *PDGFαR+/- FGF2-/-* mice did not exacerbate the already reduced OP

density or impaired proliferation observed in *PDGFαR+/-* mice (Figure 4).

Differentiation and survival of OLCs is not changed in PDGFαR heterozygotes

In vivo lineage tracing with replication-incompetent retrovirus was used to

determine the impact of decreased PDGFαR expression on differentiation of OPs into

oligodendrocytes during the course of demyelination and remyelination. Three days prior

to initiation of cuprizone treatment, NIT-GFP retrovirus was stereotactically injected into

the corpus callosum of 8-week-old mice to infect the endogenous cycling cells of the

adult white matter. Injecting with retrovirus prior to inducing demyelination allows

infection of endogenous cycling cells but not reactive astrocytes and microglia (Gensert

and Goldman, 1997; Murtie et al., submitted). Endogenous cycling cells of the adult

white matter have the potential to remyelinate after a demyelinating insult, and infection

of these cells with a heritable reporter gene can monitor OP differentiation *in vivo* during

the generation of remyelinating oligodendrocytes (Gensert and Goldman, 1997; Murtie et

al., submitted). After 6 weeks of cuprizone treatment followed by a 3-week recovery

period for remyelination, GFP-labeled cells were analyzed. Both OPs and

oligodendrocytes were labeled by retroviral GFP after recovery from demyelination.

Oligodendrocytes were identified morphologically by the presence of bifurcating

processes that form "T" intersections parallel to axons as well as by immunostaining for

the oligodendrocyte marker CC1 (Figure 5A-C). OPs were identified by double

immunostaining for the OP markers NG2 and PDGFαR (Figure 5D-G). *In vivo* OP

differentiation was assessed by determining the proportion of total GFP-labeled cells that

were identified as OPs or oligodendrocytes. This quantification indicated that

differentiation of OPs was not changed in *PDGFαR+/-* mice as compared to

PDGFαR+/+ mice (Figure 5H, I). Similar proportions of OPs and oligodendrocytes

were found in both genotypes. The remaining proportion of cells that were not identified

by cell type-specific markers had morphologies consistent with OLCs and this proportion

of cells was also not significantly different between genotypes.

PDGF acts as a survival factor for OPs and newly formed oligodendrocytes *in*

vitro (Barres et al., 1992). TUNEL analysis was completed on *PDGFαR* heterozygotes

after 6 weeks of cuprizone treatment to determine if OLC survival was affected by a

decrease in PDGFαR expression. Cell death from cuprizone toxicity should be minimal

at this time point (Mason et al., 2000). With this in mind, the 6-week cuprizone time

point should be the appropriate stage at which to test for a survival effect on OPs and

newly formed oligodendrocytes. TUNEL analysis yielded very few TUNEL+ cells in

either genotype; furthermore, there was no significant genotypic effect on cell survival

(50.76 ± 6.46 cells/mm^2 in *PDGFαR+/+* mice, n = 3; 27.83 ± 6.95cells/mm^2 in

PDGFαR+/- mice, n = 3; p = 0.063).

Absence of FGF2 rescues the oligodendrocyte repopulation deficit in PDGFαR heterozygotes

Absence of FGF2 can have a beneficial effect on oligodendroglial repopulation of

demyelinated lesions (Armstrong et al., 2002). To assess the impact of the absence of

FGF2 in the context of decreased PDGFαR expression, *PDGFαR* heterozygotes were

crossed with *FGF2* knockout mice to produce *PDGFαR+/- FGF2-/-* mice, which were

demyelinated by cuprizone ingestion. *PDGFαR+/- FGF2-/-* mice underwent the same

characteristic pattern of oligodendrocyte loss over the treatment period and significant

oligodendrocyte repopulation occurred after 3 weeks of recovery from cuprizone treatment (Figure 6A). Interestingly, the absence of FGF2 improved the oligodendrocyte density in *PDGFαR+/- FGF2-/-* mice, as compared to the deficit in *PDGFαR+/-* mice (Figure 3). The absence of FGF2 in *PDGFαR+/- FGF2-/-* mice enabled the oligodendrocyte density in non-lesioned white matter to achieve normal levels. Furthermore, comparison of lesion repopulation by oligodendrocytes in *PDGFαR+/-* mice, *FGF2-/-* mice, and *PDGFαR+/- FGF2-/-* mice expressed as a percentile of the respective lesioned wild-type mice of the same genetic background, demonstrates the nature of the combined gene disruption in *PDGFαR+/- FGF2-/-* mice (Figure 6B). These findings are consistent with distinct effects on OLCs of endogenous signaling through PDGF and FGF2 in the course of experimental demyelination and remyelination.

DISCUSSION

The influence of PDGF on OPs during early development *in vivo* has been well characterized (Calver et al., 1998; Fruttiger et al., 1999); however, the impact of PDGF on OLC responses in the adult is not well documented *in vivo*. The current study determined the impact of decreased PDGFαR expression on OLC populations in the adult normal and remyelinating CNS. We show that PDGFαR levels play a significant role in the maintenance of OPs and oligodendrocytes in the non-lesioned adult white matter. In response to demyelination, *PDGFαR* heterozygotes have a deficit in lesion repopulation by oligodendrocytes. Furthermore, the cause of this deficit was due to a general decrease in proliferation in response to cuprizone demyelination. This proliferative response was significantly reduced in *PDGFαR* heterozygotes regardless of

FGF2 genotype. In contrast, oligodendroglial repopulation of lesions in *PDGFαR* heterozygotes was significantly improved by removal of FGF2.

The current findings in non-lesioned adult CNS are consistent with previous i*n vivo* manipulation of PDGF levels that demonstrated the importance of PDGF in regulation of OP and oligodendrocyte cell density during development (Barres et al., 1993; Calver et al., 1998; Fruttiger et al., 1999). However, these reports conclude that axon number is the overriding factor that controls the final oligodendrocyte density in the non-lesioned white matter at the end of myelination. Our findings indicate that PDGFαR signaling continues to contribute to OP and oligodendrocyte cell densities in the adult CNS. Presumably, PDGFαR signaling then acts in concert with axonal signals and other growth factor pathways.

The current *in vivo* findings are consistent with the role of PDGFαR signaling *in vitro* as stimulating proliferation of OPs from adult CNS (Wolswijk and Noble, 1992; Shi et al., 1998). In response to demyelination, amplification of OP cells expressing PDGFαR and increased expression of PDGF ligand has been observed in diverse models of experimental demyelination prior to spontaneous remyelination (Redwine and Armstrong, 1998; Hinks and Franklin, 1999; Armstrong et al., 2002; Penderis et al., 2003). The present results now extend these studies to demonstrate a role for endogenous PDGFαR signaling in promoting OP proliferation in the context of a demyelinating lesion environment.

However, several studies have also implicated PDGF as having a role in OLC differentiation as well as survival of OPs and newly generated oligodendrocytes (Barres et al., 1992; Allamargot et al., 2001; Wilson et al., 2003). To evaluate OP differentiation,

we used retroviral lineage tracing over the course of demyelination and remyelination. This same retroviral lineage tracing approach showed a significant effect of FGF2 genotype on OP differentiation (% oligodendrocytes among total GFP-labeled cells = $26.04 \pm 2.45\%$ for *FGF2+/+* mice vs. $53.12 \pm 4.55\%$ for *FGF2-/-* mice; Murtie et al., submitted). The current analysis in *PDGFαR+/+* and *PDGFαR+/-* mice indicated that OP differentiation was not affected by reduction of PDGFαR expression to approximately half the wild-type expression level. However, we cannot yet rule out the possibility that minimal expression of PDGFαR could be sufficient to support normal differentiation. Additionally, an effect on survival was not detected using TUNEL analysis during the transition from demyelination to remyelination. Reduced PDGFαR expression may still be sufficient to transduce a survival signal. Furthermore, TUNEL analysis and other assays of apoptosis identify cells actively undergoing apoptosis that have not been removed by phagocytosis. Therefore, it is possible that subtle changes in cell survival are difficult to detect in our analysis.

FGF2 and FGF receptor (FGFR) levels are increased in demyelinated lesions and FGF2 signaling has significant effects during remyelination (Messersmith et al., 2000; Armstrong et al., 2002). *In vivo*, FGF2 acts as an inhibitor of OP differentiation during myelination as well as remyelination (Murtie et al., submitted). Specifically, *in vivo* retroviral lineage analysis demonstrated that FGF2 inhibits progression from the PDGFαR/NG2+ stage to the CC1+ stage, without significant effects on OP proliferation or survival assays (Armstrong et al., 2002; Murtie et al., submitted). *In vivo*, FGFR expression coincides with the progression of OLC development and is increased in demyelinated lesions (Messersmith et al., 2000; Bansal et al., 2003). However, FGFR

types can be expressed by many cell types in CNS pathologies, including reactive

astrocytes (Komoly et al., 1992; Ballabriga et al., 1997; Messersmith et al., 2000). Given

that expression of PDGF and PDGFαR is also increased in demyelinated lesions

(Redwine and Armstrong, 1998; Hinks and Franklin, 1999), FGF2 and PDGF could

possibly act simultaneously in the lesion environment.

   PDGFαR heterozygotes and *FGF2* knockout mice provided an excellent

opportunity to evaluate the potential *in vivo* interaction between PDGF and FGF2.

Cooperation between PDGF and FGF2 has been reported to convert slowly dividing OPs

from adult CNS into rapidly dividing cells *in vitro*, indicative of an important potential

role in repair of demyelinated lesions *in vivo* (Wolswijk and Noble, 1992). Accordingly,

absence of FGF2 combined with decreased expression of PDGFαR may have been

predicted to exacerbate the *PDGFαR* heterozygote effect of impaired OP proliferation

and lesion repopulation by oligodendrocytes. Our results do not support a role for FGF2

in cooperating with PDGFαR signaling for a mitogenic effect on OPs. However, *FGF2*

knockout mice have enhanced oligodendroglial repopulation of cuprizone-induced

lesions compared to wild-type controls (Armstrong et al., 2002). The current results are

consistent with a predominant effect of *FGF2* knockout as promoting lesion repopulation

in *PDGFαR+/- FGF2-/-* mice by removing FGF2 inhibition of differentiation.

   We propose a model in which endogenous PDGF and FGF2 predominantly

mediate distinct effects on OLCs in white matter (Figure 7). Specifically, *in vivo*

PDGFαR signaling regulates OP proliferation in response to demyelination while FGF2

inhibits OP differentiation during remyelination. These affects have been observed

within the CNS white matter in the normal adult and in the course of experimental

demyelination. This model does not address potential PDGF and/or FGF2 regulation of neural stem cell responses that could occur in distinct sites. Furthermore, the genetic deletions utilized here address removal of endogenous PDGFαR and FGF2 signaling. Additional potential neural stem cell and OLC responses may be elicited by exogenous administration to elevate PDGF and FGF2 levels (Lachapelle et., 2002).

 To accomplish remyelination, we show that PDGFαR signaling is critical for normal OP amplification in response to demyelination. However, generation of oligodendrocytes from this reduced OP population was improved by removal of FGF2 inhibition of differentiation. This finding is extremely important with respect to potential treatment of diseases in which oligodendrocyte regeneration is needed. To promote remyelination, attenuation of FGF2 signaling might be sufficient for overcoming reduced OP density or a lesion environment that lacks adequate support for fully exploiting the potential for oligodendrocyte regeneration.

With direct significance to the human context, OPs from human fetal tissue are responsive to PDGF and express PDGFαR (Zhang et al., 2000; Wilson et al., 2003). Furthermore, OPs that express PDGFαR can be abundant in MS lesions (Maeda et al., 2001), indicating the potential to respond to changes in PDGF expression. FGF2 is also present in MS lesions (Holley et al., 2003) and may limit successful remyelination through inhibition of endogenous OP differentiation. PDGF and FGF2 are likely to regulate OP responses in vivo in the context of multiple signals, including not only other growth factors but also cytokines and cell adhesion molecules. Understanding the interactions between various signals and resulting OLC responses will be necessary for

the success of growth factor-based treatments of demyelinating diseases.

MATERIALS AND METHODS

Animals

Mice were bred and maintained in the USUHS animal housing facility and all procedures were performed in accordance with guidelines of the National Institutes of Health and the USUHS Institutional Animal Care and Use Committee. *PDGFαR* targeted deletion mice on the C57Bl/6 genetic background were obtained from breeding heterozygous pairs (generously provided by Dr. Soriano, Fred Hutchinson Cancer Research Center). The *PDGFαR* targeted deletion replaces a 6.5 kb fragment corresponding to the signal peptide, first and second Ig domains (Soriano, 1997). *FGF2* knockout mice on the 129 Sv-Ev:Black Swiss genetic background were obtained from breeding heterozygous pairs (generously provided by Dr. Doetschman, University of Cincinnati). This *FGF2* knockout was generated by a targeted deletion replacing a 0.5 kb portion of the *FGF2* gene including 121 bp of the promoter and the entire first exon with an *Hprt* mini-gene (Zhou et al., 1998). *PDGFαR+/- FGF2-/-* mice were generated by crosses of *PDGFαR* heterozygous mice with *FGF2* knockout mice and the line was maintained on a mixed (129 Sv-Ev:Black Swiss:C57Bl/6) genetic background.

Cuprizone Experimental Demyelination

Male 8-week-old mice were placed on a diet of 0.2% (w/w) cuprizone (finely powdered oxalic bis(cyclohexylidenehydrazide); Aldrich, Milwaukee, WI) thoroughly mixed into milled chow (Harlan Teklad; Madison, WI), which was available *ad libitum*. Mice were maintained on the cuprizone diet until being returned to normal chow pellets after 6 weeks. Cuprizone ingestion results in a reproducible pattern of corpus callosum

demyelination followed by spontaneous remyelination during subsequent weeks on normal chow (Matsushima and Morell, 2001; Armstrong et al., 2002).

Tissue Preparation and Histopathological Analysis

Mice were perfused with 4% paraformaldehyde, then brains were dissected prior to overnight post-fixation in 4% paraformaldehyde (Redwine and Armstrong, 1998). Brain tissue was cryoprotected and embedded in OCT compound for immunostaining and *in situ* hybridization. For histopathology, tissue was embedded in paraffin and sections were stained with Luxol fast blue to detect myelin combined with periodic acid-Schiff reaction for monitoring the macrophage/microglial response (performed by USUHS histological service).

In Situ Hybridization

In situ hybridization and preparation of digoxigenin-labeled riboprobes were performed as previously detailed (Redwine and Armstrong, 1998; Messersmith et al., 2000). Antisense riboprobes were used to detect mRNA transcripts for PLP (gift from Dr. Lynn Hudson; National Institutes of Health; Hudson et al., 1987) and PDGFαR (gift from Dr. Bill Richardson; University College London; Fruttiger et al., 1999). The digoxigenin-labeled riboprobes were hybridized to 15-μm cryosections of brain or spinal cord tissues. Digoxigenin was detected with an alkaline phosphatase-conjugated sheep anti-digoxigenin antibody (Boehringer Mannheim, Indianapolis, IN), followed by reaction with NBT/BCIP substrate (DAKO, Carpinteria, CA). For detection of PDGFαR mRNA, the NBT/BCIP reaction was incubated overnight to amplify the signal. This protocol allowed grossly similar detection of PDGFαR mRNA signal from cells in *PDGFαR+/-* and *PDGFαR+/+* mice.

BrdU Incorporation and Detection

In situ hybridization combined with bromodeoxyuridine (BrdU) incorporation was carried out as detailed previously (Redwine and Armstrong, 1998). Mice were injected intraperitoneally with 200 mg/kg BrdU (Sigma, St. Louis, MO) at 4 hours and 2 hours prior to sacrifice. After *in situ* hybridization detection, sections were treated with HCl then incubated overnight with a monoclonal anti-BrdU antibody directly conjugated with horseradish peroxidase (diluted 1:15; Boehringer Mannheim). Peroxidase activity was detected by incubation with 3,3'-diaminobenzidine (DAB; Vector Labs, Burlingame, CA).

Immunohistochemistry

To identify OPs *in situ*, 15-µm cryosections were immunostained for NG2 and PDGFαR (Messersmith et al., 2000; Armstrong et al., 2002). Primary antibodies used were rabbit polyclonal anti-NG2 antibody (1:500; gift from Dr. William Stallcup, La Jolla, CA) and rat monoclonal anti-PDGFαR antibody (APA5 used at 1:200; Pharmingen, San Diego, CA). Donkey anti-rabbit IgG F(ab')$_2$ conjugated with Cy3 (Jackson Immunoresearch, West Grove, PA) was used to detect NG2 while the PDGFαR was detected with biotinylated donkey anti-rat IgG F(ab')$_2$ (Jackson Immunoresearch) followed by coumarin tyramide amplification (New England Nuclear, Boston, MA).

Mature oligodendrocytes were identified with CC1, which immunostains oligodendrocyte cell bodies without labeling myelin (Fuss et al., 2000). The CC1 antibody (Oncogene Research Products, Cambridge, MA) was detected with donkey anti-mouse IgG F(ab')$_2$ conjugated with Cy3 (Jackson Immunoresearch). The CC1

immunostaining conditions were previously tested to ensure that CC1 did not label astrocytes or NG2-labeled cells (Messersmith et al., 2000).

Myelin was immunostained with monoclonal antibody 8-18C5, which recognizes MOG (hybridoma cells provided by Dr. Minetta Gardinier; University of Iowa, Iowa City, IA; Linnington et al., 1984). MOG immunolabeling was detected with donkey anti-mouse IgG F(ab')$_2$ conjugated with Cy3 (Jackson Immunoresearch).

Retrovirus Production

A 293 cell line stably transfected with pNIT-GFP, a replication-incompetent retroviral expression vector encoding GFP, (provided by Dr. Fred Gage; Salk Institute, La Jolla, CA; Palmer et al., 1999) was transiently transfected with pMD.G (plasmid containing the vesicular stomatitis virus glycoprotein) and cultured for two days. Virion-containing supernatants were concentrated 100-fold by centrifugation at 50,000 x g at 4^0 C for 150 min. Viral pellets were reconstituted in Hanks balanced salt solution to a final concentration of 100x the original concentration. Titers, typically 10^5 cfu/mL, were determined by GFP expression after infection of NIH 3T3 cells with serial dilutions of concentrated virus.

Apoptosis

After 6 weeks of cuprizone treatment, adult mouse corpus callosum was analyzed for cells undergoing apoptosis. Cryosections (15 m) were processed using a modified TUNEL assay (ApopTag Plus peroxidase *in situ* apoptosis detection kit; Intergen, Purchase, NY). The 3'-OH DNA ends, generated by DNA fragmentation typically observed with apoptotic cells, were labeled with digoxigenin-dUTP using terminal deoxynucleotidyl transferase (TdT). The digoxigenin tag was then detected with an anti-

digoxigenin antibody conjugated with peroxidase to yield a dark brown reaction product with DAB substrate. The sections were lightly counterstained with methyl green to detect nuclei.

Stereotactic Surgery and Retrovirus Injection

Three days prior to cuprizone treatment, 8-week-old male mice were anesthetized with isoflurane and body temperature was maintained with 37^0 C isothermal heating pads. Heads were stabilized in the stereotactic apparatus using cushioned ear bars and a burr hole was drilled into the skull at the following coordinates: bregma –1.0 mm and 0.25 mm lateral to the sagittal suture (Franklin and Paxinos, 1997). In these adult mice, virus (10^2 cfu in 1.0 μL) was injected directly into the corpus callosum at a depth of 1.875 mm and a rate of 0.2 μL per minute. After injection, the burr hole was sealed using Gelfoam and the wound closed with a single wound clip.

After 6 weeks of cuprizone treatment and 3 weeks of recovery, mice were transcardially perfused with 3% paraformaldehyde in 0.1M phosphate buffer followed by fixation overnight at 4^0 C in 3% paraformaldehyde. Tissues to be used for immunohistochemistry were cryoprotected in 30% sucrose overnight at 4^0 C then embedded in OCT compound and stored at $–80^0$ C.

Imaging, Quantification, and Statistical Analysis

Images of *in situ* hybridization results were captured with a Spot 2 digital camera using Spot Advanced image acquisition software (Diagnostic Instruments, Sterling Heights, MI) on an Olympus IX-70 microscope (Figures 2A, B, C, 3A, B: 4x air UPLAN FL, 0.13 NA; Figure 4A: 40x air PLAN, 0.65 NA). Fluorescent images were captured using a Laser Scanning PASCAL 5 Zeiss confocal microscope (Figure 5A-G: 100x oil

PLAN APO, 1.4 NA). A stack of Z series images was acquired and the maximum projection of this image stack was generated using Zeiss Pascal 5 software. Images were prepared as panels using Adobe Photoshop.

For cell density quantification, cells expressing PLP mRNA were quantified using unbiased stereological morphometric analysis (Messersmith et al., 2000; Stereologer System Systems Planning and Analysis, Inc., Alexandria, VA). Analysis was restricted to the corpus callosum region, from the midline and extending laterally to below the cingulum in 15-µm-thick coronal sections. The unbiased stereological method could not be used appropriately for conditions with relatively few cells of interest in any particular category. Therefore, quantification of PDGFαR/BrdU single- and double-labeled categories in the corpus callosum required counting all labeled cells and measuring the area sampled (Armstrong et al., 2002). Using the Stereologer System, the thickness is sampled as part of the definition of each "dissector" volume, so that density measurements reflect cells per cubic millimeter. However, without the Stereologer System, section thickness could not be sampled in the mounted specimen, and so the density measurements are stated as cells per square millimeter.

Each category analyzed included 3 or more tissue sections per mouse and 3 or more mice per condition. Specific numbers of animals per sample are $n = 3$ except where noted in text and/or figure legends. Unpaired Student's *t*-tests were used to identify significant differences between genotypes and/or treatments. No statistical comparisons were made between mice with different genetic backgrounds (*i.e. PDGFαR+/-* mice were not compared to *FGF2-/- PDGFαR+/-* mice). The significance of proportions generated in lineage tracing was tested using the χ^2 statistical test.
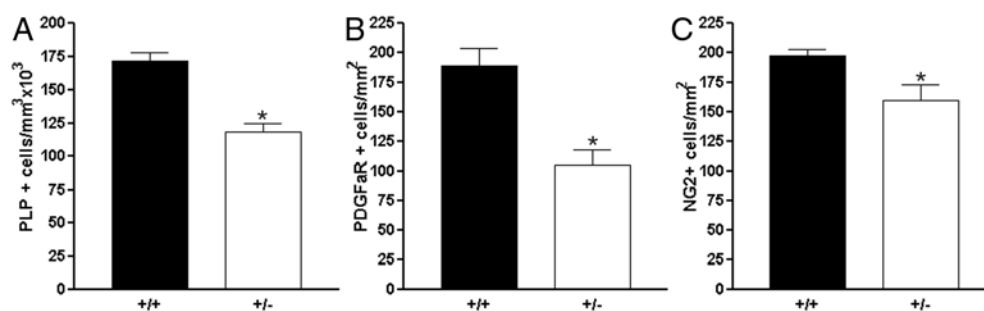
Acknowledgements

Figure 1

Figure 1: OLC populations are reduced in the non-lesioned white matter of adult PDGFαR heterozygotes. 8-week-old *PDGFαR+/+* mice (black bars) and *PDGFαR+/-* mice (white bars) were used to quantify the density of oligodendrocytes (**A**) and OPs (**B**, **C**) in the corpus callosum. (**A**) *In situ* hybridization for PLP mRNA showed that oligodendrocyte density in *PDGFαR* heterozygotes was significantly lower than in wild-type controls (* p = 0.002). (**B**, **C**) The density of OPs in the non-lesioned corpus callosum was significantly lower in *PDGFαR* heterozygotes than in wild-type controls, using OP identification by *in situ* hybridization for PDGFαR mRNA (**B**, * p = 0.003) and by NG2 immunostaining (**C**, * p = 0.015).

Figure 2
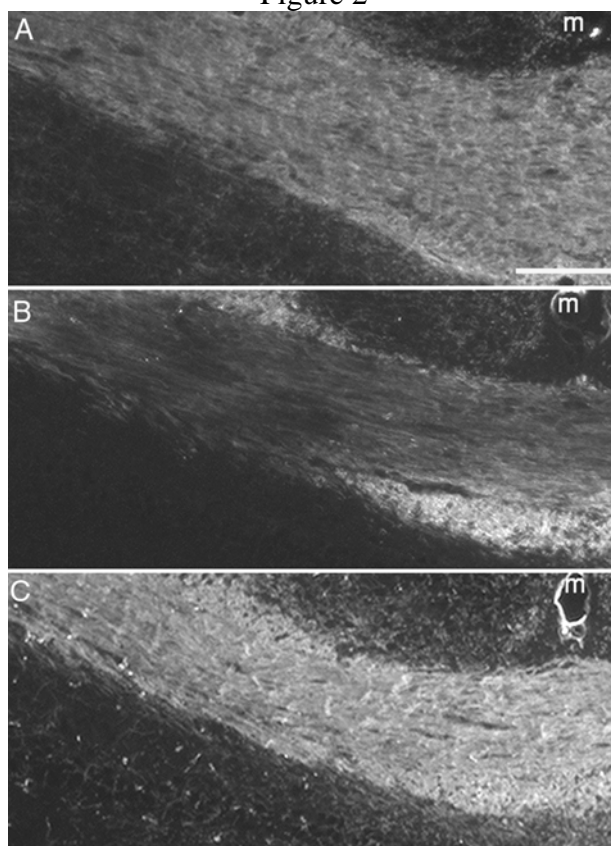
Figure 2: Demyelination and remyelination in PDGFαR heterozygotes. MOG immunostaining was used to detect myelinated fibers over the course of cuprizone treatment in *PDGFαR* heterozygotes. (**A**) Myelin is not yet consistently degenerated and phagocytosed after 3 weeks of cuprizone ingestion so that MOG immunostaining is still present in the corpus callosum. (**B**) Maximal demyelination is observed in *PDGFαR* heterozygotes after 6 weeks of cuprizone ingestion so that the corpus callosum is almost completely devoid of MOG immunostaining. (**C**) Extensive remyelination is indicated by MOG immunoreactivity throughout the corpus callosum after 6 weeks of cuprizone ingestion followed by 3 weeks of recovery on normal chow. (m = midline) Scale bar = 100 μm.
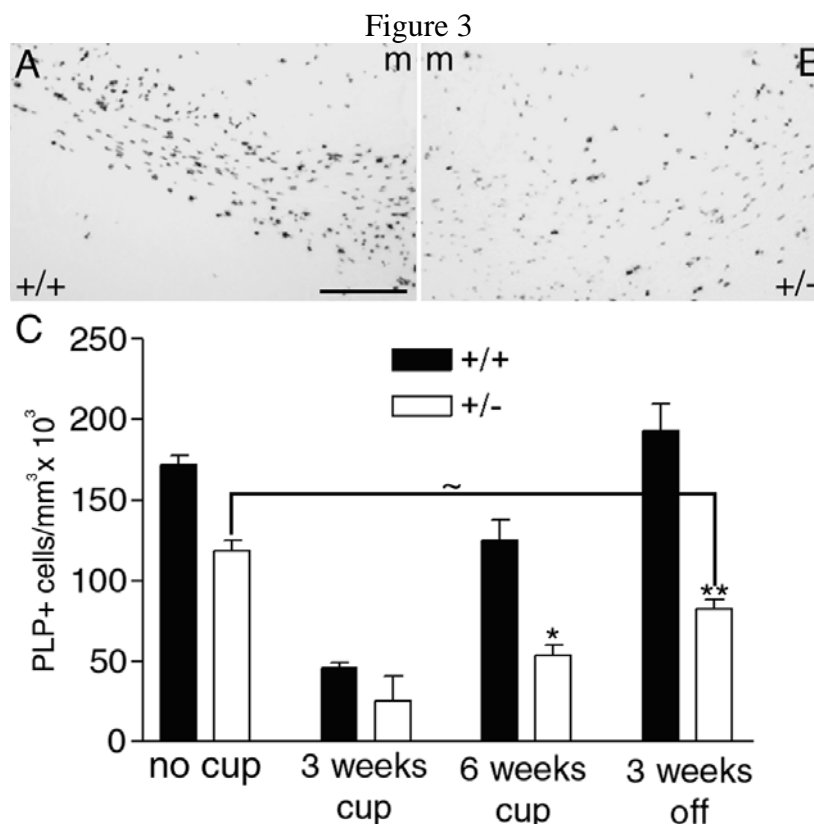
Figure 3

Figure 3: Oligodendrocyte density relative to cuprizone treatment. *In situ* hybridization for PLP mRNA was used to assess oligodendrocyte density at specific time points of cuprizone treatment and recovery. Representative images of PLP mRNA *in situ* hybridization of coronal brain sections from *PDGFαR+/+* (**A**) and *PDGFαR+/-* (**B**) mice. PDGFαR heterozygotes are not able to repopulate the lesioned corpus callosum after 3 weeks of recovery from cuprizone ingestion. (**A**, **B**; m = midline; scale bar = 100 μm) (**C**) Quantification of PLP mRNA-labeled cell density prior to cuprizone ingestion (8 weeks old; no cup), over the duration of cuprizone treatment, and after a 3-week recovery period, revealed significant deficits in oligodendrocyte density in *PDGFαR+/-* mice (white bars) as compared to *PDGFαR+/+* mice (black bars). Specifically, oligodendrocyte regeneration was significantly impaired in *PDGFαR* heterozygotes after 6 weeks of cuprizone ingestion (* p = 0.008; 6 weeks cup) and after 3 weeks of recovery (** p = 0.003; 3 weeks off). After the 3-week recovery period, oligodendrocyte density in wild-type mice returned to the level found in non-lesioned 8-week-old mice (3 weeks off vs. no cup; black bars). In contrast, oligodendrocyte density in *PDGFαR* heterozygotes after 3 weeks of recovery did not return to the level found in *PDGFαR* heterozygotes prior to demyelination (white bars, 3 weeks off vs. no cup; ~ p = 0.015).
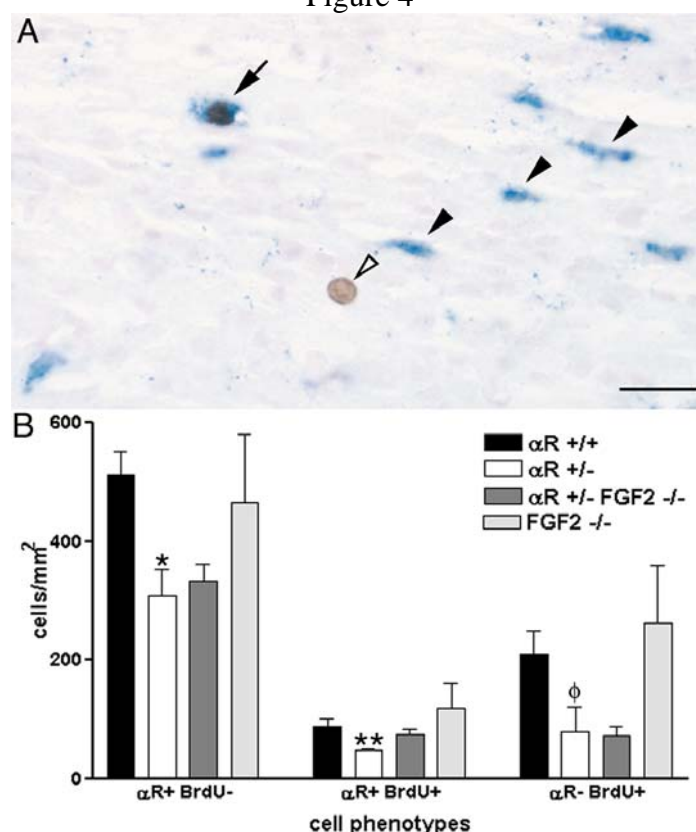
Figure 4

Figure 4: Proliferation in PDGFαR heterozygotes and PDGFαR +/- FGF2 -/- mice. (**A**) Representative image of PDGFαR mRNA *in situ* hybridization (blue cytoplasm) in combination with BrdU immunostaining (brown nuclei) in the corpus callosum of a *PDGFαR* heterozygote. (**B**) Quantification of OP amplification in *PDGFαR* wild-type mice (αR +/+, black bars) and heterozygotes (αR +/-, white bars) in comparison with *PDGFαR+/- FGF2-/-* mice (αR +/- FGF2 -/-; dark gray bars) and *FGF2-/-* mice (light gray bars). The density of cells that had not incorporated BrdU (black arrowheads in **A**; αR+ BrdU- in **B**) is significantly decreased in PDGFαR heterozygotes (αR +/+ vs. αR +/-; * p = 0.012). A significant decrease was also observed in the density of dividing OPs (black arrow in **A;** αR+ BrdU+ in **B**) (αR +/+ vs. αR +/-; ** p = 0.026). The density of BrdU-labeled cells that were not identified as OPs (white arrowhead in **A**; αR- BrdU+ in **B**) was also significantly reduced in *PDGFαR* heterozygotes (αR +/+ vs. αR +/-; φ p = 0.038). A very similar pattern to the *PDGFαR* heterozygous effect was observed in *PDGFαR* heterozygotes crossed with *FGF2* knockout mice (αR +/- FGF2 -/-). Values from previously analyzed *FGF2-/-* mice (Armstrong et al., 2002) are shown to demonstrate the similarity of *FGF2-/-* values to *PDGFαR+/+* values. This similarity indicates that the observed effect in *PDGFαR+/- FGF2-/-* is not the result of the *FGF2* gene disruption. Scale bar = 25 μm.
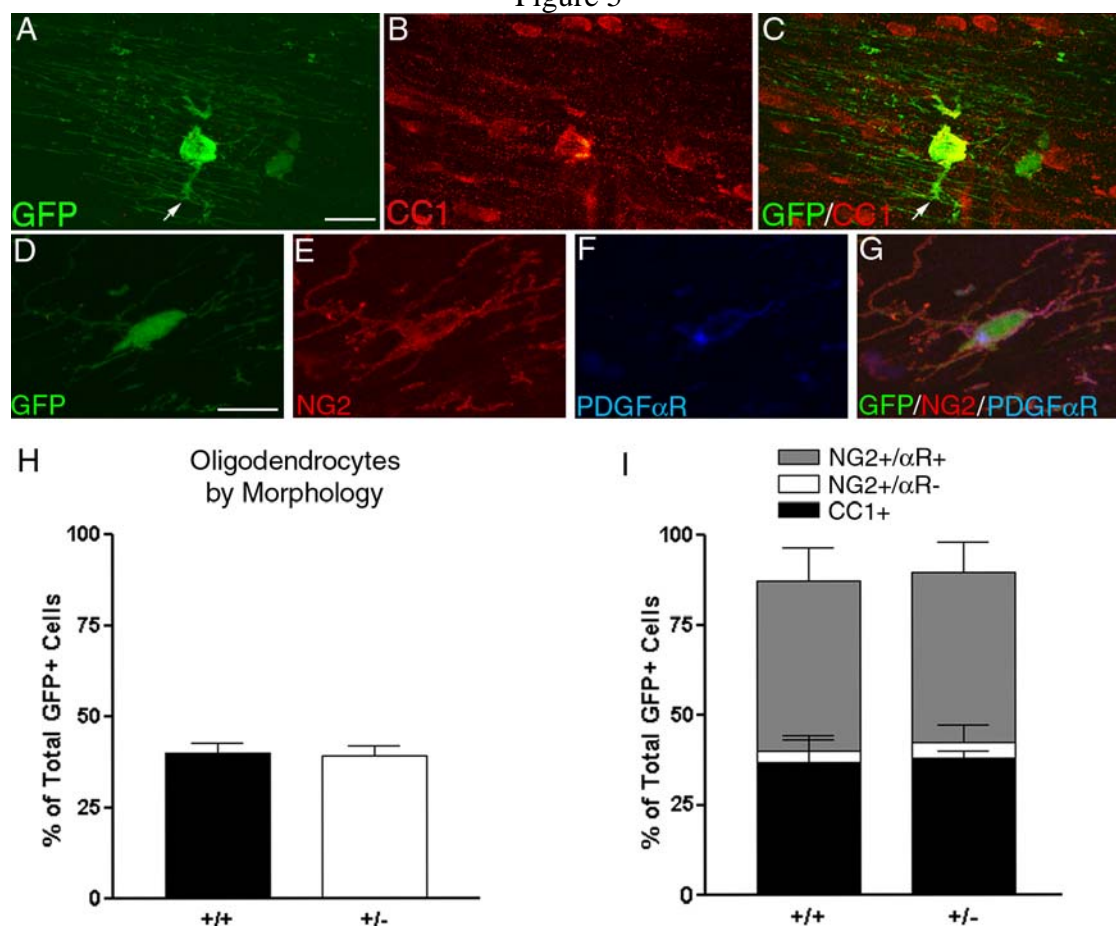
Figure 5

Figure 5: In vivo differentiation in PDGFαR heterozygotes. (**A**-**C**) Representative images of a CC1+/GFP+ oligodendrocyte in the corpus callosum of a *PDGFαR* heterozygote after 3 weeks of recovery following 6 weeks of cuprizone ingestion. CC1 immunostaining (**B**, red) is found in the cell body of a GFP+ (**A**, green) oligodendrocyte (**C**, overlap in yellow). Oligodendrocytes were also morphologically identified by the presence of bifurcated processes forming "T" intersections parallel to axon tracts (arrows). (**D**-**G**) Representative images of a PDGFαR+/NG2+/GFP+ OP in the corpus callosum of a *PDGFαR* heterozygote after 3 weeks of recovery from cuprizone ingestion. PDGFαR immunostaining (**F**, blue) is clustered at one end of the cell body with NG2 immunostaining (**E**, red) outlining the cell body and processes of a GFP+ (**D**, green) OP. (**H**) The proportion of total GFP+ cells that were morphologically identified (see text) as oligodendrocytes after 3 weeks of recovery from cuprizone treatment is not changed by *PDGFαR* genotype. (**I**) The proportions of total GFP+ cells that were identified by the cell type-specific markers CC1, PDGFαR, and NG2 is the same in *PDGFαR+/-* mice as compared to *PDGFαR+/+* mice. **A**, **D**: Scale bars = 10 μm.
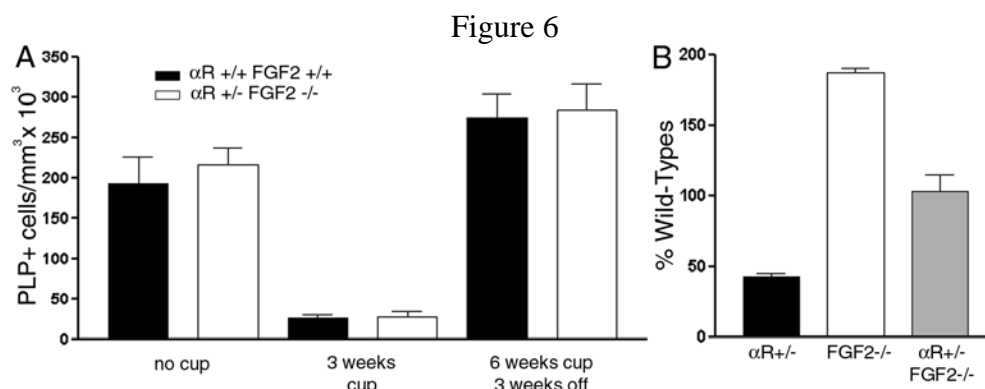
Figure 6

Figure 6: Lesion repopulation by oligodendrocytes in PDGFαR+/- FGF2-/- mice. (**A**) *In situ*
hybridization for PLP mRNA to assess oligodendrocyte density over the course of cuprizone treatment in
PDGFαR+/- FGF2-/- mice (black bars) as compared to *PDGFαR+/+ FGF2+/+* mice (white bars). The
oligodendrocyte density is the same at 8 weeks of age, prior to the start of cuprizone treatment. Similar
oligodendrocyte loss is observed in both genotypes after 3 weeks of cuprizone treatment. Similar recovery
is observed after 6 weeks of cuprizone treatment followed by 3 weeks of recovery. Oligodendrocyte
density in *PDGFαR+/- FGF2-/-* mice is statistically indistinguishable from *PDGFαR+/+ FGF2+/+* mice
at all 3 time points measured. (**B**) The oligodendrocyte repopulation response was compared between
PDGFαR+/- (black bar), *FGF2-/-* (white bar), and *PDGFαR+/- FGF2-/-* (gray bar) mice as % wild-type
from each respective line. All mice were compared after 6 weeks of cuprizone treatment followed by a 3-
week recovery period. *PDGFαR+/-* mice have a dramatically reduced repopulation response (data from
Figure 3) whereas *FGF2-/-* mice have enhanced oligodendroglial repopulation (data from Armstrong et al.,
2002). When the two gene disruptions are combined in *PDGFαR+/- FGF2-/-* mice, oligodendroglial
repopulation is quantified as an intermediary value between the two individual gene disruptions to yield the
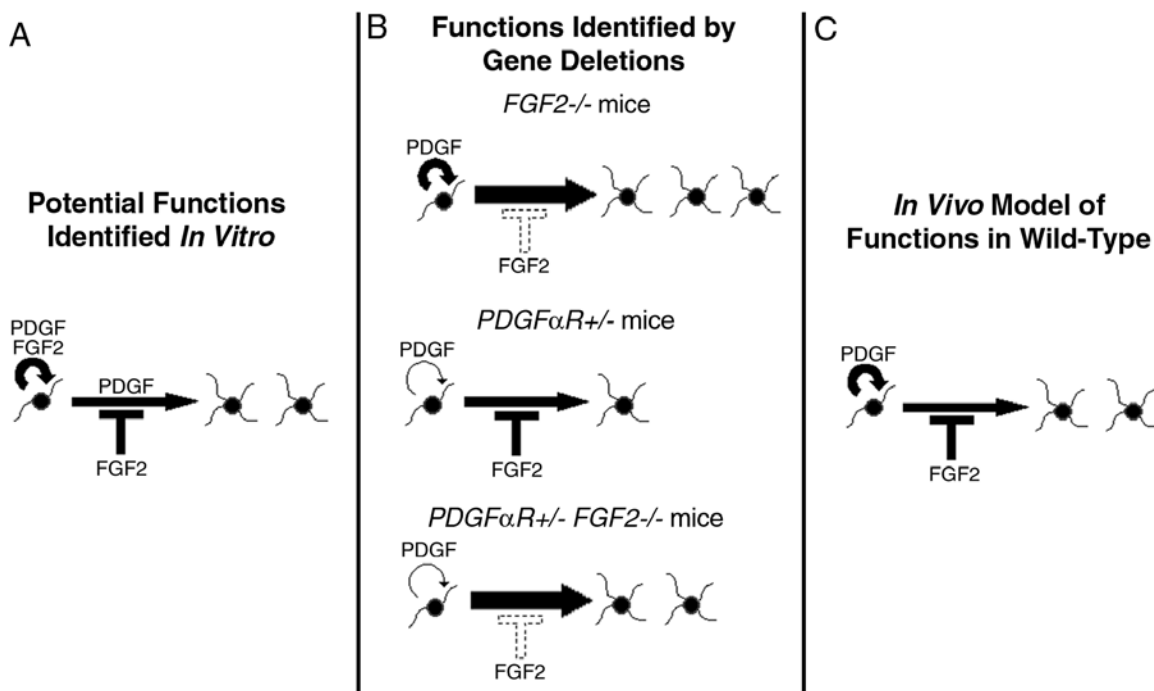equivalent of the wild-type repopulation capacity.

Figure 7

Figure 7: Proposed model for actions of endogenous PDGF and FGF2 on OLCs in the adult CNS. (**A**) *In vitro* studies predict multiple potential roles for PDGF and FGF2 *in vivo*. PDGF and FGF2 can each stimulate OP proliferation, and cooperative interaction of PDGF and FGF2 can induce OPs from adult CNS to divide more rapidly as a self-renewing line. PDGF can promote appropriately timed OP differentiation while FGF2 strongly inhibits differentiation. (**B**) Based on studies using *PDGFαR+/-* mice (current study), *FGF2-/-* mice (Armstrong et al., 2002; Murtie et al., submitted), and *PDGFαR+/- FGF2-/-* mice (current study), these growth factors do not act cooperatively *in vivo*. Reduced PDGFαR expression led to decreased OP proliferation (thin circular arrow) and fewer oligodendrocytes. Removal of FGF2 inhibition of differentiation (dotted intersecting bars) led to increased OP differentiation into oligodendrocytes. (**C**) These results in mouse models led to the propose model of endogenous PDGF and FGF2 functions. PDGF is an important OP mitogen (thick circular arrow), particularly during the OLC response to demyelination. FGF2 predominantly inhibits differentiation (solid intersecting bars) of OPs into oligodendrocytes, which is critically important during remyelination. A, B, C: Thickness of arrows corresponds with amplitude of cell response; circular arrow indicates OP proliferation; straight arrow indicates promotion of OP differentiation; intersecting bar indicates inhibition of OP differentiation.

CHAPTER 5

Discussion

Summary of Findings

Role of FGF2 during Postnatal Development

The current study, in part, sought to determine the role of FGF2 during postnatal development. Previous studies have shown that FGFR expression occurs throughout the developing CNS prior to the peak of myelination (Kuzis et al., 1995; Bansal et al., 2003). Therefore, determination of relative levels of FGF2 expression during development was critical to understanding the impact of FGF2 on myelination during postnatal development since FGFR expression is known to precede FGF2 expression. We have confirmed that FGF2 mRNA and protein expression is dramatically increased during the peak of myelination in the mouse spinal cord and thus has the potential to play a significant role in regulation of myelination (Chapter 3, Figure 1).

To determine the impact of FGF2 on oligodendrocyte development during myelination, oligodendrocyte cell density counts indicated that the normal overproduction of oligodendrocytes during the peak of myelination does not occur in *FGF2* knockout mice (Chapter 3, Figure 2). Multiple techniques were used to verify oligodendrocyte density in the myelinating spinal cord. All analyses indicated that oligodendrocyte density in the normal spinal cord peaked at P15 then declined to the density observed in the adult while oligodendrocyte density in *FGF2* knockout mice remained constant during myelination. Since there was no overproduction of oligodendrocytes in *FGF2* knockout mice during myelination, we determined if there was

a corresponding decrease in myelin. MOG immunohistochemistry in the P7 and P15 spinal cord indicated that the absence of FGF2 had no impact on the timing or amount of myelin in the developing dorsal column (Chapter 3, Figure 3).

Since the absence of FGF2 resulted in a lack of oligodendrocyte overproduction during development, we sought to determine the mechanism by which FGF2 effected oligodendrocyte development. A 4-hour terminal pulse of bromodeoxyuridine (BrdU) at P7 and P15 allowed us to identify the density of dividing and non-dividing OPs in the developing spinal cord. There was no genotypic effect on overall OP density nor was there an effect on the density of dividing and non-dividing OPs at either developmental time point (Chapter 3, Figure 6). Furthermore, OLC survival was unaffected in the developing spinal cord at P7 and P15 as determined by TUNEL analysis (Chapter 3).

Retroviral lineage tracing in the myelinating dorsal column indicated that the OPs differentiated into oligodendrocytes in greater proportions in the absence of FGF2 (Chapter 3, Figure 5), indicating that FGF2 effectively inhibits the differentiation of OPs into oligodendrocytes. Complementary techniques of immunohistochemistry and morphological analysis allowed the identification of *in vivo* cell types labeled with the retroviral reporter gene with similar results. Together these data indicate that OPs in the absence of FGF2 may not undergo the normal number of asymmetric cell divisions prior to differentiation, resulting in the observed changes in oligodendrocyte density and increased differentiation of OPs.

FGF2 and FGFR Expression and its Role in Remyelination

Prior to the current work, the role of FGF2 in remyelination was not well understood. We demonstrate that FGF2 expression is significantly upregulated during

remyelination and this increased expression corresponds with recovery of motor function from demyelination (Chapter 2, Figure 1). This increased FGF2 expression was localized to reactive astrocytes in demyelinated spinal cord lesions (Chapter 2, Figures 2 & 3).

In addition to increased FGF2 expression, the density of FGFR1 and FGFR3-labled cells were increased within demyelinated spinal cord lesions (Chapter 2, Figures 4 & 7). Identification of cell types expressing FGFRs revealed that FGFR1 is expressed by astrocytes and some, but not all, OPs in mixed glial cultures from remyelinating spinal cord (Chapter 2, Figure 5). FGFR2 was identified on oligodendrocytes in non-lesioned white matter and on astrocytes in lesioned white matter (Chapter 2, Figure 6). Finally, FGFR3 expression was localized to multiple glial cell types including astrocytes, oligodendrocytes and OPs (Chapter 2, Figure 8).

Clearly the presence of FGF2 and its high affinity receptors in remyelinating lesions sets up the possibility that FGF2 plays a central role in successful remyelination. However, recent studies have demonstrated that the absence of FGF2 actually enhances lesion repopulation by oligodendrocytes (Armstrong et al., 2002). These studies also indicated that the absence of FGF2 had no effect on OP proliferation or OLC survival. Furthermore, *in vitro* studies indicated that FGF2 may inhibit OP differentiation. In order to address this potential mechanism of action, retroviral lineage tracing was completed *in vivo*. These experiments confirmed *in vitro* results and supported a role for FGF2 as an inhibitor of OP differentiation (Chapter 3, Figure 7). These results demonstrate that removal of inhibition of differentiation can significantly improve lesion repopulation by oligodendrocytes.

Role of PDGFαR Signaling in Remyelination

Unlike FGF2, the *in vivo* role of PDGF during development is well characterized. However, the effects of PDGF signaling in remyelination are not as well studied and may have a significant impact on remyelination through manipulation of OLCs. Therefore, we examined the remyelination response in mice expressing half the normal amount of PDGFαR.

Interestingly, a surprising role for PDGFαR signaling in oligodendrocyte development was identified. *PDGFαR* heterozygotes had decreased oligodendrocyte and OP densities in control non-lesioned adult white matter (Chapter 4, Figure 1). Prior to this finding, it was not thought that PDGF played a role in normal maintenance of oligodendrocyte density in the adult white matter. Previous studies have indicated that axon number is the overriding factor that determines final oligodendrocyte number. These two findings are not in contradiction and both are likely to be critical determining factors.

Induction of demyelination using cuprizone also revealed significant deficiencies in *PDGFαR* heterozygotes. First, *PDGFαR* heterozygotes were shown to undergo the previously characterized pattern of demyelination and remyelination using MOG immunohistochemistry (Chapter 4, Figure 2). Furthermore, *PDGFαR* heterozygotes also displayed the same characteristic pattern of oligodendrocyte loss and repopulation. However, the repopulation response in *PDGFαR* heterozygotes was significantly hindered (Chapter 4, Figure 3). In fact, oligodendrocyte density in wild-type mice had returned to the density observed prior to demyelination while the density of

oligodendrocytes in *PDGFαR* heterozygotes did not return to the density observed prior to demyelination (Chapter 4, Figure 3).

This deficiency in oligodendroglial repopulation was accounted for by significant decreases in overall OP density, dividing OP density, and non-dividing OP density in response to demyelination (Chapter 4, Figure 4). In contrast, no significant genotypic effects on OP differentiation or OLC survival were observed during remyelination (Chapter 4, Figure 5).

Interaction of PDGF and FGF2 during Remyelination

Several *in vitro* studies have demonstrated a potential interaction between PDGF and FGF2 as OP mitogens (Bogler et al., 1990, McKinnon et al., 1990). To test this potential interaction *in vivo*, *PDGFαR* heterozygotes were crossed with *FGF2* knockout mice and demyelination was induced using cuprizone. Analysis of OP proliferation in response to demyelination revealed that the absence of FGF2 did not further impair OP proliferation as might have been predicted from *in vitro* results (Chapter 4, Figure 4). After recovery from demyelination, *PDGFαR+/- FGF2 -/-* mice displayed oligodendroglial lesion repopulation similar to that seen in wild-type mice (Chapter 4, Figure 6). Specifically, the absence of FGF2 rescued the oligodendroglial lesion repopulation deficit observed in *PDGFαR* heterozygotes.

Contribution of Present Findings

In Vitro vs. *In Vivo* Roles of PDGF and FGF2

Identification of the effects of PDGF and FGF2 on the oligodendrocyte lineage has largely been carried out *in vitro*. These experiments have demonstrated several potential effects of these growth factors on the OLCs. Specifically, PDGF and FGF2 have both been identified as potent mitogens for neonatal and adult OPs alike (Bogler et al., 1990, McKinnon et al., 1990; Wolswijk and Noble, 1992; Shi et al., 1998; Frost et al., 2002). In combination with previous studies characterizing the effects of PDGF on OLCs during *in vivo* development (Calver et., 1998; Fruttiger et al., 1999), the current study confirms the *in vitro* identification of PDGF as an *in vivo* OP mitogen. Furthermore, FGF2 has been identified *in vitro* as an inhibitor of OP differentiation (Bansal and Pfeiffer, 1997). The current results have also confirmed this as an *in vivo* role for FGF2 during development and remyelination. However, *in vitro* findings do not always translate into *in vivo* roles. It seems clear based on current results that FGF2 does not appear to play a significant role in OLC survival or proliferation *in vivo* as might be predicted from *in vitro* experiments (Bogler et al., 1990; McKinnon et al., 1990; Muir and Compston, 1996).

Comparison of *in vitro* and *in vivo* results is not always as simple as it may appear. For example, we demonstrated that decreased PDGFαR expression *in vivo* has no detectable effect on OLC survival. These results do not eliminate the possibility that PDGF acts as a survival factor for OPs and newly formed oligodendrocytes as has been demonstrated *in vitro* (Barres et al., 1992). First, TUNEL analysis may not be a definitive assessment of long-term survival *in vivo*. Since dying cells are phagocytosed

and do not accumulate *in vivo*, TUNEL analysis simply determines the relative density of

dying cells at a given time. Therefore subtle changes in density of dying cells may not be

detected using TUNEL or other conventional assays of survival. Furthermore, this lack

of a survival effect on OLCs in *PDGFαR* heterozygotes may simply represent the

possibility that minimal PDGFαR expression is sufficient to transduce a survival signal.

The same can be said for the lack of an effect on OP differentiation in *PDGFαR*

heterozygotes; and this is the difficulty with interpreting results from decreased

expression levels rather than complete elimination of protein expression.

   In vitro experiments are not always meant to identify potential *in vivo* roles. For

example, cell transplantation is becoming a potentially attractive treatment for numerous

diseases and pathologies. In fact animal models of demyelination and dysmyelination

have been used to assess the potential benefits of cell transplants (reviewed in McDonald

and Howard, 2002; Inoue et al., 2003; Pluchino et al., 2003). Optimization of cell

transplant treatment protocols will likely require *in vitro* manipulation of cell populations

in order to induce cells to acquire specific characteristics. Additionally, *in vivo* studies

will be required to determine the potential cellular responses transplanted cells will have

to their new environment.

Current Findings in the Context of Previous *In Vivo* Studies

   As stated previously, PDGF and FGF2 have already been shown to have

significant effects *in vivo*. In light of the current results, these studies can be revisited for

further assessment. Previous studies in which exogenous PDGF was focally administered

to demyelinated lesions resulted in significant increases in OP density and

oligodendrocyte density in addition to increases in remyelination (Allamargot et al.,

2001). These observational findings may now potentially be explained by increased proliferation of OPs as a result of increased PDGF concentration. Interestingly, these studies also found a significant increase in oligodendrocyte density. Consistent with these results, the current study finds decreased oligodendrocyte density in *PDGFαR* heterozygotes during remyelination. These consistent results either represent an effect of altered OP proliferation or an effect on oligodendrocytes themselves. The latter would be an unexpected mechanism of action since oligodendrocytes do not express detectable amounts of PDGFαR.

In comparison to previous studies where PDGF signaling, and potentially other RTKs, was pharmacologically inhibited during remyelination (McKay et al., 1997; McKay et al., 1998), the current results are in complete agreement. Both studies observe decreased oligodendrocyte density as a result of decreased PDGF signaling. Trapidil mediated inhibition of PDGF signaling also resulted in decreased remyelination of lesions. The current study also attempted to quantify the extent of remyelination using MOG immunohistochemistry (data not shown); however, the variability seen in recovery of MOG expression after cuprizone demyelination was so great that a meaningful comparison could not be made.

The current results using *FGF2* knockout mice in cuprizone demyelination appear to contradict previous findings that artificially elevated levels of FGF2 encourage recovery and remyelination from EAE. However, a few critical observations must be made. First, artificially elevating levels of FGF2 may not necessarily represent the same cellular effects as eliminating endogenous FGF2 altogether. As previously stated, FGF signaling involves an extremely complex network of ligands, high and low affinity

receptors, and different concentrations of FGF2 may differentially influence various cell types based on FGFR expression profiles. Furthermore, the current results investigating the role of FGF2 in development do not reflect the results seen during remyelination despite a common mechanism of action. This clearly indicates that FGF2 acts in the context of other signals. Therefore, the apparent contradiction in results may be the result of the timing and level of FGF2 administration. Ruffini et al. utilized the EAE model of demyelination with remyelination and observed an improvement in clinical symptoms and enhanced remyelination. Furthermore, a difference in demyelinating model is not likely to be significant since experiments comparing two demyelinating models in the absence of FGF2 had similar results (Armstrong et al., 2002).

In addition to the different lesion environments between animal models of demyelination, there are also likely to be significant environmental differences between the myelinating and remyelinating CNS. The current results indicate that the removal of FGF2 during development does not have the same effect on oligodendrocyte density that is observed during remyelination (Chapter 3, Figure 2; Armstrong et al., 2002). These apparently contradictory results may reflect the interaction of FGF2 with other signals that regulate oligodendrocyte density during myelination and remyelination. For example, axonal signals regulate oligodendrocyte density during development (Trapp et al., 1997, Calver et al., 1998; Barres and Raff, 1999). One of these putative signals could be the Notch pathway. Notch1 expression has been shown to be induced by FGF2 in a cell line with an immature oligodendrocyte phenotype (Bongarzone et al., 2000). Furthermore, interaction of Notch1 on OLCs with neuronal Jagged1 inhibits further maturation of OLCs and inhibits their expression of myelin proteins (Wang et al., 1998).

These data indicate a potential model by which FGF2 mediates OLC maturation in conjunction with the Notch pathway. Specifically, increased FGF2 expression during development may upregulate OLC expression of Notch1 which then binds neuronal Jagged1, effectively inhibiting further maturation of OLCs.

Current Model for PDGF and FGF2 *In Vivo*

Based on the current results, we can now begin to propose a unifying model that describes the effects of PDGF and FGF2 on the oligodendrocyte lineage *in vivo*. *In vitro*
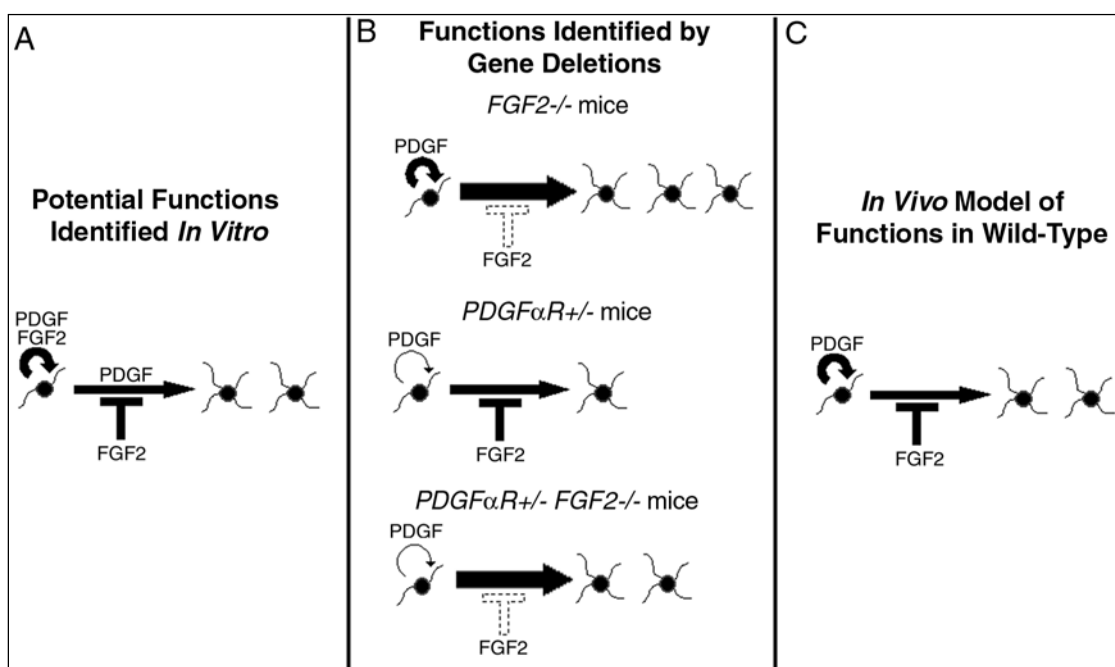
Figure 1: Proposed in vivo model for the action of PDGF and FGF2 on the oligodendrocyte lineage based on current results.

experiments would predict that PDGF and FGF2 cooperatively act as OP mitogens (Bogler et al., 1990; McKinnon et al., 1990). Furthermore, PDGF has been shown to potentially promote OLC maturation (Allamargot et al., 2001; Wilson et al., 2003) while FGF2 has been shown to inhibit OP differentiation (reviewed in Bansal and Pfeiffer, 1997).

The current *in vivo* results using *PDGFαR* heterozygotes and *FGF2* knockout mice in the context of previous *in vivo* studies of these growth factors support the proposed model (Figure 1). Specifically, the predominant role for PDGF is as an OP mitogen *in vivo* during myelination (Calver et al, 1998, Fruttiger et al., 1999) as well as during remyelination (current results). Furthermore, an effect of PDGF on OP differentiation or OLC survival was not detected *in vivo* (current results). PDGF has also been shown to have profound effects on oligodendrocyte density through its role as an OP mitogen.

Prior to the current results, FGF2 may have been expected to act as an OP mitogen alone and in combination with PDGF (Bogler et al, 1990; McKinnon et al, 1990), as an inhibitor of differentiation (Bansal and Pfeiffer, 1997), and as a pro-apoptotic signal to mature oligodendrocytes (Muir and Compston, 1996). The current results demonstrate that the predominant role for FGF2 *in vivo* is as an inhibitor of OP differentiation and not as a mitogen or pro-apoptotic agent.

Future Experiments

Clearly it is necessary to extend the current studies in order to fully address the effects of PDGF and FGF2 on the oligodendrocyte lineage *in vivo*. The most promising area in which these studies may be advanced is in potentially tailoring growth factor treatment of animal models of demyelination. Specifically, several questions could be addressed: would systemic or localized administration of PDGF during the peak in OP proliferation during remyelination enhance the remyelination response? Additionally, would inhibition of FGF2 signaling during late remyelination enhance the remyelination response?

The impaired remyelination response in *PDGFαR* heterozygotes represents a unique opportunity to study other factors that may potentially promote remyelination in an environment that does not support a significant recovery response. As was demonstrated with FGF2, other factors with known effects on the oligodendrocyte lineage such as insulin-like growth factor I (IGF-1) or neuregulin might be tested using *PDGFαR* heterozygotes. Ideally, alternative transgenics would be used to assess these types of interactions. The omnipresent criticism of classical knockout mice is the fact that they have developed in the absence of a specific factor; and the true role of this factor may have been masked by some form of compensation. Conditional-inducible knockouts or the use of cell-specific signal inhibition through the use of dominant-negative proteins would be the ideal approach to assess the impact of any given factor.

Smaller scale experiments that would further the interpretation of the current results include in-depth analysis of proliferation in *PDGFαR* heterozygotes and *FGF2* knockout mice. A 4 hour terminal pulse of BrdU is useful for identification of dividing cell populations since it does not allow for OLC differentiation; however, longer pulses of BrdU would be a more sensitive approach that may reveal subtle changes in the rate of cell proliferation despite the loss of the ability to accurately identify dividing cell types.

The potential interaction of these growth factors with other factors that influence OLC responses was previously alluded to with the discussion of the potential interaction of FGF2 and Notch signaling. These types of studies clearly need to be completed to understand the context in which these growth factors act. It would be beneficial to use complimentary models of demyelination and remyelination, such as the MHV-A59 and

cuprizone models, to assess the impact of immunoregulatory molecules and the presence of lymphocytes on the interaction of factors such as Notch and FGF2.

Growth Factor Treatment of Demyelinating Diseases

Growth factor treatment of demyelinating diseases is a potentially promising approach that may influence multiple treatment strategies. The most obvious application of growth factor treatment of demyelination would be to induce remyelination through the proliferation, differentiation, survival, and myelination of endogenous OLCs that are present in the adult human CNS (Armstrong et al., 1992; Chang et al., 2002). As stated earlier, these approaches have already been tested with promising findings in animal models of demyelination (Allamargot et al., 2001; Ruffini et al., 2001; Lachapelle et al., 2002). These studies have demonstrated the impact of administration of exogenous PDGF and FGF2. In addition to these studies, administration of other factors such as IGF-1 and nerve growth factor (NGF) has shown promising results in animal models of demyelination (Yao et al., 1995; Villoslada et al., 2000). However, inhibition of growth factor signals such as FGF2 may improve regeneration (Armstrong et al, 2002; current results).

While simple administration or inhibition of growth factor signals may be a promising treatment strategy, timing and route of administration must be studied further. For example, IGF-1 treatment of EAE showed promising effects during the acute phase but not the chronic phase of EAE (Canella et al., 2000; O'Leary et al., 2002). The current results also allude to the importance of timing in administration of treatment. Specifically, administration of exogenous PDGF and FGF2 during early stages of recovery may improve OP proliferation while inhibiting their differentiation. Then,

inhibition of FGF2 signaling may effectively encourage the differentiation of the amplified population of OPs. Using experiments that determine the net result of variations in the timing and route of administration would optimize treatment protocols and may prove extremely beneficial.

Another potential benefit of growth factors in treatment of demyelinating disease may be through *in vitro* manipulation of stem cells with the intention of transplant. The overwhelming evidence demonstrating the influence of growth factors on stem cells and OLCs *in vitro* may be used to manipulate cell lineages prior to transplant. One of the possible dangers of stem cell transplants as a treatment strategy is the potential for tumor formation as a result of transplantation of immature cell types. Growth factors may potentially be used to amplify cells *in vitro* while also inducing their commitment to a specific lineage.

Together, the results of the current study have demonstrated the need for *in vivo* analysis of *in vitro* effects of growth factors on the oligodendrocyte lineage. Furthermore, they also demonstrate the importance of environmental context in which growth factors act. This was specifically addressed with opposite results observed using the same *FGF2* knockout mice during myelination and remyelination. All of these factors have supported the potential benefits of growth factor-based treatments while also identifying potential risks.

REFERENCES

Allamargot C, Pouplard-Barthelaix A, Fressinaud C (2001) A single intracerebral microinjection of platelet-derived growth factor (PDGF) accelerates the rate of remyelination in vivo. Brain Res 918:28-39.

Armstrong RC, Harvath L, Dubois-Dalcq ME (1990) Type 1 astrocytes and oligodendrocyte-type 2 astrocyte glial progenitors migrate toward distinct molecules. J Neurosci Res 27:400-407.

Armstrong RC, Dorn HH, Kufta CV, Friedman E, Dubois-Dalcq ME (1992) Pre-oligodendrocytes from adult human CNS. J Neurosci 12:1538-1547.

Armstrong RC (1998) Isolation and characterization of immature oligodendrocyte lineage cells. Methods 16:282-292.

Armstrong RC, Le TQ, Frost EE, Borke RC, Vana AC (2002) Absence of fibroblast growth factor 2 promotes oligodendroglial repopulation of demyelinated white matter. Journal of Neuroscience 22:8574-8585.

Auguste P, Gursel DB, Lemiere S, Reimers D, Cuevas P, Carceller F, Di Santo JP, Bikfalvi A (2001) Inhibition of fibroblast growth factor/fibroblast growth factor receptor activity in glioma cells impedes tumor growth by both angiogenesis-dependent and -independent mechanisms. Cancer Res 61:1717-1726.

Ballabriga J, Pozas E, Planas AM, Ferrer I (1997) bFGF and FGFR-3 immunoreactivity in the rat brain following systemic kainic acid administration at convulsant doses: localization of bFGF and FGFR-3 in reactive astrocytes, and FGFR-3 in reactive microglia. Brain Res 752:315-318.

Bansal R, Kumar M, Murray K, Morrison RS, Pfeiffer SE (1996) Regulation of FGF

receptors in the oligodendrocyte lineage. Mol Cell Neurosci 7:263-275.

Bansal R, Pfeiffer SE (1997) Regulation of oligodendrocyte differentiation by fibroblast growth factors. Adv Exp Med Biol 429:69-77.

Bansal R, Lakhina V, Remedios R, Tole S (2003) Expression of FGF receptors 1, 2, 3 in the embryonic and postnatal mouse brain compared with Pdgfralpha, Olig2 and Plp/dm20: implications for oligodendrocyte development. Dev Neurosci 25:83-95.

Baron W, de Jonge JC, de Vries H, Hoekstra D (2000) Perturbation of myelination by activation of distinct signaling pathways: an in vitro study in a myelinating culture derived from fetal rat brain. J Neurosci Res 59:74-85.

Barres BA, Hart IK, Coles HS, Burne JF, Voyvodic JT, Richardson WD, Raff MC (1992) Cell death and control of cell survival in the oligodendrocyte lineage. Cell 70:31-46.

Barres BA, Raff MC (1993) Proliferation of oligodendrocyte precursor cells depends on electrical activity in axons. Nature 361:258-260.

Barres BA, Raff MC (1999) Axonal control of oligodendrocyte development. J Cell Biol 147:1123-1128.

Baumann N, Pham-Dinh D (2001) Biology of oligodendrocyte and myelin in the mammalian central nervous system. Physiol Rev 81:871-927.

Belachew S, Chittajallu R, Aguirre AA, Yuan X, Kirby M, Anderson S, Gallo V (2003) Postnatal NG2 proteoglycan-expressing progenitor cells are intrinsically multipotent and generate functional neurons. J Cell Biol 161:169-186.

Bergsten E, Uutela M, Li X, Pietras K, Ostman A, Heldin CH, Alitalo K, Eriksson U

(2001) PDGF-D is a specific, protease-activated ligand for the PDGF beta-receptor. Nat Cell Biol 3:512-516.

Blight AR (1993) Remyelination, revascularization, and recovery of function in experimental spinal cord injury. Adv Neurol 59:91-104.

Bogler O, Wren D, Barnett SC, Land H, Noble M (1990) Cooperation between two growth factors promotes extended self-renewal and inhibits differentiation of oligodendrocyte-type-2 astrocyte (O-2A) progenitor cells. Proc Natl Acad Sci U S A 87:6368-6372.

Bongarzone ER, Byravan S, Givogri MI, Schonmann V, Campagnoni AT (2000) Platelet-derived growth factor and basic fibroblast growth factor regulate cell proliferation and the expression of notch-1 receptor in a new oligodendrocyte cell line. J Neurosci Res 62:319-328.

Bruck W, Kuhlmann T, Stadelmann C (2003) Remyelination in multiple sclerosis. J Neurol Sci 206:181-185.

Calver AR, Hall AC, Yu WP, Walsh FS, Heath JK, Betsholtz C, Richardson WD (1998) Oligodendrocyte population dynamics and the role of PDGF in vivo. Neuron 20:869-882.

Cannella B, Pitt D, Capello E, Raine CS (2000) Insulin-like growth factor-1 fails to enhance central nervous system myelin repair during autoimmune demyelination. Am J Pathol 157:933-943.

Chang A, Tourtellotte WW, Rudick R, Trapp BD (2002) Premyelinating oligodendrocytes in chronic lesions of multiple sclerosis. N Engl J Med 346:165-173.

Chen MS, Huber AB, van der Haar ME, Frank M, Schnell L, Spillmann AA, Christ F, Schwab ME (2000) Nogo-A is a myelin-associated neurite outgrowth inhibitor and an antigen for monoclonal antibody IN-1. Nature 403:434-439.

Claesson-Welsh L (1996) Mechanism of action of platelet-derived growth factor. Int J Biochem Cell Biol 28:373-385.

Crowe MJ, Bresnahan JC, Shuman SL, Masters JN, Beattie MS (1997) Apoptosis and delayed degeneration after spinal cord injury in rats and monkeys. Nat Med 3:73-76.

Dal Canto MC, Kim BS, Miller SD, Melvold RW (1996) Theiler's Murine Encephalomyelitis Virus (TMEV)-Induced Demyelination: A Model for Human Multiple Sclerosis. Methods 10:453-461.

Decker L, Avellana-Adalid V, Nait-Oumesmar B, Durbec P, Baron-Van Evercooren A (2000) Oligodendrocyte precursor migration and differentiation: combined effects of PSA residues, growth factors, and substrates. Mol Cell Neurosci 16:422-439.

Deng CX, Wynshaw-Boris A, Shen MM, Daugherty C, Ornitz DM, Leder P (1994) Murine FGFR-1 is required for early postimplantation growth and axial organization. Genes Dev 8:3045-3057.

Dono R, Texido G, Dussel R, Ehmke H, Zeller R (1998) Impaired cerebral cortex development and blood pressure regulation in FGF-2-deficient mice. Embo J 17:4213-4225.

Dumont RJ, Okonkwo DO, Verma S, Hurlbert RJ, Boulos PT, Ellegala DB, Dumont AS (2001) Acute spinal cord injury, part I: pathophysiologic mechanisms. Clin Neuropharmacol 24:254-264.

Fields-Berry SC, Halliday AL, Cepko CL (1992) A recombinant retrovirus encoding

    alkaline phosphatase confirms clonal boundary assignment in lineage analysis of

    murine retina. Proc Natl Acad Sci U S A 89:693-697.

Franklin KBJ, Paxinos G (1997) The mouse brain in stereotaxic coordinates. San Diego:

    Academic Press.

Frost EE, Nielsen JA, Le TQ, Armstrong RC (2003) PDGF and FGF2 regulate

    oligodendrocyte progenitor responses to demyelination. J Neurobiol 54:457-472.

Fruttiger M, Karlsson L, Hall AC, Abramsson A, Calver AR, Bostrom H, Willetts K,

    Bertold CH, Heath JK, Betsholtz C, Richardson WD (1999) Defective

    oligodendrocyte development and severe hypomyelination in PDGF-A knockout

    mice. Development 126:457-467.

Fuss B, Mallon B, Phan T, Ohlemeyer C, Kirchhoff F, Nishiyama A, Macklin WB (2000)

    Purification and analysis of in vivo-differentiated oligodendrocytes expressing the

    green fluorescent protein. Dev Biol 218:259-274.

Gensert JM, Goldman JE (1996) In vivo characterization of endogenous proliferating

    cells in adult rat subcortical white matter. Glia 17:39-51.

Gensert JM, Goldman JE (1997) Endogenous progenitors remyelinate demyelinated

    axons in the adult CNS. Neuron 19:197-203.

Gilbertson DG, Duff ME, West JW, Kelly JD, Sheppard PO, Hofstrand PD, Gao Z,

    Shoemaker K, Bukowski TR, Moore M, Feldhaus AL, Humes JM, Palmer TE,

    Hart CE (2001) Platelet-derived growth factor C (PDGF-C), a novel growth factor

    that binds to PDGF alpha and beta receptor. J Biol Chem 276:27406-27414.

Goddard DR, Berry M, Butt AM (1999) In vivo actions of fibroblast growth factor-2 and

insulin-like growth factor-I on oligodendrocyte development and myelination in the central nervous system. J Neurosci Res 57:74-85.

Goddard DR, Berry M, Kirvell SL, Butt AM (2001) Fibroblast growth factor-2 inhibits myelin production by oligodendrocytes in vivo. Mol Cell Neurosci 18:557-569.

Goldman JE (2003) What are the characteristics of cycling cells in the adult central nervous system? J Cell Biochem 88:20-23.

Grossman SD, Rosenberg LJ, Wrathall JR (2001) Temporal-spatial pattern of acute neuronal and glial loss after spinal cord contusion. Exp Neurol 168:273-282.

Hart IK, Richardson WD, Heldin CH, Westermark B, Raff MC (1989) PDGF receptors on cells of the oligodendrocyte-type-2 astrocyte (O-2A) cell lineage. Development 105:595-603.

Heldin CH, Westermark B (1999) Mechanism of action and in vivo role of platelet-derived growth factor. Physiol Rev 79:1283-1316.

Hinks GL, Franklin RJ (1999) Distinctive patterns of PDGF-A, FGF-2, IGF-I, and TGF-beta1 gene expression during remyelination of experimentally-induced spinal cord demyelination. Mol Cell Neurosci 14:153-168.

Hiremath MM, Saito Y, Knapp GW, Ting JP, Suzuki K, Matsushima GK (1998) Microglial/macrophage accumulation during cuprizone-induced demyelination in C57BL/6 mice. J Neuroimmunol 92:38-49.

Holley JE, Gveric D, Newcombe J, Cuzner ML, Gutowski NJ (2003) Astrocyte characterization in the multiple sclerosis glial scar. Neuropathol Appl Neurobiol 29:434-444.

Houtman JJ, Fleming JO (1996) Pathogenesis of mouse hepatitis virus-induced

demyelination. J Neurovirol 2:361-376.

Hudson LD, Berndt JA, Puckett C, Kozak CA, Lazzarini RA (1987) Aberrant splicing of proteolipid protein mRNA in the dysmyelinating jimpy mutant mouse. Proc Natl Acad Sci U S A 84:1454-1458.

Inoue M, Honmou O, Oka S, Houkin K, Hashi K, Kocsis JD (2003) Comparative analysis of remyelinating potential of focal and intravenous administration of autologous bone marrow cells into the rat demyelinated spinal cord. Glia 44:111-118.

Jiang F, Levison SW, Wood TL (1999) Ciliary neurotrophic factor induces expression of the IGF type I receptor and FGF receptor 1 mRNAs in adult rat brain oligodendrocytes. J Neurosci Res 57:447-457.

Jiang F, Frederick TJ, Wood TL (2001) IGF-I synergizes with FGF-2 to stimulate oligodendrocyte progenitor entry into the cell cycle. Dev Biol 232:414-423.

Keirstead HS, Levine JM, Blakemore WF (1998) Response of the oligodendrocyte progenitor cell population (defined by NG2 labelling) to demyelination of the adult spinal cord. Glia 22:161-170.

Klinghoffer RA, Mueting-Nelsen PF, Faerman A, Shani M, Soriano P (2001) The two PDGF receptors maintain conserved signaling in vivo despite divergent embryological functions. Mol Cell 7:343-354.

Komoly S, Hudson LD, Webster HD, Bondy CA (1992) Insulin-like growth factor I gene expression is induced in astrocytes during experimental demyelination. Proc Natl Acad Sci U S A 89:1894-1898.

Kono K, Ueba T, Takahashi JA, Murai N, Hashimoto N, Myoumoto A, Itoh N,

Fukumoto M (2003) In vitro growth suppression of human glioma cells by a 16-mer oligopeptide: a potential new treatment modality for malignant glioma. J Neurooncol 63:163-171.

Kuzis K, Reed S, Cherry NJ, Woodward WR, Eckenstein FP (1995) Developmental time course of acidic and basic fibroblast growth factors' expression in distinct cellular populations of the rat central nervous system. J Comp Neurol 358:142-153.

Lachapelle F, Avellana-Adalid V, Nait-Oumesmar B, Baron-Van Evercooren A (2002) Fibroblast growth factor-2 (FGF-2) and platelet-derived growth factor AB (PDGF AB) promote adult SVZ-derived oligodendrogenesis in vivo. Mol Cell Neurosci 20:390-403.

Lannes-Vieira J, Gehrmann J, Kreutzberg GW, Wekerle H (1994) The inflammatory lesion of T cell line transferred experimental autoimmune encephalomyelitis of the Lewis rat: distinct nature of parenchymal and perivascular infiltrates. Acta Neuropathol (Berl) 87:435-442.

Larsen PH, Wells JE, Stallcup WB, Opdenakker G, Yong VW (2003) Matrix metalloproteinase-9 facilitates remyelination in part by processing the inhibitory NG2 proteoglycan. J Neurosci 23:11127-11135.

Lavi E, Das Sarma J, Weiss SR (1999) Cellular reservoirs for coronavirus infection of the brain in beta2-microglobulin knockout mice. Pathobiology 67:75-83.

Levison SW, Young GM, Goldman JE (1999) Cycling cells in the adult rat neocortex preferentially generate oligodendroglia. J Neurosci Res 57:435-446.

Li X, Ponten A, Aase K, Karlsson L, Abramsson A, Uutela M, Backstrom G, Hellstrom M, Bostrom H, Li H, Soriano P, Betsholtz C, Heldin CH, Alitalo K, Ostman A,

Eriksson U (2000) PDGF-C is a new protease-activated ligand for the PDGF alpha-receptor. Nat Cell Biol 2:302-309.

Li AW, Murphy PR (2000) Expression of alternatively spliced FGF-2 antisense RNA transcripts in the central nervous system: regulation of FGF-2 mRNA translation. Mol Cell Endocrinol 170:233-242.

Linnington C, Webb M, Woodhams PL (1984) A novel myelin-associated glycoprotein defined by a mouse monoclonal antibody. J Neuroimmunol 6:387-396.

Liu X, Mashour GA, Webster HF, Kurtz A (1998) Basic FGF and FGF receptor 1 are expressed in microglia during experimental autoimmune encephalomyelitis: temporally distinct expression of midkine and pleiotrophin. Glia 24:390-397.

Lu QR, Yuk D, Alberta JA, Zhu Z, Pawlitzky I, Chan J, McMahon AP, Stiles CD, Rowitch DH (2000) Sonic hedgehog--regulated oligodendrocyte lineage genes encoding bHLH proteins in the mammalian central nervous system. Neuron 25:317-329.

Lu QR, Sun T, Zhu Z, Ma N, Garcia M, Stiles CD, Rowitch DH (2002) Common developmental requirement for Olig function indicates a motor neuron/oligodendrocyte connection. Cell 109:75-86.

Lucchinetti C, Bruck W, Parisi J, Scheithauer B, Rodriguez M, Lassmann H (1999) A quantitative analysis of oligodendrocytes in multiple sclerosis lesions. A study of 113 cases. Brain 122 (Pt 12):2279-2295.

Lucchinetti C, Bruck W, Parisi J, Scheithauer B, Rodriguez M, Lassmann H (2000) Heterogeneity of multiple sclerosis lesions: implications for the pathogenesis of demyelination. Ann Neurol 47:707-717.

Ludwin SK (1997) The pathobiology of the oligodendrocyte. J Neuropathol Exp Neurol 56:111-124.

Maeda Y, Solanky M, Menonna J, Chapin J, Li W, Dowling P (2001) Platelet-derived growth factor-alpha receptor-positive oligodendroglia are frequent in multiple sclerosis lesions. Ann Neurol 49:776-785.

Magy L, Mertens C, Avellana-Adalid V, Keita M, Lachapelle F, Nait-Oumesmar B, Fontaine B, Baron-Van Evercooren A (2003) Inducible expression of FGF2 by a rat oligodendrocyte precursor cell line promotes CNS myelination in vitro. Exp Neurol 184:912-922.

Mallon BS, Shick HE, Kidd GJ, Macklin WB (2002) Proteolipid promoter activity distinguishes two populations of NG2-positive cells throughout neonatal cortical development. J Neurosci 22:876-885.

Mason JL, Jones JJ, Taniike M, Morell P, Suzuki K, Matsushima GK (2000) Mature oligodendrocyte apoptosis precedes IGF-1 production and oligodendrocyte progenitor accumulation and differentiation during demyelination/remyelination. J Neurosci Res 61:251-262.

Mason JL, Ye P, Suzuki K, D'Ercole AJ, Matsushima GK (2000) Insulin-like growth factor-1 inhibits mature oligodendrocyte apoptosis during primary demyelination. J Neurosci 20:5703-5708.

Mason JL, Langaman C, Morell P, Suzuki K, Matsushima GK (2001) Episodic demyelination and subsequent remyelination within the murine central nervous system: changes in axonal calibre. Neuropathol Appl Neurobiol 27:50-58.

Mason JL, Goldman JE (2002) A2B5+ and O4+ Cycling progenitors in the adult

forebrain white matter respond differentially to PDGF-AA, FGF-2, and IGF-1. Mol Cell Neurosci 20:30-42.

Matsushima GK, Morell P (2001) The neurotoxicant, cuprizone, as a model to study demyelination and remyelination in the central nervous system. Brain Pathol 11:107-116.

Matthews MA, Duncan D (1971) A quantitative study of morphological changes accompanying the initiation and progress of myelin production in the dorsal funiculus of the rat spinal cord. J Comp Neurol 142:1-22.

Matthews AE, Weiss SR, Paterson Y (2002) Murine hepatitis virus--a model for virus-induced CNS demyelination. J Neurovirol 8:76-85.

Maxwell M, Galanopoulos T, Neville-Golden J, Hedley-Whyte ET, Antoniades HN (1998) Cellular localization of PDGF mRNAs in developing human forebrain. Neuropathol Appl Neurobiol 24:337-345.

McDonald JW, Howard MJ (2002) Repairing the damaged spinal cord: a summary of our early success with embryonic stem cell transplantation and remyelination. Prog Brain Res 137:299-309.

McKay JS, Blakemore WF, Franklin RJ (1997) The effects of the growth factor-antagonist, trapidil, on remyelination in the CNS. Neuropathol Appl Neurobiol 23:50-58.

McKay JS, Blakemore WF, Franklin RJ (1998) Trapidil-mediated inhibition of CNS remyelination results from reduced numbers and impaired differentiation of oligodendrocytes. Neuropathol Appl Neurobiol 24:498-506.

McKinnon RD, Matsui T, Dubois-Dalcq M, Aaronson SA (1990) FGF modulates the

PDGF-driven pathway of oligodendrocyte development. Neuron 5:603-614.

McKinnon RD, Smith C, Behar T, Smith T, Dubois-Dalcq M (1993) Distinct effects of
bFGF and PDGF on oligodendrocyte progenitor cells. Glia 7:245-254.

Messersmith DJ, Murtie JC, Le TQ, Frost EE, Armstrong RC (2000) Fibroblast growth
factor 2 (FGF2) and FGF receptor expression in an experimental demyelinating
disease with extensive remyelination. Journal of Neuroscience Research 62:241-
256.

Morell P, Barrett CV, Mason JL, Toews AD, Hostettler JD, Knapp GW, Matsushima GK
(1998) Gene expression in brain during cuprizone-induced demyelination and
remyelination. Mol Cell Neurosci 12:220-227.

Moscatelli D (1987) High and low affinity binding sites for basic fibroblast growth factor
on cultured cells: absence of a role for low affinity binding in the stimulation of
plasminogen activator production by bovine capillary endothelial cells. J Cell
Physiol 131:123-130.

Muir DA, Compston DA (1996) Growth factor stimulation triggers apoptotic cell death in
mature oligodendrocytes. J Neurosci Res 44:1-11.

Navas S, Seo SH, Chua MM, Sarma JD, Lavi E, Hingley ST, Weiss SR (2001) Murine
coronavirus spike protein determines the ability of the virus to replicate in the
liver and cause hepatitis. J Virol 75:2452-2457.

Nishiyama A, Yu M, Drazba JA, Tuohy VK (1997) Normal and reactive NG2+ glial cells
are distinct from resting and activated microglia. J Neurosci Res 48:299-312.

Nunes MC, Roy NS, Keyoung HM, Goodman RR, McKhann G, 2nd, Jiang L, Kang J,
Nedergaard M, Goldman SA (2003) Identification and isolation of multipotential

neural progenitor cells from the subcortical white matter of the adult human brain. Nat Med 9:439-447.

O'Leary MT, Hinks GL, Charlton HM, Franklin RJ (2002) Increasing local levels of IGF-I mRNA expression using adenoviral vectors does not alter oligodendrocyte remyelination in the CNS of aged rats. Mol Cell Neurosci 19:32-42.

Oh LY, Denninger A, Colvin JS, Vyas A, Tole S, Ornitz DM, Bansal R (2003) Fibroblast growth factor receptor 3 signaling regulates the onset of oligodendrocyte terminal differentiation. J Neurosci 23:883-894.

Olson JK, Croxford JL, Calenoff MA, Dal Canto MC, Miller SD (2001) A virus-induced molecular mimicry model of multiple sclerosis. J Clin Invest 108:311-318.

Ortega S, Ittmann M, Tsang SH, Ehrlich M, Basilico C (1998) Neuronal defects and delayed wound healing in mice lacking fibroblast growth factor 2. Proc Natl Acad Sci U S A 95:5672-5677.

Palmer TD, Markakis EA, Willhoite AR, Safar F, Gage FH (1999) Fibroblast growth factor-2 activates a latent neurogenic program in neural stem cells from diverse regions of the adult CNS. J Neurosci 19:8487-8497.

Penderis J, Shields SA, Franklin RJ (2003) Impaired remyelination and depletion of oligodendrocyte progenitors does not occur following repeated episodes of focal demyelination in the rat central nervous system. Brain 126:1382-1391.

Pfeiffer SE, Warrington AE, Bansal R (1993) The oligodendrocyte and its many cellular processes. Trends Cell Biol 3:191-197.

Pluchino S, Quattrini A, Brambilla E, Gritti A, Salani G, Dina G, Galli R, Del Carro U, Amadio S, Bergami A, Furlan R, Comi G, Vescovi AL, Martino G (2003)

Injection of adult neurospheres induces recovery in a chronic model of multiple sclerosis. Nature 422:688-694.

Prineas JW, Barnard RO, Kwon EE, Sharer LR, Cho ES (1993) Multiple sclerosis: remyelination of nascent lesions. Annals of Neurology 33:137-151.

Pringle NP, Mudhar HS, Collarini EJ, Richardson WD (1992) PDGF receptors in the rat CNS: during late neurogenesis, PDGF alpha-receptor expression appears to be restricted to glial cells of the oligodendrocyte lineage. Development 115:535-551.

Raine CS, Wu E (1993) Multiple sclerosis: remyelination in acute lesions. Journal of Neuropathology & Experimental Neurology 52:199-204.

Rapraeger AC, Krufka A, Olwin BB (1991) Requirement of heparan sulfate for bFGF-mediated fibroblast growth and myoblast differentiation. Science 252:1705-1708.

Redwine JM, Armstrong RC (1998) In vivo proliferation of oligodendrocyte progenitors expressing PDGFalphaR during early remyelination. J Neurobiol 37:413-428.

Richardson WD, Pringle N, Mosley MJ, Westermark B, Dubois-Dalcq M (1988) A role for platelet-derived growth factor in normal gliogenesis in the central nervous system. Cell 53:309-319.

Riva MA, Mocchetti I (1991) Developmental expression of the basic fibroblast growth factor gene in rat brain. Brain Res Dev Brain Res 62:45-50.

Ruffini F, Furlan R, Poliani PL, Brambilla E, Marconi PC, Bergami A, Desina G, Glorioso JC, Comi G, Martino G (2001) Fibroblast growth factor-II gene therapy reverts the clinical course and the pathological signs of chronic experimental autoimmune encephalomyelitis in C57BL/6 mice. Gene Ther 8:1207-1213.

Saksela O, Moscatelli D, Sommer A, Rifkin DB (1988) Endothelial cell-derived heparan

sulfate binds basic fibroblast growth factor and protects it from proteolytic degradation. J Cell Biol 107:743-751.

Sauvageot CM, Stiles CD (2002) Molecular mechanisms controlling cortical gliogenesis. Curr Opin Neurobiol 12:244-249.

Schwab ME, Schnell L (1989) Region-specific appearance of myelin constituents in the developing rat spinal cord. J Neurocytol 18:161-169.

Schwab ME (2002) Increasing plasticity and functional recovery of the lesioned spinal cord. Prog Brain Res 137:351-359.

Shi J, Marinovich A, Barres BA (1998) Purification and characterization of adult oligodendrocyte precursor cells from the rat optic nerve. J Neurosci 18:4627-4636.

Shing Y, Folkman J, Sullivan R, Butterfield C, Murray J, Klagsbrun M (1984) Heparin affinity: purification of a tumor-derived capillary endothelial cell growth factor. Science 223:1296-1299.

Shuman SL, Bresnahan JC, Beattie MS (1997) Apoptosis of microglia and oligodendrocytes after spinal cord contusion in rats. J Neurosci Res 50:798-808.

Simpson PB, Armstrong RC (1999) Intracellular signals and cytoskeletal elements involved in oligodendrocyte progenitor migration. Glia 26:22-35.

Soriano P (1997) The PDGF alpha receptor is required for neural crest cell development and for normal patterning of the somites. Development 124:2691-2700.

Spassky N, Olivier C, Perez-Villegas E, Goujet-Zalc C, Martinez S, Thomas J, Zalc B (2000) Single or multiple oligodendroglial lineages: a controversy. Glia 29:143-148.

Stohlman SA, Bergmann CC, van der Veen RC, Hinton DR (1995) Mouse hepatitis

virus-specific cytotoxic T lymphocytes protect from lethal infection without

eliminating virus from the central nervous system. J Virol 69:684-694.

Swanborg RH (2001) Experimental autoimmune encephalomyelitis in the rat: lessons in

T-cell immunology and autoreactivity. Immunol Rev 184:129-135.

Touriol C, Morillon A, Gensac MC, Prats H, Prats AC (1999) Expression of human

fibroblast growth factor 2 mRNA is post-transcriptionally controlled by a unique

destabilizing element present in the 3'-untranslated region between alternative

polyadenylation sites. J Biol Chem 274:21402-21408.

Trapp BD, Nishiyama A, Cheng D, Macklin W (1997) Differentiation and death of

premyelinating oligodendrocytes in developing rodent brain. J Cell Biol 137:459-

468.

Vaccarino FM, Schwartz ML, Raballo R, Nilsen J, Rhee J, Zhou M, Doetschman T,

Coffin JD, Wyland JJ, Hung YT (1999) Changes in cerebral cortex size are

governed by fibroblast growth factor during embryogenesis. Nat Neurosci 2:246-

253.

Vaccarino FM, Schwartz ML, Raballo R, Rhee J, Lyn-Cook R (1999) Fibroblast growth

factor signaling regulates growth and morphogenesis at multiple steps during

brain development. Curr Top Dev Biol 46:179-200.

van Heyningen P, Calver AR, Richardson WD (2001) Control of progenitor cell number

by mitogen supply and demand. Curr Biol 11:232-241.

Villoslada P, Hauser SL, Bartke I, Unger J, Heald N, Rosenberg D, Cheung SW, Mobley

WC, Fisher S, Genain CP (2000) Human nerve growth factor protects common

marmosets against autoimmune encephalomyelitis by switching the balance of T

helper cell type 1 and 2 cytokines within the central nervous system. J Exp Med

191:1799-1806.

Wang S, Sdrulla AD, diSibio G, Bush G, Nofziger D, Hicks C, Weinmaster G, Barres BA

(1998) Notch receptor activation inhibits oligodendrocyte differentiation. Neuron

21:63-75.

Weiner LP (1973) Pathogenesis of demyelination induced by a mouse hepatitis. Arch

Neurol 28:298-303.

Williamson JS, Sykes KC, Stohlman SA (1991) Characterization of brain-infiltrating

mononuclear cells during infection with mouse hepatitis virus strain JHM. J

Neuroimmunol 32:199-207.

Wilson HC, Onischke C, Raine CS (2003) Human oligodendrocyte precursor cells in

vitro: phenotypic analysis and differential response to growth factors. Glia

44:153-165.

Wolswijk G, Munro PM, Riddle PN, Noble M (1991) Origin, growth factor responses,

and ultrastructural characteristics of an adult-specific glial progenitor cell. Ann N

Y Acad Sci 633:502-504.

Wolswijk G, Noble M (1992) Cooperation between PDGF and FGF converts slowly

dividing O-2Aadult progenitor cells to rapidly dividing cells with characteristics

of O-2Aperinatal progenitor cells. J Cell Biol 118:889-900.

Wolswijk G (2002) Oligodendrocyte precursor cells in the demyelinated multiple

sclerosis spinal cord. Brain 125:338-349.

Woodruff RH, Franklin RJ (1999) Demyelination and remyelination of the caudal

cerebellar peduncle of adult rats following stereotaxic injections of lysolecithin, ethidium bromide, and complement/anti-galactocerebroside: a comparative study. Glia 25:216-228.

Xu X, Weinstein M, Li C, Naski M, Cohen RI, Ornitz DM, Leder P, Deng C (1998) Fibroblast growth factor receptor 2 (FGFR2)-mediated reciprocal regulation loop between FGF8 and FGF10 is essential for limb induction. Development 125:753-765.

Yamaguchi TP, Harpal K, Henkemeyer M, Rossant J (1994) fgfr-1 is required for embryonic growth and mesodermal patterning during mouse gastrulation. Genes Dev 8:3032-3044.

Yao DL, Liu X, Hudson LD, Webster HD (1995) Insulin-like growth factor I treatment reduces demyelination and up-regulates gene expression of myelin-related proteins in experimental autoimmune encephalomyelitis. Proc Natl Acad Sci U S A 92:6190-6194.

Yayon A, Klagsbrun M, Esko JD, Leder P, Ornitz DM (1991) Cell surface, heparin-like molecules are required for binding of basic fibroblast growth factor to its high affinity receptor. Cell 64:841-848.

Ye P, Li L, Richards RG, DiAugustine RP, D'Ercole AJ (2002) Myelination is altered in insulin-like growth factor-I null mutant mice. J Neurosci 22:6041-6051.

Yeh HJ, Silos-Santiago I, Wang YX, George RJ, Snider WD, Deuel TF (1993) Developmental expression of the platelet-derived growth factor alpha-receptor gene in mammalian central nervous system. Proc Natl Acad Sci U S A 90:1952-1956.

Zhang SC, Ge B, Duncan ID (2000) Tracing human oligodendroglial development in vitro. J Neurosci Res 59:421-429.

Zhou M, Sutliff RL, Paul RJ, Lorenz JN, Hoying JB, Haudenschild CC, Yin M, Coffin JD, Kong L, Kranias EG, Luo W, Boivin GP, Duffy JJ, Pawlowski SA, Doetschman T (1998) Fibroblast growth factor 2 control of vascular tone. Nat Med 4:201-207.

List of Figures

Contributions

Tuan Le—Chapter 2-Figures 6 and 8; Chapter 3-Figures 2, 3, and 6; Chapter 4-Figure 4

Donna Messersmith—Chapter 2-Figures 1, 2, and 3

Adam Vana—Chapter 4-Figure 6

Yong-Xing Zhou—Chapter 3-Figure 1; Chapter 4-Figures 4 and 6